FACULTAD DE CIENCIAS

Departamento de Química Inorgánica

PROGRAMA OFICIAL DE DOCTORADO EN QUÍMICA

TESIS DOCTORAL

MATERIALES BIOINSPIRADOS

BASADOS EN BACTERIAS.

APLICACIONES BIOMÉDICAS

Ana Isabel González Garnica

Granada, noviembre 2017

MATERIALES BIOINSPIRADOS BASADOS EN BACTERIAS. APLICACIONES BIOMÉDICAS

Memoria de Tesis Doctoral presentada por
Ana Isabel González Garnica
para aspirar al título de Doctor por la
Universidad de Granada

Fdo. Ana Isabel González Garnica

LOS DIRECTORES DE LA TESIS DOCTORAL:

D. José Manuel Domínguez Vera
Catedrático del Departamento de Química Inorgánica
Instituto de Biotecnología
Universidad de Granada
y
Dª. Natividad Gálvez Rodríguez
Profesora titular del Departamento de Química Inorgánica
Universidad de Granada

La doctoranda Ana Isabel González Garnica y los directores de la Tesis José Manuel Domínguez Vera y Natividad Gálvez Rodríguez garantizamos, al firmar esta Tesis Doctoral, que el trabajo ha sido realizado por la doctoranda bajo la dirección de los directores de la Tesis y hasta donde nuestro conocimiento alcanza, en la realización del trabajo, se han respetado los derechos de otros autores a ser citados, cuando se han utilizado sus resultados o publicaciones.
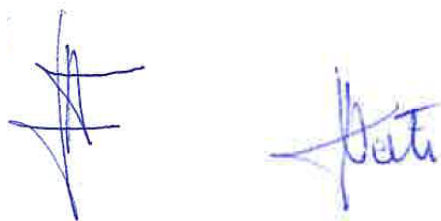
Granada, noviembre 2017

La Doctoranda

Fdo.: Ana Isabel González Garnica

Los Directores de la Tesis

Fdo.: José Manuel Domínguez Vera y Natividad Gálvez Rodríguez

Los resultados del trabajo de investigación realizado durante el desarrollo de esta Tesis Doctoral han dado lugar a la publicación de algunos artículos cuyos indicios de calidad son:

- González, A., Gálvez, N., Clemente-León M., & Domínguez-Vera, J. M. (2015). Electrochromic polyoxometalate material as a sensor of bacterial activity. ***Chemical Communications*, *51*, 10119-10122**.

INDICIOS DE CALIDAD:

Datos del Journal Citation Reports

- Impact Factor: 6.567
- Categorías (incluyendo Nº de revistas y posición revistas): CHEMISTRY, MULTIDISCIPLINARY - SCIE, 163 revistas, posición 21 de 163
- Cuartil: Q1
- Número de citas recibidas: 9

RESUMEN Y ESTRUCTURA DE LA TESIS DOCTORAL

En esta Tesis Doctoral se ha pretendido indagar en aspectos concretos de la maquinaria química de una bacteria probiótica, como *Lactobacillus fermentum*, muy frecuente en diferentes floras del cuerpo humano. En particular la Tesis se centra en explorar la actividad reductora de la bacteria y su capacidad para generar biofilms a través de la formación de exopolisacáridos (EPS). El conocimiento adquirido se ha utilizado para abordar problemas de salud en los que, de forma directa o indirecta, esta bacteria está involucrada.

Los resultados experimentales obtenidos y la discusión de los mismos se presentan en este trabajo divididos en 7 capítulos.

En el **primer capítulo,** se revisan los conceptos básicos del tema de investigación en el que se enmarca la presente Tesis Doctoral y la motivación de la mismo en el contexto actual. Se hace una revisión bibliográfica del uso de microorganismos para la síntesis de nanopartículas metálicas, y más concretamente del uso de EPS en diferentes aplicaciones biotecnológicas y biomédicas. Asimismo se proponen estos EPS como plataformas para la preparación de nuevos nanomateriales con propiedades ópticas mejoradas. Por último, se introduce la cepa *Lactobacillus fermentum* y se revisan las aplicaciones que hoy en día encuentra dicho probiótico en nutrición y medicina.

En el **segundo capítulo,** se ha evaluado la actividad reductora de *L. fermentum* usando un polioxometalato electrocrómico, que pasa de color amarillo pálido a azul intenso cuando es reducido. A partir de esta metodología simple, se ha podido demostrar que la actividad reductora de *L. fermentum* correlaciona con su fortaleza metabólica, de tal forma

que cuando la bacteria se encuentra en medios de cultivos óptimos produce la reducción de dicho polioxometalato, mientras que en medios de cultivos pobres, este poder de reducción disminuye significativamente.

Por tanto, esta metodología permite evaluar la presencia y fortaleza del probiótico en diferentes ambientes químicos, lo cual ha permitido, además, estudiar cual es el efecto de algunos fármacos sobre este probiótico. En particular se ha analizado el efecto de omeprazol y vancomicina sobre la viabilidad de dicho probiótico. Omeprazol es un fármaco utilizado masivamente en tratamientos de úlcera y gastritis y vancomicina, uno de los antibióticos de amplio rango más consumidos. Entorno a estos dos fármacos ha existido siempre la duda de si su consumo habitual podría dañar la flora bacteriana a nivel digestivo. En este sentido, los resultados ponen de manifiesto que omeprazol no tienen ningún efecto sobre la capacidad reductora de *L. fermentum* y por tanto sobre su fortaleza. Mientras que vancomicina reduce el poder reductor de *L. fermentum* hasta niveles prácticamente despreciables, poniendo de manifiesto que genera una muerte o daño severo sobre esta cepa.

En el **tercer capítulo,** se ha extendido la idea de que el cese de la actividad metabólica de las bacterias provoca una disminución de metabolitos excretados al medio para desarrollar un sensor para la diagnosis de vaginosis bacteriana. Esta infección afecta en torno al 10-15% de la población femenina mundial. En ella, la flora vaginal típica constituida por bacterias del tipo lactobacillus, que excretan ácido láctico al medio como producto mayoritario, se ve alterada por el crecimiento de

bacterias patógenas de carácter anaeróbico que excretan ácidos grasos de cadena corta, siendo el ácido acético el más abundante.

Los métodos actuales de diagnosis se basan en la toma de muestra para detectar las posibles bacterias patógenas presentes, lo que necesita tiempo y conlleva un coste y dificultad elevados. Se ha desarrollado un método de diagnosis basado en detectar los metabolitos típicos excretados por las bacterias. El cambio de color de amarillo a azul de un polioxometalato electrocrómico, al ser reducido en una muestra que contiene ácido láctico y tras aplicar luz ultravioleta, es la señal que indica el estado de la flora vaginal. La intensidad de color es mayor cuanto mayor es la concentración de dicho ácido y por tanto más "sana" es la muestra. Por tanto, se ha diseñado un método de diagnosis más rápido, barato y sencillo que los actualmente utilizados.

En el **cuarto capítulo,** se ha dado un paso vital para entender porque las bacterias probióticas contribuyen al aumento de la absorción de hierro en el tracto gastrointestinal. La reducción de Fe(III) a Fe(II) es esencial para que el hierro sea absorbido en duodeno. Se ha determinado que la actividad ferrireductasa de *L. fermentum* se debe a una molécula excretada por esta bacteria, el ácido *p*-hidroxifenilláctico (HPLA). Mediante su capacidad para reducir Fe(III), HPLA favorece la absorción de Fe(II) a través de los canales DMT1 de los enterocitos. HPLA estaría, por tanto, actuando como lo hace la proteína ferrireductora DcytB, proteína de membrana que va ligada a los canales DMT1 en el enterocito.

HPLA ha sido aislada del sobrenadante de un cultivo de *L. fermentum* mediante el empleo de cromatografía líquida de alta resolución y

posteriormente ha sido caracterizada utilizando las técnicas de resonancia magnética nuclear y espectrometría de masas. En un segundo paso se han llevado a cabo diferentes experimentos, entre ellos un experimento *in vitro*, para confirmar que los probióticos aumentan la absorción de Fe en el tracto gastrointestinal debido a la excreción de HPLA. Estos resultados han permitido proponer por primera vez un mecanismo que explique el por qué del efecto promotor de los probióticos en absorción de hierro. Este descubrimiento abre nuevas vías para el tratamiento de la deficiencia de hierro en humanos, uno de los desordenes nutricionales más comunes y extendidos en el mundo.

En el **quinto capítulo**, se ha llevado a cabo la identificación de los EPS que componen el biofilm de *L. fermentum*. Los EPS son los componentes mayoritarios en un biofilm bacteriano y están muy implicados en el desarrollo de las funciones de la bacteria. En el caso de bacterias probióticas, los EPS están relacionados con la adhesión y colonización de estas bacterias al epitelio, un proceso fundamental para que los probióticos puedan realmente llevar a cabo su papel beneficioso para la salud.

Tras aislar y purificar los EPS sintetizados en un cultivo donde sacarosa es la fuente de carbono, se ha llevado a cabo su identificación mediante el empleo de resonancia magnética nuclear. De este modo, se ha determinado que los EPS de *L. fermentum* en estas condiciones son dos homopolisacáridos: dextran y levan. Dextran es un polímero de glucosa y levan de fructosa. Ambos polímeros presentan propiedades que los hacen ser de interés para aplicaciones biotecnológicas en la industria alimentaria y farmacéutica.

En el **sexto capítulo**, se han aprovechado los EPS de *L. fermentum* como plataforma de soporte de nanopartículas de oro (AuNPs). Las AuNPs esféricas, en forma de bastón (rods) y prismas se adhieren y agregan en los EPS. Además, se ha puesto de manifiesto que los EPS son capaces de sintetizar y acoplar AuNPs por sí mismos a partir de Au(III) en disolución.

Mediante UV-vis se ha determinado que la agregación de AuNPs sobre EPS genera nuevas bandas de absorción, que acompañan a la banda de resonancia del plasmón de la superficie (SPR) típica de las nanopartículas de oro. Por ejemplo, en el caso de las nanopartículas con forma de prismas, la nueva banda de absorción se sitúa a muy baja energía, sobre 1100 nm, lo que aumenta el interés de las propiedades ópticas de estos sistemas.

Con el empleo de microscopía electrónica de transmisión se ha confirmado la agregación de las AuNPs en el EPS. A su vez, se ha llevado a cabo un experimento SERS para aumentar la señal Raman que tiene la rodamina B (una molécula modelo para este tipo de estudios) depositada sobre AuNPs aisladas empleando para ello estos sistemas AuNPs-EPS. En el caso del sistema AuNPs con forma de prismas sobre EPS se observa que la intensidad de la señal Raman de la rodamina aumenta dos órdenes de magnitud, mientras que para el resto de tipos de AuNPs no se ha encontrado ningún efecto. Esto ha sido explicado mediante un estudio por microscopía electrónica de transmisión con tomografía, donde se han observado diferencias en la forma en la que los EPS soportan las AuNPs, siendo el caso de los prismas de oro el único en el que el espacio entre

partículas está disponible para albergar las moléculas de rodamina B y por tanto aumentar su señal Raman.

Por último, en el **séptimo capítulo**, se recogen las conclusiones generales de esta tesis doctoral. En ellas se realiza un resumen de todo el trabajo realizado y se exponen y comentan los resultados más significativos.

SUMMARY

In this doctoral Thesis, the investigation of the specific aspects of the chemical machinery of a probiotic bacterium, such as *Lactobacillus fermentum*, which is very common in different floras of the human body, is intended. In particular, the Thesis is focused on exploring the bacterium's reducing activity and its capacity to generate biofilms through the formation of exopolysaccharides (EPS). The acquired knowledge is employed to address some health problems in which this bacterium is directly or indirectly implied.

The experimental results obtained and their discussion are presented in this report divided into 7 chapters.

In the **first chapter**, the basic concepts of the research topic in which the present Thesis is defined and its motivation in the current context are reviewed. A bibliography review regarding the use of microorganisms for the synthesis of metallic nanoparticles is done, concretely and more specifically, the use of the EPS in different biotechnological and biomedical applications. Furthermore, these EPS have been proposed as platforms for the preparation of new nanomaterials with improved optical properties. Finally, the *Lactobacillus fermentum* strain is presented and the main applications in nutrition and medicine of this prebiotic are reviewed.

In the **second chapter**, the reducing activity of *L. fermentum* is evaluated by using an electrochromic polyoxometalate which change from pale yellow to powerful blue when it is reduced. From this simple methodology, it has been able to demonstrate that the reducing activity of *L. fermentum* is correlated with its metabolic strength. Thus, when the

bacterium is in an optimal culture media, it produces the reduction of this polyoxometalate, whereas in a poor media, this reducing power significantly decreases.

Therefore, this methodology allows the evaluation of the probiotic's presence and strength in different chemical environments, and also studying the effect of some drugs against this probiotic. In particular, the effect of omeprazole and vancomycin has been evaluated against the viability of this probiotic. Omeprazole is a massive used drug for ulcer and gastritis treatment, and vancomycin, one of the antibiotics broadly more consumed. There has always existed a doubt around these two drugs regarding whether or not its usual consumption damages the bacterial flora at the intestinal level. In this sense, the results expose that omeprazole has not any effect against the reducing capacity of *L. fermentum*, and in consequence its strength. However, vancomycin decreases the reducing power of *L. fermentum* up to practically insignificant levels, which provokes death or serious damage to this strain.

In the **third chapter**, the idea that the stoppage of the metabolic activity of the bacteria provokes a decrease of excreted metabolites in the media, is extended to develop a sensor for the diagnosis of bacterial vaginosis. This infection affects approximately 10-15% of women in the general female population. In this, the typical vaginal flora, which is constituted of lactobacillus bacteria and excretes lactic acid out to the media, is altered by the growth of pathogenic anaerobic bacteria that excrete short chain fatty acids out, being the acetic acid the most abundant.

The current diagnosis methods are based on the sample gathering to detect the presence of possible pathogenic bacteria, which requires time and a huge cost and difficulty. A diagnosis method based on the detection of the typical excreted metabolites by the bacteria has been developed. The change of colour from yellow to blue of an electrochromic polyoxometalate when it is reduced in a sample containing lactic acid and after using ultraviolet light, is the signal that indicates the state of the vaginal flora. The intensity of the colour is higher when higher is the acid concentration and thus more 'healthy' is the sample. Therefore, a faster, cheaper and easier diagnosis method than the current approaches has been designed.

In the **fourth chapter**, a vital step towards understanding why probiotic bacteria increase iron absorption in the gastrointestinal tract has been taken. Reduction of Fe(III) to Fe(II) is essential for iron absorption in the duodenum. It has been determined that the ferric-reducing activity of *L. fermentum* is due to an excreted molecule, *p*-hydroxyphenyllactic acid (HPLA), by this bacteria. By reducing Fe(III), HPLA boosts Fe(II) absorption through the DMT1 channels of enterocytes. Thus, HPLA would be acting in the same way that the ferric-reducing protein DcytB, a membrane protein that is linked to the DMT1 channels in the enterocyte, does.

HPLA has been isolated from the supernatant of a *L. fermentum* culture by the employment of high resolution liquid chromatography and afterwards has been characterized using nuclear magnetic resonance and mass spectroscopy techniques. In a secondary step, several experiments have been carried out, among them an *in vitro* experiment, to confirm

that probiotics increase the Fe absorption in the gastrointestinal tract due to the excretion of HPLA. These results have allowed, for the first time, to propose a mechanism that explains the reason for probiotic to promote iron absorption. This discovery opens new avenues for the treatment of iron deficiency in humans, one of the most common and widespread nutritional disorders in the world.

In the **fifth chapter**, the identification of the EPS that compound the biofilm of *L. fermentum* has been carried out. The EPS are the main components of a bacterial biofilm and they are highly implied in the development of the bacterial functions. In the case of the probiotic bacteria, the EPS are related with the epithelial adhesion and colonization of these bacteria, a fundamental process needed in the beneficial role of the probiotic for the human health.

After isolating and purifying the EPS, synthesized in a culture where sucrose is the carbon source, their identification by employing nuclear magnetic resonance has been carried out. In this way, it has been determined that the EPS of *L. fermentum* in these culture conditions are two homopolysaccharides: dextran and levan. Dextran is a glucose polymer and levan a fructose one. Both polymers have properties of interest for biotechnological applications in food and pharmaceutical industries.

In the **sixth chapter**, it has been taken advantage of the EPS of *L. fermentum* as a platform to support gold nanoparticles (AuNPs). Spherical, rods and prisms nanoparticles aggregate when deposited onto

EPS. Moreover, the EPS of *L. fermentum* produce gold aggregates from a Au(III) solution on their own.

UV-vis spectra of aggregated AuNPs shows new absorbance peaks, together with the typical band of the surface plasmon resonance (SPR) of gold nanoparticles. For example, in the case of gold nanoprisms, the new absorption band appears at a very low energy centered at 1100 nm. This fact increases the interest of the optical properties of these systems.

By using transmission electron microscopy it has been confirmed the AuNPs aggregation onto EPS. At the same time, it has been carried out a SERS experiment to increase the Raman signal of deposited rhodamine B (a model molecule for this type of studies) over isolated AuNPs by using these AuNPs-EPS systems. In the case of gold nanoprisms onto EPS, a rhodamine Raman signal intensity two times higher has been observed, whereas no effect has been found with the other types of AuNPs. This fact has been explained by a transmission electron microscopy tomography study where several differences in the way in which AuNPs are deposited onto the EPS have been observed. Only the gold nanoprisms aggregate, in which gold interparticle surfaces were exposed to RhB, showed a drastic increase of intensity in the Raman spectrum of RhB.

Finally, in the **seventh chapter**, the general conclusions of this doctoral Thesis are included. In them, all the work and the most significant results are exposed, discussed and summarized.

ÍNDICE

CHAPTER 1.

INTRODUCTION

.

1.1 MAKING MODERN CHEMISTRY

1.1.1 Material science and the nano-revolution

The history of our civilization goes hand in hand with materials, which have been essential in human supervivence.[1] "M*aterials science*" involves investigating the relationships that exist between structures and properties of materials, to produce, on the basis of these structure-property correlations, better and better materials with a predetermined set of properties.[2]

The behavior that a material has in response to any exterior stimulus can be defined as a property. Properties are directly related with the final structure of a material and depend of its shape or size. [2-3] For this reason, the design of a material requires the control not only over its chemical structure at atomic level but also, the control over structuration of the material at microscopic level.

In last decades, the concept of advanced materials is specially related to two concepts or approaches: nanotechnology and/or self assembly processes inspired by nature.[2, 4]

It was Richard Feynman who first dreamed with the idea of manipulating materials at the atomic and molecular scale in 1959 with his famous talk 'There is plenty of room at the bottom'. Although he is credited for the initiation of the nanotechnologycal revolution,[5-6] it was not until 1968, with the discovery of molecular beam epitaxy in the Bell Laboratories, when the dream started to become true.[7] Later, in 1974,

the term 'nanotechnology' was first used by Norio Taniguchi to refer to the design of materials on the nanoscale.[8]

The most appropriate definition for nanotechnology in the context of this work is that of the National Nanotechnology Initiative: *'nanotechnology is the research and technology development at the atomic, molecular, or macromolecular levels, in the length scale of 1–100 nm range, to provide a fundamental understanding of phenomena and materials at the nanoscale and to create and integrate them into larger material components, systems, and architectures that have novel properties and functions because of their small and/or intermediate size'.*[5, 9] So it is the change in their properties in comparison to their bulk counterparts what make nanoscale materials such as interesting. Some properties that can change depending on the size are for instance, optical (e.g., gold, silver), electrical (e.g., carbon), physical (e.g., gold, Si, PbS), and chemical (e.g., gold, palladium, platinium).[5]

Nanotechnology can be applied to many different disciplines depending on what the systems designed or the properties developed are. When the field of application of the nanotechnology is medicine, it is called Nanomedicine. Therefore, Nanomedicine makes use of the multidisciplinary science of Nanotechnology to apply its development to the diagnosis and therapy in health and medicine fields, generating new materials with these specific applications.[10] One of the most important topics of the nanomedicine is biomedicine, the branch of medicine based on the study of illness from a biological (or biochemical) and physiological perspective.

A faster and more preventive diagnosis is achieved with the use of novel contrast agents or the improvement of traditional ones, as well as a correct therapy and an easier follow-up of diseases with strategies such as drug delivery, regenerative medicine or anti-tumor photothermal therapy are also arised.[11] These and other disciplines have improved thanks to nanotechnology, for example gene sequencing, tissue engineering, cancer diagnosis or stem cell research.[12]

Nanoparticles (NPs), which are discrete entities with three dimensions of the order of 100 nm or less,[13] are the main elements that nanomedicine uses for diagnosis and therapy. These particles have unique mechanical, thermal, electrical, magnetic and optical properties, due to size-dependent surface and quantum effects, absent in individual atoms and bulk materials. Furthermore, the nanoparticle surface can be chemically tuned, by coupling functional groups, for specific goals, especially for driving the nanoparticle to the desired target The advantages of using nanoparticles as carriers (summarized in Figure 1) are: i) Their shape, size and surface properties can protect encapsulated agents from degradation by endogeneous defense mechanisms when they are introduced in the biological medium; ii) nanoparticles can be targeted to specific organs, tissues and cells due to the functionalization of their surface; iii) the controlled release of drugs as target areas is also possible using a nanocarrier matrix; iv) nanocarries should be no toxic and be safely excreted from the body.[14]

Methods of synthesis of nanoparticles have been traditionally classified depending on the applied approach: "bottom-up" or "top-

down". In the bottom-up approach, traditionally related to chemistry, atoms assemble to conform a nanoparticle. On the contrary, the top-down approach is based on physical methods, breaking down a bulk material until the nanoparticle size. These traditional methods are generally quite expensive and potentially hazardous due to the biological and environmental toxicity of the chemicals used.[15]
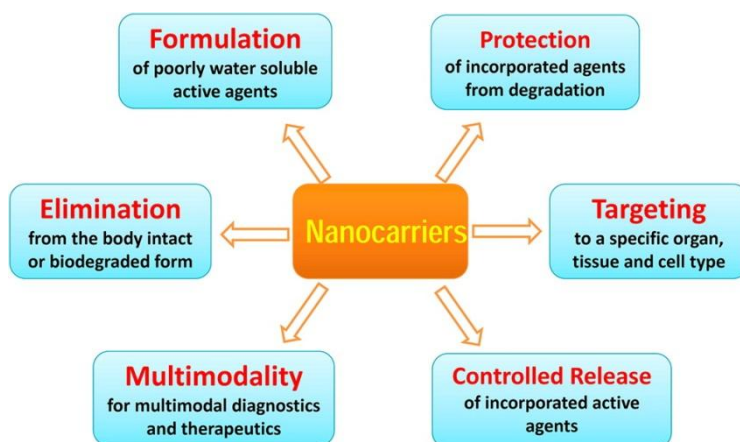
Figure 1. Advantages of nanocarrier formulations in medicine.[14]

An eco-friendly approach is becoming more and more usual as people and industry are becoming more conscious with environmental issues. The key of the eco-friendly approach is the bio-inspiration and use of green-chemistry where traditional toxic chemical compounds are replaced by the use of biological material or microorganisms (bacteria, funghi, yeast, etc.) to obtain metallic nanoparticles.

1.1.2 Microorganisms: synthesizing nanoparticles

Organisms such as bacteria are capable of synthesizing inorganic materials by themselves. The first approach to produce these natural

inorganic materials has been the use of the microorganism itself in our laboratories to reproduce (bio-mimic approach) what these organisms do in their natural habits. However, researching now is trying to obtain these natural materials by using other microorganisms that do not necessarily produce these materials as part of their metabolism, but that might if adequate conditions are implemented.[16]

The use of living microorganisms to synthesize metallic nanoparticles is a relatively recent approach. The biosynthesis allows controlling size and morphology of nanoparticles, which are crucial parameters for obtaining the desired properties.

In most cases, the experimental process to analyze the ability of a microorganism to produce nanoparticles has been carried out as a screening assay, in which the bacterial reducing activity is tested by adding the bacteria in their different metabolic phases to metallic ions solutions. The most typical examples are devoted to gold and silver nanoparticles, but it has also applied to other metals as platinum, palladium, selenium, tellurium and copper. Table 1 shows different bacteria and metal nanoparticles produced by them.

The first example describing the synthesis of nanoparticles by bacteria was in 1980s[17] and dealt with the use of *Bacillus subtilis* to produce gold nanoparticles. Since then, many other examples of bacteria producing gold nanoparticles from gold ions have been reported. In some cases, some correlations between bacteria and shape and size of gold nanoparticles have been described. For example, bacterium *Rhodopseudomonas capsulate* produces different nanoparticle shapes by

monitoring pH and gold ions concentration.[18] The presence of oxygen is another parameter that affect size and shape of the nanoparticles. In the case of *Actinobacter* sp. triangular and hexagonal shapes (30-50 nm), along with some spherical nanoparticles, were obtained in the absence of molecular oxygen. However, the same reaction at lower pH lead up to a decrease in particle size (10 nm), whereas in the presence of molecular oxygen, a completely different morphology resulted.[19]

Bacteria	Metal
Bacillus subtilis	Au
Shewanella algae	Au
Rhodopseudomonas capsulate	Au
Pseudomonas aeruginosa	Au
Lactobacilli strains	Au
Ralstonia metallidurans	Au
Shewanella oneidensis	Au
Lactobacilli strains	Ag
Pseudomonas stutzeri AG259	Ag
Lactobacillus strains (*fermentum* LMG 8900, *farciminis* LMG 9189, *garvieae* LMG8162, *brevis* LMG 11437, *parabuchneri* LMG 11772, *rhamnosus* LMG 18243, *plantarum* LMG 24830/LMG24832, *mucosae*)	Ag
Lactobacillus fructivorans	Ag
Pedicoccus pentosaceus LMG 9445	Ag
Morganella morganii Subgroup (A, B, C, D, E, F, G1, G2)	Ag
Morganella morganii RP42	Ag
Morganella psychrotolerans	Ag
Shewanella algae	Pt
Desulfovibrio desulfuricans	Pd
Sulfurospirillum barnesii	Se
Bacillus selenitireducens	Se
Selnihalanaerobacter shriftii	Se
Pseudomonas alkaliphila	Se
Sulfurospirillum barnesii	Te
Bacillus selenitireducens	Te
Serratia sp.	Cu
Escherichia coli	Cu
Lactobacilli strains	Au–Ag

Table 1. List of different metal nanoparticles synthesized by microorganisms. (Modified from Bansal, *et al.*)[16]

Although it is well known that silver ions are toxic to most microbial cells, there are some bacteria that have developed a resistance by reducing Ag^+ to form Ag nanoparticles.[20-21] The shape control of Ag

nanoparticles is also possible by monitoring the bacterial growth kinetics using different temperatures.[22]

Other metallic nanoparticles have also been synthesized by bacteria with interesting potential for several applications in material science. For example, platinum nanoparticles[23] have huge interest as anticancer agent because they may be more effective than platinum. Palladium nanoparticles have interest in catalysis as it has been demonstrated that are superior to conventional palladium catalysists.[24] In addition, selenium and tellurium nanoparticles are of interest in semiconductor industry,[25] and copper ones may be an economical alternative to gold and silver nanoparticles.[26] Furthermore, fluorescent cadmium sulfide (CdS) nanoparticles has been found in the cytoplasm of human breast cancer cells when administer coupled to *L. fermentum*, pointing out a possible carrier role of *L. fermentum* of therapeutic anti-cancer drugs.[27]

The biochemical mechanism of metal ions reduction by bacteria is still not well defined but two different approaches have been envisaged: 1) the bacteria may have a defensive mechanism against toxic stimuli, as Ag^+ 2) chemical compounds with redox activity at the bacterial membrane or excreted during bacterial growth have the ability to reduce ions to metal atoms, which would form nanoparticles.[16, 28] The same reducing molecule or other could act as well as coating to prevent aggregation and control the final size.

For example*, Lactobacillus fermentum* is also able to synthesize silver nanoparticles in different ways. Firstly, the supernatant of a *L. fermentum* culture has been used as reductant, obtaining extracellular and stable

spherical nanoparticles (no agglomeration was found after months) of around 15 nm of diameter.[29] The bacteria have been also used as a reducing and capping agent to produce nanoparticles of 11 nm totally associated to the bacteria.[30] In addition, excreted exopolysaccharides from these bacteria have produced and coated silver nanoparticles which exhibit antibacterial activity.[31]

Regardless of the unsolved mechanism, the possibility of producing nanoparticles by bacteria is an alternative approach with interest itself. Likewise, the use of excreted molecules or metabolites by bacteria might be of great interest both for material science and biomedicine.

1.2 MICROORGANISMS: A NATURAL SOURCE OF METABOLITES

Knowing the way in which microorganisms live in the nature and how they interact with human may constitute a good strategy to decode the possible mechanisms implied in the production of nanoparticles and materials in general. In this section, the bacteria way of living in natural environment and in human body is reviewed, focusing on the different compounds secreted out by these cells and their possible implications in material production for further applications in biomedicine and biotechnology.

### 1.2.1 Biofilms: more than a way of living

The idea of a bacterial culture living isolated in the nature is far from the reality. Bacteria cohabit in populations, forming polymicrobial aggregates in which each population adhere to the other and/or to its surface or interface, that is, forming the so called *bacterial biofilms*.[32] A

biofilm can be defined as 'a mass of bacteria enclosed in a protective matrix and associated with a surface or interface'.[33] In biofilms, from 10^8 to 10^{11} cells per gram (both prokaryotic and eukaryotic) are found comprising many different species (a self-specie biofilm is very strange) interacting (socially and physically) one to another, what makes possible that bacteria acquire properties that were not predictable on their free-living state.[34]

In a biofilm formation, bacteria work in a group, in the same way in which humans live in cities, so biofilms have been described as 'city of microbes'. Looking for suiting our needs, we choose a city and neighborhood to live. In the same way, the bacterium (an individual planktonic cell) choose its neighborhood when it founds a surface where to interact with other microbes that live there, up to create a stable association being one more member of the colony. From this moment, the biofilm is erected, as a 3D complex matrix, in the same way that buildings in a community are. Finally, a dispersion of the biofilm can be produced and planktonic cells restart the colonization of new substrates closing the cycle.[35] This process is schematized in Figure 2.

This matrix formation is not a simple process and depends on many aspects such as the amount and type of available nutrients; the extracellular material synthesis and secretion; shear stress; and possible competition between the biofilm's habitant microorganism.[34] In addition, the matrix confers to the microorganisms structural and functional benefits (hydration, resources accumulation, digestive capacity and protection against antimicrobial) and facilitates the interactions between

cells enhancing their metabolic capacity and resistance to antimicrobials.[34, 36]
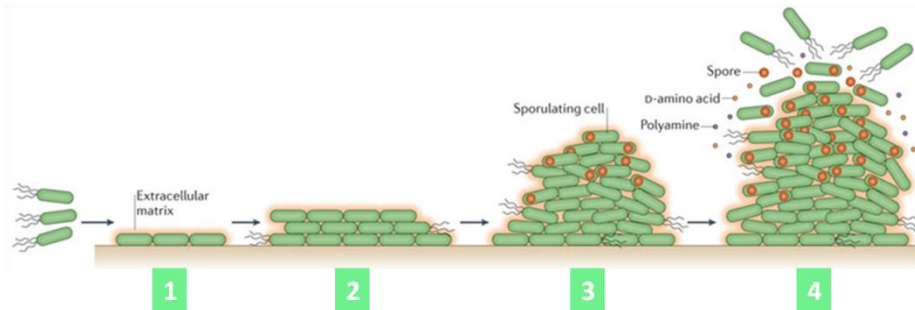
Figure 2. Process of biofilm formation (modified from Vlamakis *et al.*).[37] 1) Initial reversible attachment of microbes to surface. 2) Permanent attachment and early vertical development (start of the 3D structure). 3) Mature biofilm formed. 4) Dispersal of more microbes.

1.2.1.1 Biofilms composition and structure

The matrix of a biofilm is constituted in its major part of water (up to 97%) and extracellular polymeric substances (EPS) secreted out by the microorganisms that live in the biofilm. The EPS abbreviation may cause some confusion because it is sometimes used to refer to the 'extracellular polysaccharides' or 'exopolysaccharides', which are defined as the most abundant components of the extracellular polymeric substances group. Nevertheless, protein, nucleic acids, lipids and humic substances (non-degraded dead organic matter) are also components.[38] Extracellular polymeric substances have several roles in biofilm functions, which are described in Table 2. As it will be of interest in this work, from now, EPS will refer to exopolysaccharides.

Function	Relevance for biofilms	EPS components involved
Adhesion	Allows the initial steps in the colonization of abiotic and biotic surfaces by planktonic cells, and the long-term attachment of whole biofilms to surfaces	Polysaccharides, proteins, DNA and amphiphilic molecules
Aggregation of bacterial cells	Enables bridging between cells, the temporary immobilization of bacterial populations, the development of high cell densities and cell–cell recognition	Polysaccharides, proteins and DNA
Cohesion of biofilms	Forms a hydrated polymer network (the biofilm matrix), mediating the mechanical stability of biofilms (often in conjunction with multivalent cations) and, through the EPS (capsule, slime or sheath), determining biofilm architecture, as well as allowing cell–cell communication	Neutral and charged polysaccharides, proteins (such as amyloids and lectins), and DNA
Retention of water	Maintains a highly hydrated microenvironment around biofilm organisms, leading to their tolerance of dessication in water-deficient environments	Hydrophilic polysaccharides and, possibly, proteins
Protective barrier	Confers resistance to nonspecific and specific host defences during infection, and confers tolerance to various antimicrobial agents (for example, disinfectants and antibiotics), as well as protecting cyanobacterial nitrogenase from the harmful effects of oxygen and protecting against some grazing protoza	Polysaccharides and proteins
Sorption of organic compounds	Allows the accumulation of nutrients from the environment and the sorption of xenobiotics (thus contributing to environmental detoxification)	Charged or hydrophobic polysaccharides and proteins
Sorption of inorganic ions	Promotes polysaccharide gel formation, ion exchange, mineral formation and the accumulation of toxic metal ions (thus contributing to environmental detoxification)	Charged polysaccharides and proteins, including inorganic substituents such as phosphate and sulphate
Enzymatic activity	Enables the digestion of exogenous macromolecules for nutrient acquisition and the degradation of structural EPS, allowing the release of cells from biofilms	Proteins
Nutrient source	Provides a source of carbon-, nitrogen- and phosphorus-containing compounds for utilization by the biofilm community	Potentially all EPS components
Exchange of genetic information	Faciliates horizontal gene transfer between biofilm cells	DNA
Electron donor or acceptor	Permits redox activity in the biofilm matrix	Proteins (for example, those forming pili and nanowires) and, possibly, humic substances
Export of cell components	Releases cellular material as a result of metabolic turnover	Membrane vesicles containing nucleic acids, enzymes, lipopolysaccharides and phospholipids
Sink for excess energy	Stores excess carbon under unbalanced carbon to nitrogen ratios	Polysaccharides
Binding of enzymes	Results in the accumulation, retention and stabilization of enzymes through their interaction with polysaccharides	Polysaccharides and enzymes

Table 2. Functions of extracellular polymeric substances in bacterial biofilms.[39] (EPS refers to extracellular polymeric substances in this table).

Extracellular polymeric substances are considered 'the dark matter of bifilms' because their biochemical characterization is something really difficult to achieve due to the large range of matrix biopolymers as well as the fact that the composition may vary depending on the environment.[40] Despite this, a theoretical principle of structure was established by Mayer *et al*. when defined London forces, electrostatic interactions and hydrogen bonds as the three basics weak interactions that conform the structure of a biofilm.[41] Subsequence studies have determined that the architecture of biofilms depends on more things that the simple chemical interactions.

The hydrodynamic conditions, nutrients' concentration, bacterial motility, cellular communication, proteins and EPS can modify the morphology significantly. For example, alginate has been defined to be involved in biofilms formation where *Pseudomonas aeruginosa* is a member and acetyl groups or calcium ions also influence this structure.[39]

Different strategies have been applied for the isolation and characterization of extracellular polymeric substances. In the so-called destructive approach, chemical methods are used consisting of the extraction and isolation of the extracellular polymeric substances from the cells. In these methods centrifugation, filtration, heating, blending and sonication are the main steps before using exchanger resins or precipitation with EtOH (usually used for the exopolysaccharides extraction). After the isolation, several characterization techniques have been employed to unravel its chemical structure and morphology, such as Transmission Electron Microscopy (TEM), infrared and Raman spectroscopies, nuclear magnetic resonance, among others. From these

techniques, information on lipids, proteins, amino acids and polysaccharides is recovered. On the other hand, the non-destructive methods apply the same kind of microscopy and spectroscopic techniques to obtain information of the whole structure of the biofilm. In any case, full analysis of the chemical composition and structure is extraordinarily complex.[42-43]

Recently, modern techniques are being used for the extracellular polymeric substances characterization. Atomic force microscopy (AFM) has allowed, by the first time, making a deep insight into the nanostructure and composition of some biofilm[40]. When coupled to Raman spectroscopy (RM) the resolution increased and provided information of macromolecules at different growth stages of the bacteria. In addition, optical coherence tomography[45-46] (a high-resolution medical and biological imaging technology similar to ultrasound) and sum-frequency-generation (SFG) spectroscopy[47-49] (a surface-specific non-linear optical technique) seems to be complementary techniques for a better chemical and structural characterization.

There is not perfect isolation or characterization methods for extracellular polymeric substances. The combination of several techniques seems to be nowadays the best strategy to identify and characterize the components of the biofilm. A rigorous identification is needed, not only to know more about the way of living of the microorganisms, but also because understanding the way in which the different components interact with each other is of great interest for
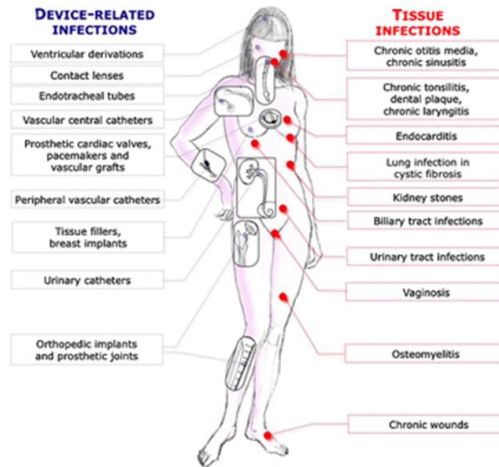
applications in food, pharmaceutical, biomedical, bioremediation and bioleaching industries, where new bioinspired materials are emerging day by day.

1.2.1.2 Biofilms of pathogenic organisms

One of the main functions of a biofilm is the protection of the living colony by acting as a protective barrier. This is why the biofilm has a crucial role in the resistance against antibiotics. The World Health Organization stated in April 2014 that *'this serious threat is no longer a prediction for the future, it is happening right now in every region of the world and has the potential to affect anyone, of any age, in any country. Antibiotic resistance—when bacteria change so antibiotics no longer work in people—is now a major threat to public health'*. In this context, one of the most hopeful treatments is precisely to weaken or destroy off the biofilm.

Biofilms colonize not only biological surfaces, such as human tissues but also medical devices (see Figure 3). The most known microorganisms implied in medical devices colonization are staphylococci and bacterium *P. aeruginosa*. In human infections, biofilms are found on implants, dental caries, periodontitis, otitis media, bilary tract infections, intra-amniotic infections, pneumonia, etc.[50] Millions of dollars are dedicated every year for avoiding infection through medical devices and treatment of biofilms formation in different tissues.[51]

Figure 3. Sites of major device-related and soft tissue biofilm-related infections.[51]

1.2.1.3 Biotechnological applications of the EPS

Bacterial EPS are of huge interest in biotechnology. They are used in cosmetic, pharmaceutical, biomedicine and food industries, where traditional polymers do not achieve all the requirements of purity and properties. Some of these EPS correspond to xanthan gum, gellan, alginate, glucans (cellulose, curdlan and dextran), hyaluronan, succinoglycan and levan and are currently commercially exploited. Table 3 summarizes the origin, composition, properties and main applications of these EPS.

In the medicine field, some bacterial EPS are approved to be used in specific applications. Dextran is used as a blood plasma volume expander to control de wound shock. In the case of gellan, it is well used in oral, ophthalmic and nasal drug formulations, and hyaluronic acid, on his behalf, is employed in eye surgery and intraarticular injections in osteoarthritis.[52]

EPS	Bacteria genera	Components	Main Properties	Main Applications
Xanthan gum	*Xanthomonas*	Glucose, mannose, Glucuronic acid, acetate, pyruvate	Hydrocolloid (high viscosity yield at low shear rates even at low concentrations; stability over wide temperature, pH and salt concentrations ranges)	Foods, petroleum industry, pharmaceuticals, cosmetics and personal care products, agriculture
Gellan	*Sphingomonas*	Glucose, rhamnose Glucuronic acid, Acetate, glycerate	Hydrocolloid (stability over wide pH range), gelling capacity, thermoreversible gels	Foods, pet food, phatmaceuticals, research (agar substitute and gel electrophoresis)
Alginate	*Azetobacter Pseudomonas*	Glucuronic acid, mannuronic acid, acetate	Hydrocolloid, gelling capacity, film-forming	Food hydrocolloid, medicine (surgical dressings, wound management, controlled drug release)
Cellulose	*Gluconacetobacter, Agrobacterium, Aerobacter Achromobacter, Azotobacter Rhizobium, Sarcina, Salmonella*	Glucose	High crystallinity, insolubility in most solvents, high tensile , strength, moldability	Foods (indigestible fiber), biomedical (wound healing, tissue engineered, blood vessels, audio speaker diaphragms)
Dextran	*Leuconostoc Streptococcus Lactobacillus*	Glucose	Non-ionic, good stability, newtonian fluid behavior	Foods, pharmaceutical industry (blood volume expander), chromatographic media
Curdlan		Glucose	Gel-forming ability, water insolubility, edible and non-toxic, biological activity	Foods, pharmaceutical industry, heavy metal removal, concrete additive
Hyaluronan	*Pseudomonas aeruginosa Streptococci*	Glucuronic acid, acetylglucosmine	Biological activity, highly hydrophilic, biocompatible	Medicine, solid culture media
Succinoglycan		Glucose, galactose, acetate, pyruvate, succinate, 3-hydroxybutyrate	Viscous shear thinning aqueous solutions, acid stability	Food, oil recovery
Levan		Fructose	Low viscosity, high water solubility, biological activity (anti-tumor activity, anti-inflammatory), adhesive strength, film-forming capacity	Food (prebiotic), feed, medicines, cosmetics, industry

Table 3. Origin, composition, properties and main applications of the most extensively studied bacterial EPS. (Modified from Freitas *et al.*).[53]

One particular ability of the EPS is that they can be used as drug carries due to their ability to form hydrogels. Preparation and encapsulation (self-assemble) of drug nanoparticles, make these drugs be more efficient and less toxic than the non-encapsulated ones. Xanthan and alginate have been used in drug delivery, the first as a drug controlled release carrier, and the second, in cell microencapsulation as microsphere vectors.[52] Selenium, iron, cobalt, gold and silver nanoparticles have been capped with levan, obtaining more protective effect on human intestinal cells and high stability.[54]

Other possible biomedical applications that are currently under study are drug-targeting, anticancer capacity, recombinant macromolecular function, vaccines preparations, gen delivery, cell encapsulation and tissue engineering.[52]

Other more recent EPS identified from bacteria are GaloctoPol[55] and FucoPol.[56] The first one is synthesized by *Pseudomonas oleovorans* and it is composed of galactose. The second one is synthesized by Enterobacter and consists of fucose. Both bacteria are found on glycerol by-product in biodiesel industry and have potential properties such as viscosity and film-forming, emulsifying and flocculating capacity which allow them to be used in food, cosmetic and pharmaceutical industry as hydrocolloid, coatings and packages. In addition, the fucose content of FucoPol renders this polymer biological active as anti-carcinogenic, anti-inflammatory and anti-aging agents. Likewise, they can function as prebiotics due to its fuco-oligosaccharides content.[53]

In this thesis, a new example of bacterial EPS isolation and characterization will be described in Chapter 5. These EPS are really useful coating agents of gold nanoparticles, as shown in Chapter 6.

1.2.2 Human Microbiota

The microbiota is the sum of all microorganisms, including bacteria, archaea, eukaryotes and viruses, that reside in and/or on a host or a specified part of a host.[57] In humans, colonization starts at birth by mother's vagina or skin contact an afterwards by intake of breast milk. About 10^{14} bacteria co-habit in the intestine at adult age. Ten times over the number of cells in the human body! Most of these microorganisms reside in the gastrointestinal tract (GI) but they colonise practically every part of the human body exposed to the external environment, as skin, mouth, respiratory cavity and urogenital tract.[57-59]

Around 1000 species of aerobic, anaerobic and facultative anaerobic bacteria are found in the GI, being the anaerobic ones the most numerous. This complex community is called gut microbiota and its specific composition is really difficult to determine as it depends of the location in GI due to intestinal motility, pH, redox potential, nutrient supplies, host secretions, etc. (See Figure 4).

The pH changes from stomach (pH < 3) to colon (neutral pH), which favours an increase in the density of bacteria. Approximately, 10^4 cells of *bacili, catenabacteria, enterococci and lactobacilli* are found in stomach. 10^2-10^4 *lactobacilli, streptococci, veillonellae, staphylococci, actinobacilli*, and yeasts are in the duodenum (pH 4-5). From here to the ileum, the density reaches 10^6-10^8 and finally at the colon and feaces the number of

bacteria reaches 10^{10}-10^{12}, being the anaerobes the most predominant.[57, 59-61]
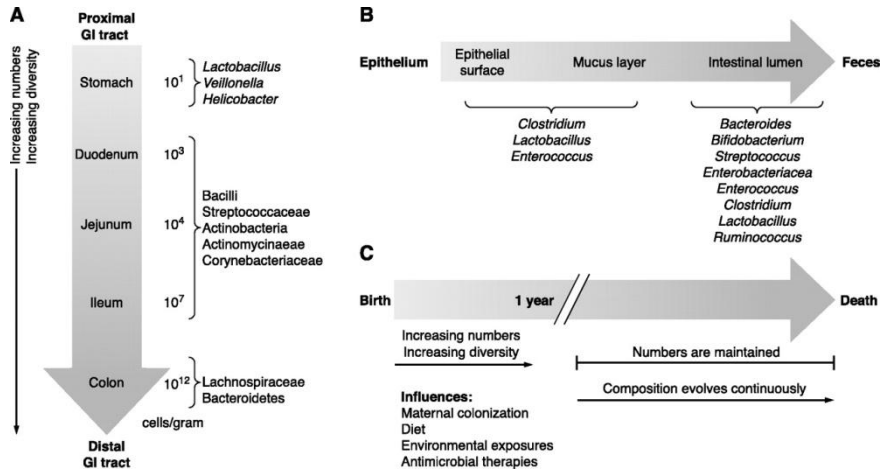
Figure 4. Spatial and temporal aspects of intestinal microbiota composition. A: variations in microbial numbers and composition across the length of the gastrointestinal tract. B: longitudinal variations in microbial composition in the intestine. C: temporal aspects of microbiota establishment and maintenance and factors influencing microbial composition. (From Sekirov, *et. al*)[62]

The high range of metabolic and biochemical activities developed by bacteria's combined genomas (also known as microbiome) makes possible to consider the gut microbiota as an additional organ with its own functions.[63-64] Each person has its own microbiota but the basic colonizers and genes are shared among individuals. People who shared their life together also share their microbiota composition and it is even shared with their pets' ones.[65]

Gut microbiota plays a principal role at metabolic, nutritional, physiological and immunological processes in the human body. For example, bacteria of the gut microbiota obtain energy from the

metabolism of non-digestible polysaccharides (impossible to metabolize by human's enzymes) to produce vital vitamins, amino-acids and/or short-chain fatty acids (SCFA); favour the differentiation of the host's intestinal epithelium and immune system; protect against pathogens by mechanisms such as colonisation resistance and production of antimicrobial compounds; and have a key role in tissue homeostasis (including the bone).[57, 59]

For the adequate performance of all of these functions, a correct beneficial relationship between both, the host and its microbiota, is needed. However, it can be altered, among others, by some aspects like the composition of the microbial community as well as by the host diet. Accordingly, the preservation of the beneficial interactions between the mutualistic organisms is a key requirement for health.

1.2.2.1 The natural microbiota and its role in health and disease

One of the main points under researching is the effect that the ability of the microbiota to metabolize non-digestible molecules might have in the host. As living organisms, microbes need to acquire energy to grow and reproduce. These processes take place in the colon whit the fermentation (saccharolytic fermentation) of carbohydrates, that have not been absorbed in the upper GI tract. The fermentation of polysaccharides (pectins, hemicelluloses, gums, insulin and resistant starches), oligosaccharides (raffinose, galactoligosaccharides and dextrins), sugars (non-absorbed lactose and non-absorbed fructose) and polyols (mannitol, lactitol and isomalt) produces SCFAs (acetic, propionic and butyric acids) and lactic acid (also converted to propionic and acetic

acid by microbes). SCFAs allow uptaking of water and salts and can also be a source of energy to the host when are absorbed. Butyric acid can impact growth and differentiation of epithelial colon cells. Some hydrogen gases are also produced in the fermentation products and these may contribute to the equilibrium of the microbiota.[66]

Microbes from the microbiota not only produce metabolites by the fermentation in the colon. In some others parts of the GI tract metabolites are also produced. Some of the main chemical metabolites production in which host microbiota is implied (including the ones from the saccharolytic fermentation) are described in Table 4.

Metabolites	Related bacteria	Potential biological functions
Short-chain fatty acids: acetate, propionate, butyrate, isobutyrate, 2-methylpropionate, valerate, isovalerate, hexanoate	Clostridial clusters IV and XIVa of Firmicutes, including species of *Eubacterium*, *Roseburia*, *Faecalibacterium*, and *Coprococcus*	Decreased colonic pH, inhibit the growth of pathogens; stimulate water and sodium absorption; participate in cholesterol synthesis; provide energy to the colonic epithelial cells, implicated in human obesity, insulin resistance and type 2 diabetes, colorectal cancer.
Bile acids: cholate, hyocholate, deoxycholate, chenodeoxycholate, etc.	*Lactobacillus*, *Bifidobacteria*, *Enterobacter*, *Bacteroides*, *Clostridium*	Absorb dietary fats and lipid-soluble vitamins, facilitate lipid absorption, maintain intestinal barrier function, signal systemic endocrine functions to regulate triglycerides, cholesterol, glucose and energy homeostasis.
Choline metabolites: methylamine, dimethylamine, trimethylamine, trimethylamine-*N*-oxide, dimethylglycine, betaine	*Faecalibacterium prausnitzii*, *Bifidobacterium*	Modulate lipid metabolism and glucose homeostasis. Involved in nonalcoholic fatty liver disease, dietary induced obesity, diabetes, and cardiovascular disease.
Phenolic, benzoyl, and phenyl derivatives: benzoic acid, hippuric acid, 4-cresol, 4-cresyl sulfate, 4-hydroxyphenylacetate, phenylacetate, etc.	*Clostridium difficile*, *F.prausnitzii*, *Bifidobacterium*, *Subdoligranulum*, *Lactobacillus*	Detoxification of xenobiotics; indicate gut microbial composition and activity; utilize polyphenols. Urinary hippuric acid may be a biomarker of hypertension and obesity in humans. Urinary 4-hydroxyphenylacetate, 4-cresol, and phenylacetate are elevated in colorectal cancer. Urinary 4-cresyl sulfate is elevated in children with severe autism.

Metabolites	Related bacteria	Potential biological functions
Indole derivatives: N-acetyltryptophan, indoleacetate, indoleacetylglycine (IAG), indole, indoxyl sulfate, indole-3-propionate, melatonin, melatonin 6-sulfate, serotonin, 5-hydroxyindole	*Clostridium sporogenes, E. coli*	Protect against stress-induced lesions in the GI tract; modulate expression of proinflammatory genes, increase expression of anti-inflammatory genes, strengthen epithelial cell barrier properties. Implicated in GI pathologies, brain-gut axis, and a few neurological conditions.
Vitamins: vitamin K, vitamin B12, biotin, folate, thiamine, riboflavin, pyridoxine	*Bifidobacterium*	Provide complementary endogenous sources of vitamins, strengthen immune function, exert epigenetic effects to regulate cell proliferation.
Polyamines: putrescine, cadaverine, spermidine, spermine	*Campylobacter jejuni, Clostridium saccharolyticum*	Exert genotoxic effects on the host, anti-inflammatory and antitumoral effects. Potential tumor markers.
Lipids: conjugated fatty acids, LPS, peptidoglycan, acylglycerols, sphingomyelin, cholesterol, phosphatidylcholines, phosphoethanolamines, triglycerides	*Bifidobacterium, Roseburia, Lactobacillus, Klebsiella,Enterobacter, Citrobacter, Clostridium*	Impact intestinal permeability, activate intestinebrain-liver neural axis to regulate glucose homeostasis; LPS induces chronic systemic inflammation; conjugated fatty acids improve hyperinsulinemia, enhance the immune system and alter lipoprotein profiles. Cholesterol is the basis for sterol and bile acid production.
Others: D-lactate, formate, methanol, ethanol, succinate, lysine, glucose, urea, α-ketoisovalerate, creatine, creatinine, endocannabinoids, 2-arachidonoylglycerol (2-AG), *N*-arachidonoylethanolamide, LPS, etc.	*Bacteroides, Pseudobutyrivibrio, Ruminococcus, Faecalibacterium, Subdoligranulum, Bifidobacterium, Atopobium, Firmicutes, Lactobacillus*	Direct or indirect synthesis or utilization of compounds or modulation of linked pathways including endocannabinoid system.

Table 4. Gut bacteria and the metabolites they contribute. (Modified from Nicholson, *et al.*)[67]

Probiotics and prebiotics

The aim of manipulate the gut microbiota to improve health is one of the main researching strategies nowadays. To reach it, several strategies can be applied, such as the incorporation of positive bacteria to the gut

or the administration of molecules that are well known to have a beneficial effect in the host.

The first one who proposed that some bacteria could be beneficial for human health was the Nobel prize winner Metchnikoff at the beginning of the twentieth century,[68] but it was not until some years later when the word *probiotics* was firstly used to refer to substances required for health. It exists numerous definitions for this concept, but the most widely accepted is that proposed by the FAO (Food and Agricultural Organization) and WHO (World Health Organization) in 2011: '*Live microorganisms which, when administered in adequate amounts, confer a health benefit on the host*'.[69] Probiotics are transient, but some of them belong to commensal typical species. Although some actions have been reported, the mechanism in which these microbes interact with the gut and which benefits have each of the different species to the host is something still under researching. For example, probiotics take part in pathogens action and adherence inhibition, intestinal epithelial cells tight junction reinforcement, availability of substrates for commensal bacterial growth or the interaction with immune system components.[70]

The *prebiotic* concept is much more modern, it appeared in 1995 when Gibson and Roberfroid defined a prebiotic as '*a nondigestible food ingredient that beneficially affects the host by selectively stimulating the growth and/or activity of one or a limited number of bacteria in the colon, and thus improves host health*'.[71] Although, this original definition has suffered from criticism and there is an absence of a consensus definition, some basic premises are in all the definitions. A substance that is considered to be a prebiotic must have a beneficial physiological effect or

improve host health, whereas not all the functional foods can be considered as prebiotics, only those whose benefits are mediated by modulation of the gut microbiota or by changes in the microbial community structure. Then, a prebiotic affects to host health by modulating its microbiota.[72] In this line, the FAO defined a prebiotic in 2008 as a *'nonviable food component that confers a health benefit on the host associated with modulation of the microbiota'*,[73] being this one the accepted definition by the EFSA (European Food Safety Authority) for the regulation of prebiotics in Europe.

The implication of prebiotics, probiotics or the combination of both (synbiotics) in human health is still under researching but many studies in animal models have shown important data. *Bifidobacterium, Lactobacillus, Propionibacterium* and *Eubacterium* bacteria have been described as probiotics and their effect is believed to be related with the production of metabolites when these bacteria take part in fermentation of carbohydrates. At the same time, prebiotics have been identified as the responsible of the increment of the *bifidobacteria* and *lactobacilli* proportion in the gut microbiota upon other groups of bacteria.[66]

In IBD (inflammatory bowel disease)[74] and IBS (irritable bowel syndrome)[75], probiotics and prebiotics have been checked under the idea of finding a treatment, however, results are not very clear. Although some probiotics seems to be effective, other are not. Even for the ones that have a good response more experiments are needed to determine the correct doses and strains.

Probiotics have also been tested to treat some affections related with brain.[76] The administration of probiotics in rats conducted to the reduction of dopamine and the normalization of depression-like behaviour (*B. longum* subsp. *infantis* str. 356244), anxiety normalization (*B. longum* str. NCC3001) and the prevention of stress-induced memory dysfunction (*Lactobacillus rhamnosus* str. R0011 and *Lactobacillus helveticus* str. R0052). However, these studies indicate that the response to probiotic or their fermentation products accumulation depends in the behavioural parameter under study and on the model used to perturb it.[77]

The mineral absorption is related with prebiotics. Contribution of prebiotics helps in calcium, magnesium, iron, selenium, copper, zinc and silver absorption and an increment in growth and skeletal mass in rats and human has been shown.[66] For instance, soluble corn fiber (SCF) has been determined as a prebiotic because of it contribution to calcium absorption increment.[78]

In addition, probiotics can restore the balanced microbiota in urogenital medicine, for example in the case of bacterial vaginosis, where an imbalance of the natural vaginal microbiota provokes an infection. They can even be preventive and the diary intake of product containing probiotics is recommended.[79]

Finally, the interest of prebiotic and probiotic and their potential to be applied in treatments, has made them be tested also for upper respiratory tract infection (URTI), in the reduction of infections and in allergic conditions (atopy, atopic eczema or allergic rhinitis). In all of

these cases promising results have appeared although further research is still needed.[66]

Knowing the mechanism of action of the gut microbiota could be a good alternative to understand how the beneficial role of prebiotics and probiotics is carried out, what molecules are the responsible and by which bacteria they are produced.

1.2.2.2 Which bacteria do make what?

Establishing biological links between bacteria and what they produce is not an easy process, but scientists are working on it. Several methods can be used. Sequencing methods can provide a DNA sequence reconstruction and study the ability of organisms to carry out metabolic functions. Nevertheless, they cannot define the functionality of particular bacteria under different environmental and complex conditions. In vitro experiments may be an alternative. Preparing different systems that mimic the gut, in which dietary residues such as carbohydrates, proteins and amino acids are the substrates, is a good strategy to isolate the metabolites produced. Then, using different microscopy and spectroscopy techniques, these metabolites are characterized and associated with their bacterial origin.[67]

A good example of this can be found in Chapter 4 of this work, where a molecule related with iron absorption was isolated and characterized by Magnetic Nuclear Resonance (MNR) from an in vitro *Lactobacillus fermentum* culture. Another example related to iron metabolism is the fact that bifidobacteria produce siderophores (molecules with high iron-affinity).[80] Furthermore, lactoferrin (LF) a globular protein with a high

affinity for iron, has been reported to have bifidogenic effects, that is, it is able to promote bifidobacteria growth, specially *Bifidobacterium bifidum*.[81]

In addition, other possible probiotics for minerals absorption have also been studied in vitro. For example, *Enterococcus durans* has been proposed as a good carrier for selenium to be used in feed trails, due to its ability to accumulate and incorporate large amounts of this mineral.[82]

It is important to take into account that in vitro models are not a perfect simulation of in vivo situation, however, useful information is obtained from these simulations, making easier further work in animals and human models.

1.3 *LACTOBACILLUS FERMENTUM*: FROM PROBIOTIC TO MATERIAL

Lactobacillus bacteria (genus *Lactobacillus*) are gram-positive, non-spore-forming and rod-shaped bacteria. They conform a major part of the lactic acid bacteria group, that is, they take part in the metabolism of sugars to produce lactic acid. More than 120 different species of this genus have been identified and they can be found in the human microbiota as well as in other body sites. For example, in women they can be found at the vaginal tract or breast milk.

One of their most known features is their ability to work as probiotics (as it has been described before) and their use in fermented food industry: milk, yogur, cheese, beer, cocoa, kefir, etc.

Moreover, lactobacilli present other properties that makes them useful for applications in materials science. Numerous species of lactobacillus have been tested as functional biomaterials under the use of green chemistry. The interest of using a probiotic bacteria goes further than the idea of making green chemistry to produce nanoparticles, these bacteria could be used as direct materials in the organism, both for diagnosis and therapy.

In the context of this thesis, we will describe several applications that have been reported for the *Lactobacillus fermentum* specie.

Firstly, materials containing these bacteria in food industry have been prepared. For example, it has been possible the encapsulation of *L. fermentum* in alginate-fenugreek gum-locust bean gum (AFL) matrix, which allows its viability preservation and toleration of GI.[83]

Another worrying issue in food industry, is the pathogens growth in food products. Antimicrobial and antibiotics compounds are daily used to avoid their growth. *L. fermentum* has been successfully identified as an alternative to these compound because it can be itself an antimicrobial system due to the secretion of substances out of its cell wall.[84] The substances secreted out could be related too with antioxidants properties[85-86] which are also good qualified in this industry. For example, this antioxidant capacity has been evaluated in the improvement of pork meat.[87] In addition, the antimicrobial activity of *L. fermentum* has also been tested in others areas such as fuel ethanol production, where the use of antibiotics is not possible.[88] A suggested mechanism for this activity has been described with the identification in a *L. fermentum*

culture, of a NADH-dependent d-lactate dehydrogenase (d-LDH) with high reducing activity to phenylpyruvate (PPA) to give phenyllactic acid (PLA), which is a novel antimicrobial compound.[89]

Our group has also been working with *L. fermentum*, concretely with the strain CECT5716, to generate new materials. This strain was isolated from breast milk and patented by Biosearch Life (WO 2004003235 A2).[90] Under the commercial name of HEREDITUM® LC40 has the EFSA and FDA licences, which guaranties its security.

The *L. fermentum* serves as a platform to arrange superparamagnetic nanoparticles of maghemite, giving rise to the first living magnet at room temperature so far reported.[91] These "artificial magnetic bacteria has been patented as a new iron supplement for iron deficiency anemy. In addition, these bacteria are able to reduced Au(III) to produce gold nanoparticles. Furthermore, following a combined approach a 'two-in-one' magneto-optical bacteria could be produced.[92]

Apart from the applications of these materials, understanding the chemical machinery of *L. fermentum* operating in these processes may be a good strategy for creating new materials for new applications.

Along this thesis, the knowledge of the chemical machinery of the *L. fermentum* has been used for different applications in different contexts: as sensor of metabolic activity of probiotics, as promoting agent of iron absorption and as platforms to produce gold aggregates of different optical properties.

1.4 OBJECTIVES

Through this work we have tried to explore specific aspects of the chemical machinery of probiotic bacteria that could serve as inspiration, either for the creation of new materials or for designing new diagnostic and therapy approaches of pathologies associated with the presence of these bacteria in our body.

This study has been focused on a probiotic bacterium, *Lactobacillus fermentum.* Lactobacilli are the most common natural bacterial strains of our body and are found not only in the digestive flora, but also in specific sites, such as skin, mouth, respiratory cavity and urogenital tract. Because of their importance and occurrence in our body, we thought that, focusing on this probiotic, the research approach that we intended to carry out in this work would be of high impact. Moreover, this approach could be extended in the future to other probiotics.

This work has had three specific objectives:

1. The study of the reducing capacity of *L. fermentum* in order to correlate its redox activity with its strength. Achieving this correlation would allow, on the one hand, to develop a test to evaluate the presence and activity level of this probiotic in specific sites of our body, and on the other hand, to develop a test to analyze the effect (positive or negative) of certain drugs on this healthy probiotic.

In this sense it is appropriate to point out that the destruction of the bacterial flora at the digestive level by the action of some drugs, such as antibiotics, gives rise to health problems. Therefore, the development of

a test to evaluate the action of drugs on *L. fermentum*, one of the most important bacteria of our flora, would be very useful in the understanding of the contraindications of these drugs.

Also, a large number of bacterial infections occur as a consequence of a weakening of the native and healthy bacterial flora in favor of an increase of pathological bacteria. Therefore, the development of a test that would allow measuring the decrease of *L. fermentum* activity, would be very useful for the early detection of these infections.

2. The isolation and identification of the bacterium metabolites related with the iron absorption in our body. As mentioned in the introduction, it is known that the presence of probiotics in the intestinal flora facilitates the absorption of iron and prevents the development of iron deficiencies and/or anemia. However, nowadays the relationship between the presence of probiotics and the iron absorption is still completely unknown. In this work we intend to identify which molecules excreted by *L. fermentum* may be involved in facilitating iron absorption. Determining this type of molecules and their mechanism of action would allow developing new approaches for the adequate supplementation of iron, a crucial aspect for health.

3. The isolation and identification of the EPS of this bacterium, and its use as a platform for the synthesis of nanomaterials. As discussed throughout along this thesis, the EPS have essential role in the bacterium. However, there are very few examples in the literature of rigorous characterization of EPS from probiotic bacteria. Likewise, we intend to use these EPS as a platform for the preparation of nanomaterials. In

particular, we aim to use the EPS surface to host gold nanoparticles. Since the optical properties of gold nanoparticles depend on their degree of aggregation, we plan to control the degree of aggregation and therefore the optical properties of these gold nanomaterials.

1.5 REFERENCES

1. Drexler, K. E., *Engines of Creation: The Coming Era of Nanotechnology*. Anchor Books: New York, 1986.

2. Callister, J., *Materials science and engineering : an introduction*. 7th ed.; John Wiley & Sons, Inc.: New York, 2007.

3. Mitchell, B. S., *An introduction to materials engineering and science for chemical and materials engineers*. John Wiley & Sons, Inc.: New Jersey, 2004.

4. Williams, D. F., On the nature of biomaterials. *Biomaterials* **2009,** *30* (30), 5897-5909.

5. Devadasu, V. R.; Bhardwaj, V.; Kumar, M. N. V. R., Can Controversial Nanotechnology Promise Drug Delivery? *Chemical Reviews* **2013,** *113* (3), 1686-1735.

6. Toumey, C., Plenty of room, plenty of history. *Nature Nanotechnology* **2009,** *4* (12), 783-784.

7. Riehemann, K.; Schneider, S. W.; Luger, T. A.; Godin, B.; Ferrari, M.; Fuchs, H., Nanomedicine – challenge and perspectives. *Angewandte Chemie (International ed. in English)* **2009,** *48* (5), 872-897.

8. Taniguchi, N., *Proceedings of the International Conference on Production Engineering: Tokyo, 1974; [held at the Prince Hotel, Tokyo, from August 26 to August 29, 1974]*. Japan Society of Precision Engineering: 1974.

9. Auffan, M.; Rose, J.; Bottero, J.-Y.; Lowry, G. V.; Jolivet, J.-P.; Wiesner, M. R., Towards a definition of inorganic nanoparticles from an environmental, health and safety perspective. *Nature Nanotechnology* **2009,** *4* (10), 634-641.

10. Kantor, L. W., NIH Roadmap for Medical Research. *Alcohol Research & Health* **2008,** *31* (1), 12-13.

11. Wu, J.; Li, Z., Applications of nanotechnology in biomedicine. *Chinese Science Bulletin* **2013,** *58* (35), 4515-4518.

12. Silva, G. A., Introduction to nanotechnology and its applications to medicine. *Surgical Neurology* **2004,** *61* (3), 216-220.

13. SCENIHR, The existing and proposed definitions relating to products of nanotechnologies. *European Commission* **2008**.

14. Chen, G.; Roy, I.; Yang, C.; Prasad, P. N., Nanochemistry and Nanomedicine for Nanoparticle-based Diagnostics and Therapy. *Chemical Reviews* **2016,** *116* (5), 2826-2885.

15. Ahmed, S.; Annu; Ikram, S.; Yudha S, S., Biosynthesis of gold nanoparticles: A green approach. *Journal of Photochemistry and Photobiology B: Biology* **2016,** *161*, 141-153.

16. Bansal, V.; Bharde, A.; Ramanathan, R.; Bhargava, S. K., Inorganic materials using 'unusual' microorganisms. *Advances in Colloid and Interface Science* **2012,** *179–182*, 150-168.

17. Beveridge, T. J.; Murray, R. G., Sites of metal deposition in the cell wall of Bacillus subtilis. *Journal of Bacteriology* **1980,** *141* (2), 876-87.

18. He, S.; Guo, Z.; Zhang, Y.; Zhang, S.; Wang, J.; Gu, N., Biosynthesis of gold nanoparticles using the bacteria Rhodopseudomonas capsulata. *Materials Letters* **2007,** *61* (18), 3984-3987.

19. Bharde, A.; Kulkarni, A.; Rao, M.; Prabhune, A.; Sastry, M., Bacterial Enzyme Mediated Biosynthesis of Gold Nanoparticles. *Journal of Nanoscience and Nanotechnology* **2007,** *7* (12), 4369-4377.

20. Klaus, T.; Joerger, R.; Olsson, E.; Granqvist, C.-G., Silver-based crystalline nanoparticles, microbially fabricated. *Proceedings of the National Academy of Sciences* **1999,** *96* (24), 13611-13614.

21. Silver, S., Bacterial silver resistance: molecular biology and uses and misuses of silver compounds. *FEMS Microbiology Reviews* **2003,** *27* (2-3), 341-53.

22. Ramanathan, R.; O'Mullane, A. P.; Parikh, R. Y.; Smooker, P. M.; Bhargava, S. K.; Bansal, V., Bacterial Kinetics-Controlled Shape-Directed Biosynthesis of Silver Nanoplates Using Morganella psychrotolerans. *Langmuir* **2011,** *27* (2), 714-719.

23. Lengke, M. F.; Fleet, M. E.; Southam, G., Synthesis of Platinum Nanoparticles by Reaction of Filamentous Cyanobacteria with Platinum(IV)–Chloride Complex. *Langmuir* **2006,** *22* (17), 7318-7323.

24. Yong, P.; Rowson, N. A.; Farr, J. P.; Harris, I. R.; Macaskie, L. E., Bioreduction and biocrystallization of palladium by Desulfovibrio desulfuricans NCIMB 8307. *Biotechnology and Bioengineering* **2002,** *80* (4), 369-79.

25. Murray, C. B.; Norris, D. J.; Bawendi, M. G., Synthesis and characterization of nearly monodisperse CdE (E = sulfur, selenium, tellurium) semiconductor nanocrystallites. *Journal of the American Chemical Society* **1993,** *115* (19), 8706-8715.

26. Bansal, V.; Jani, H.; Du Plessis, J.; Coloe, P. J.; Bhargava, S. K., Galvanic Replacement Reaction on Metal Films: A One-Step Approach to Create Nanoporous Surfaces for Catalysis. *Advanced Materials* **2008,** *20* (4), 717-723.

27. Raj, R.; Das, S., Development and application of anticancer fluorescent CdS nanoparticles enriched Lactobacillus bacteria as therapeutic microbots for human breast carcinoma. *Applied Microbiology and Biotechnology* **2017,** *101* (13), 5439-5451.

28. Suresh, A. K.; Pelletier, D. A.; Wang, W.; Broich, M. L.; Moon, J.-W.; Gu, B.; Allison, D. P.; Joy, D. C.; Phelps, T. J.; Doktycz, M. J., Biofabrication of discrete spherical gold nanoparticles using the metal-reducing bacterium Shewanella oneidensis. *Acta Biomaterialia* **2011,** *7* (5), 2148-2152.

29. Behin Omidi, S. J. H., Mansour Bayat, Kambiz Larijani, Biosynthesis of Silver Nanoparticles by Lactobacillus fermentum. *Bulletin of Environment, Pharmacology and Life Sciences* **2014,** *3* (12), 6.

30. Sintubin, L.; De Windt, W.; Dick, J.; Mast, J.; van der Ha, D.; Verstraete, W.; Boon, N., Lactic acid bacteria as reducing and capping agent for the fast and efficient production of silver nanoparticles. *Applied Microbiology and Biotechnology* **2009,** *84* (4), 741-749.

31. Adebayo-Tayo, B. C.; Popoola, A. O., Biogenic synthesis and antimicrobial activity of Silver nanoparticle using exopolysaccharides from Lactic Acid bacteria. *International Journal of Nano Dimension* **2017,** *8* (1), 61-69.

32. Costerton, J. W.; Lewandowski, Z.; Caldwell, D. E.; Korber, D. R.; Lappin-Scott, H. M., Microbial Biofilms. *Annual Review of Microbiology* **1995,** *49* (1), 711-745.

33. Moshynets, O. V.; Spiers, A. J., Viewing Biofilms within the Larger Context of Bacterial Aggregations. In *Microbial Biofilms - Importance and Applications*, Dhanasekaran, D.; Thajuddin, N., Eds. InTech: Rijeka, 2016; p Ch. 01.

34. Flemming, H.-C.; Wingender, J.; Szewzyk, U.; Steinberg, P.; Rice, S. A.; Kjelleberg, S., Biofilms: an emergent form of bacterial life. *Nature reviews. Microbiology* **2016,** *14* (9), 563-575.

35. Watnick, P., Kolter R., Biofilm, City of Microbes. *Journal of Bacteriology* **2000,** *182* (10), 4.

36. Davies, D. G.; Parsek, M. R.; Pearson, J. P.; Iglewski, B. H.; Costerton, J. W.; Greenberg, E. P., The Involvement of Cell-to-Cell Signals in the Development of a Bacterial Biofilm. *Science* **1998,** *280* (5361), 295-298.

37. Vlamakis, H.; Chai, Y.; Beauregard, P.; Losick, R.; Kolter, R., Sticking together: building a biofilm the Bacillus subtilis way. *Nature reviews. Microbiology* **2013,** *11* (3), 157-168.

38. Wingender, J.; Neu, T. R.; Flemming, H.-C., What are Bacterial Extracellular Polymeric Substances? In *Microbial Extracellular Polymeric Substances: Characterization, Structure and Function*, Wingender, J.; Neu, T. R.; Flemming, H.-C., Eds. Springer Berlin Heidelberg: Berlin, Heidelberg, 1999; pp 1-19.

39. Flemming, H.-C.; Wingender, J., The biofilm matrix. *Nature reviews. Microbiology* **2010,** *8*, 623.

40. Hans-Curt Flemming, T. R. N., Daniel J Wozniak, The EPS Matrix: The "House of Biofilm Cells". *Journal of Bacteriology* **2007,** *189* (22), 3.

41. Mayer, C.; Moritz, R.; Kirschner, C.; Borchard, W.; Maibaum, R.; Wingender, J.; Flemming, H.-C., The role of intermolecular interactions: studies on model systems for bacterial biofilms. *International Journal of Biological Macromolecules* **1999,** *26* (1), 3-16.

42. Neu, T. R.; Lawrence, J. R., In Situ Characterization of Extracellular Polymeric Substances (EPS) in Biofilm Systems. In *Microbial Extracellular Polymeric Substances: Characterization, Structure and Function*, Wingender, J.; Neu, T. R.; Flemming, H.-C., Eds. Springer Berlin Heidelberg: Berlin, Heidelberg, 1999; pp 21-47.

43. Pan, M.; Zhu, L.; Chen, L.; Qiu, Y.; Wang, J., *Detection Techniques for Extracellular Polymeric Substances in Biofilms: A Review*. 2016; Vol. 11.

44. James, S. A.; Powell, L. C.; Wright, C. J., Atomic Force Microscopy of Biofilms: Imaging, Interactions, and Mechanics. In *Microbial Biofilms - Importance and Applications*, Dhanasekaran, D.; Thajuddin, N., Eds. InTech: Rijeka, 2016; p Ch. 06.

45. Haisch, C.; Niessner, R., Visualisation of transient processes in biofilms by optical coherence tomography. *Water Research* **2007,** *41* (11), 2467-72.

46. Xi, C.; Marks, D.; Schlachter, S.; Luo, W.; Boppart, S. A., High-resolution three-dimensional imaging of biofilm development using optical coherence tomography. *Journal of Biomedical Optics* **2006,** *11* (3), 34001.

47. Shen, Y. R., A few selected applications of surface nonlinear optical spectroscopy. *Proceedings of the National Academy of Sciences of the United States of America* **1996,** *93* (22), 12104-12111.

48. Morita, A.; Hynes, J. T., A theoretical analysis of the sum frequency generation spectrum of the water surface. *Chemical Physics* **2000,** *258* (2), 371-390.

49. Howell, C.; Diesner, M.-O.; Grunze, M.; Koelsch, P., Probing the Extracellular Matrix with Sum-Frequency-Generation Spectroscopy. *Langmuir* **2008,** *24* (24), 13819-13821.

50. de la Fuente-Núñez, C.; Reffuveille, F.; Fernández, L.; Hancock, R. E. W., Bacterial biofilm development as a multicellular adaptation: antibiotic resistance and new therapeutic strategies. *Current Opinion in Microbiology* **2013,** *16* (5), 580-589.

51. Römling, U.; Kjelleberg, S.; Normark, S.; Nyman, L.; Uhlin, B. E.; Åkerlund, B., Microbial biofilm formation: a need to act. *Journal of Internal Medicine* **2014,** *276* (2), 98-110.

52. Moscovici, M., Present and future medical applications of microbial exopolysaccharides. Frontiers in Microbiology 2015, 6 (1012).

53. Freitas, F.; Alves, V. D.; Reis, M. A., Advances in bacterial exopolysaccharides: from production to biotechnological applications. *Trends in Biotechnology* **2011,** *29* (8), 388-98.

54. Sutapa Biswas Majee, D. A., Gopa Roy Biswas, Rheological Behavior and Pharmaceutical Applications of BacterialExopolysaccharides. Journal of Applied Pharmaceutical Science 2017, 7 (9), 224-232.

55. Freitas, F.; Alves, V. D.; Pais, J.; Costa, N.; Oliveira, C.; Mafra, L.; Hilliou, L.; Oliveira, R.; Reis, M. A. M., Characterization of an extracellular polysaccharide produced by a Pseudomonas strain grown on glycerol. *Bioresource Technology* **2009,** *100* (2), 859-865.

56. Freitas, F.; Alves, V. D.; Torres, C. A. V.; Cruz, M.; Sousa, I.; Melo, M. J.; Ramos, A. M.; Reis, M. A. M., Fucose-containing exopolysaccharide produced by the newly isolated Enterobacter strain A47 DSM 23139. *Carbohydrate Polymers* **2011,** *83* (1), 159-165.

57. Sommer, F.; Backhed, F., The gut microbiota - masters of host development and physiology. *Nature reviews. Microbiology* **2013,** *11* (4), 227-238.

58. Savage, D. C., Microbial Ecology of the Gastrointestinal Tract. *Annual Review of Microbiology* **1977,** *31* (1), 107-133.

59. Gerritsen, J.; Smidt, H.; Rijkers, G. T.; de Vos, W. M., Intestinal microbiota in human health and disease: the impact of probiotics. *Genes & Nutrition* **2011,** *6* (3), 209-240.

60. O'May, G. A.; Reynolds, N.; Macfarlane, G. T., Effect of pH on an In Vitro Model of Gastric Microbiota in Enteral Nutrition Patients. *Applied and Environmental Microbiology* **2005,** *71* (8), 4777-4783.

61. Chuan-Sheng Lin, C. J. C., Chia-Chen Lu, Jan Martel, David M. Ojcius, Yun-Fei Ko, John D. Young, Hsin-Chih Lai, Impact of the Gut Microbiota, Prebiotics, and Probiotics on Human Health and Disease. *Biomedical journal* **2014,** *37*, 9.

62. Sekirov, I.; Russell, S. L.; Antunes, L. C. M.; Finlay, B. B., Gut Microbiota in Health and Disease. *Physiological Reviews* **2010,** *90* (3), 859-904.

63. Umu, Ö. C. O.; Oostindjer, M.; Pope, P. B.; Svihus, B.; Egelandsdal, B.; Nes, I. F.; Diep, D. B., Potential applications of gut microbiota to control human physiology. *Antonie van Leeuwenhoek* **2013,** *104* (5), 609-618.

64. Gill, S. R.; Pop, M.; DeBoy, R. T.; Eckburg, P. B.; Turnbaugh, P. J.; Samuel, B. S.; Gordon, J. I.; Relman, D. A.; Fraser-Liggett, C. M.; Nelson, K. E., Metagenomic Analysis of the Human Distal Gut Microbiome. *Science (New York, N.Y.)* **2006,** *312* (5778), 1355-1359.

65. Peccia, J.; Kwan, S. E., Buildings, Beneficial Microbes, and Health. *Trends in microbiology 24* (8), 595-597.

66. Binns, N., *Probiotics, Prebiotics and the Gut Microbiota*. ILSI Europe: 2013.

67. Nicholson, J. K.; Holmes, E.; Kinross, J.; Burcelin, R.; Gibson, G.; Jia, W.; Pettersson, S., Host-Gut Microbiota Metabolic Interactions. *Science* **2012,** *336* (6086), 1262.

68. Metchnikoff, I. I., *The Prolongation of Life: Optimistic Studies*. Springer Publishing Company: 2004.

69. Food; Nations, A. O. o. t. U.; Organization, W. H., *Probiotics in Food: Health and Nutritional Properties and Guidelines for Evaluation*. Food and Agriculture Organization of the United Nations: 2006.

70. Sanders, M. E., Impact of Probiotics on Colonizing Microbiota of the Gut. *Journal of Clinical Gastroenterology* **2011,** *45*, S115-S119.

71. Gibson, G. R.; Roberfroid, M. B., Dietary Modulation of the Human Colonic Microbiota: Introducing the Concept of Prebiotics. *The Journal of Nutrition* **1995,** *125* (6), 1401-1412.

72. Hutkins, R. W.; Krumbeck, J. A.; Bindels, L. B.; Cani, P. D.; Fahey, G.; Goh, Y. J.; Hamaker, B.; Martens, E. C.; Mills, D. A.; Rastal, R. A.; Vaughan, E.; Sanders, M. E., Prebiotics: why definitions matter. *Current Opinion in Biotechnology* **2016,** *37* (Supplement C), 1-7.

73. Pineiro, M.; Asp, N.-G.; Reid, G.; Macfarlane, S.; Morelli, L.; Brunser, O.; Tuohy, K., FAO Technical Meeting on Prebiotics. *Journal of Clinical Gastroenterology* **2008,** *42*, S156-S159.

74. Shanahan, F., Editorial: probiotics in inflammatory bowel disease—wrong organisms, wrong disease, or flawed concepts? *Alimentary Pharmacology & Therapeutics* **2017,** *46* (6), 632-633.

75. Dimidi, E.; Rossi, M.; Whelan, K., Irritable bowel syndrome and diet: where are we in 2018? *Current Opinion in Clinical Nutrition & Metabolic Care* **2017,** *20* (6), 456-463.

76. Fung, T. C.; Olson, C. A.; Hsiao, E. Y., Interactions between the microbiota, immune and nervous systems in health and disease. *Nature Neuroscience* **2017,** *20* (2), 145-155.

77. Collins, S. M.; Surette, M.; Bercik, P., The interplay between the intestinal microbiota and the brain. *Nature reviews. Microbiology* **2012,** *10* (11), 735-742.

78. Skrypnik, K., Suliburska, J. , Association between the gut microbiota and mineral metabolism. *Journal of the Science of Food and Agriculture* **2017**.

79. Homayouni, A.; Bastani, P.; Ziyadi, S.; Mohammad-Alizadeh-Charandabi, S.; Ghalibaf, M.; Mortazavian, A. M.; Mehrabany, E. V., Effects of Probiotics on the Recurrence of Bacterial Vaginosis: A Review. *Journal of Lower Genital Tract Disease* **2014,** *18* (1), 79-86.

80. Vazquez-Gutierrez, P.; Lacroix, C.; Jaeggi, T.; Zeder, C.; Zimmerman, M. B.; Chassard, C., Bifidobacteria strains isolated from stools of iron deficient infants can efficiently sequester iron. *BMC Microbiology* **2015,** *15* (1), 3.

81. Oda, H.; Wakabayashi, H.; Yamauchi, K.; Abe, F., Lactoferrin and bifidobacteria. *BioMetals* **2014,** *27* (5), 915-922.

82. Pieniz, S.; Andreazza, R.; Mann, M. B.; Camargo, F.; Brandelli, A., Bioaccumulation and distribution of selenium in Enterococcus durans. *Journal of Trace Elements in Medicine and Biology* **2017,** *40* (Supplement C), 37-45.

83. Damodharan, K.; Palaniyandi, S. A.; Yang, S. H.; Suh, J. W., Co-encapsulation of lactic acid bacteria and prebiotic with alginate-fenugreek gum-locust bean gum matrix: Viability of encapsulated bacteria under simulated gastrointestinal condition and during storage time. *Biotechnology and Bioprocess Engineering* **2017,** *22* (3), 265-271.

84. Karami, S.; Roayaei, M.; Zahedi, E.; Bahmani, M.; Mahmoodnia, L.; Hamzavi, H.; Rafieian-Kopaei, M., Antifungal effects of Lactobacillus species isolated from local dairy products. *International Journal of Pharmaceutical Investigation* **2017,** *7* (2), 77-81.

85. Persichetti, E.; De Michele, A.; Codini, M.; Traina, G., Antioxidative capacity of Lactobacillus fermentum LF31 evaluated in vitro by oxygen radical absorbance capacity assay. *Nutrition* **2014,** *30* (7), 936-938.

86. Pourramezan, Z.; Kasra Kermanshahi, R.; Oloomi, M.; Aliahmadi, A.; Rezadoost, H., In vitro study of antioxidant and antibacterial activities of Lactobacillus probiotic spp. *Folia Microbiologica* **2017**.

87. Wang, A. N.; Yi, X. W.; Yu, H. F.; Dong, B.; Qiao, S. Y., Free radical scavenging activity of Lactobacillus fermentum in vitro and its antioxidative effect on growing–finishing pigs. *Journal of Applied Microbiology* **2009,** *107* (4), 1140-1148.

88. Rich, J. O.; Bischoff, K. M.; Leathers, T. D.; Anderson, A. M.; Liu, S.; Skory, C. D., Resolving bacterial contamination of fuel ethanol fermentations with beneficial bacteria – An alternative to antibiotic treatment. *Bioresource Technology* **2017,** *247* (Supplement C), 357-362.

89. Chen, L.; Bai, Y.; Fan, T.-P.; Zheng, X.; Cai, Y., Characterization of a d-Lactate Dehydrogenase from Lactobacillus fermentum JN248 with High Phenylpyruvate Reductive Activity. *Journal of Food Science* **2017,** *82* (10), 2269-2275.

90. Xaus, P. J.; Martin, J. R.; Rodriguez, G. J. M.; Boza, P. J.; JIMENEZ, L. J., Probiotic strains, a process for the selection of them, compositions thereof, and their use. Google Patents: 2004.

91. Martín, M.; Carmona, F.; Cuesta, R.; Rondón, D.; Gálvez, N.; Domínguez-Vera, J. M., Artificial Magnetic Bacteria: Living Magnets at Room Temperature. *Advanced Functional Materials* **2014,** *24* (23), 3489-3493.

92. Carmona, F.; Martín, M.; Gálvez, N.; Dominguez-Vera, J. M., Bioinspired Magneto-optical Bacteria. *Inorganic chemistry* **2014,** *53* (16), 8565-8569.
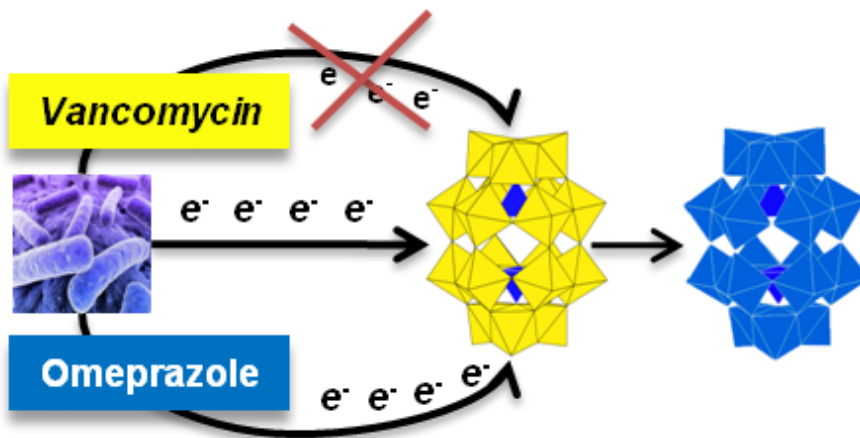
CHAPTER 2.

ELECTROCHROMIC POLYOXOMETALATE MATERIAL AS A SENSOR OF BACTERIAL ACTIVITY

2.1 INTRODUCTION

Polyoxometalates (POMs) have attracted a lot of attention due to their applications in diverse fields such as catalysis, biomedicine and materials science.[1-10] Their structures can be described as molecular fragments of close-packed metal oxides with the general formula $[X_xM_mO_y]^{n-}$ (where M = Mo, W, V, *etc*. and X = P, Si, As, *etc*.).[11]

One of the most important properties of POMs, which gives rise to their main applications, is their ability to accept electrons yielding mixed-valence species. This ability means POMs are very good electrochromic materials. A living organism can be an electron donor for a POM, and this is of paramount interest because in such a case switching of the chromic properties of the POM can be directly related to a certain biological activity, i.e., to life itself.

Some microorganisms are known for their ability to reduce metal cations, which has been exploited for the eco-friendly synthesis of zero-valent metal nanoparticles.[12-17] However, this property has not been exploited in other fields beyond the preparation of nanoparticles.

We want to open a new avenue: since the properties of metallic materials depend on the oxidation states of metal cations present in the structure, the possibility of using living organisms to reduce the metal cations in certain materials offers promising routes to develop new protocols for measuring their biological activity and to be used as a tool to establish an *ex vivo* experimental framework for testing the effect of certain drugs on the metabolism of the microorganisms. Detection and

determination of bacterial activity are often performed in reference to toxic bacteria. However, the determination of healthy bacteria in some biological fluids and, in particular, the study of how some drugs can affect this healthy function are also of interest.

An approach based on switching of the electrochromic properties of a material in order to the monitor cell metabolism has been developed for the first time. We have studied how *Lactobacillus fermentum* is capable of acting as an electron donor for the electrochromic POM $[P_2Mo^{VI}_{18}O_{62}]^{6-}$. It is well known that this probiotic bacterium has a positive effect on the maintenance of human health since it constitutes part of our natural microbiota, thus playing an important role in promoting the immune system activity, defence against infections and anti-inflammatory properties. This protocol can be extended to the observation of other reducing bacteria.

As the reductive ability of *L. fermentum* correlates directly to its bacterial activity (synthesis and secretion of extracellular reducing molecules), the protocol is useful for *ex vivo* screening to measure how specific drugs can affect the activity of the bacterium. Thus, the influence of the antibiotic vancomycin and the proton pump inhibitor omeprazole on the activity of this bacterium have been evaluated by simply monitoring the reductive power of *L. fermentum* with respect to $[P_2Mo^{VI}_{18}O_{62}]^{6-}$ in the presence of these drugs.

The electrochromic POM $[P_2Mo^{VI}_{18}O_{62}]^{6-}$ has been used to assess the activity of the bacterium *L. fermentum*. This POM is reduced by the addition of various specific number of electrons, leading to a family of

mixed-valence $Mo^{VI}Mo^V$ species with a characteristic deep blue colour ("heteropoly blues"), which are easily detected by UV-vis spectroscopy.[18-19]

2.2 RESULTS AND DISCUSSION

As shown in Figure 1, upon incubating $[P_2Mo^{VI}_{18}O_{62}]^{6-}$ in a culture of *L. fermentum*, a large band centred at 800 nm gradually develops, which confirms that the POM is reduced by the bacterium. It means that the redox capacity of the bacterium is at least higher than 0.5 V *vs*. SCE, which is the potential at which $[P_2Mo^{VI}_{18}O_{62}]^{6-}$ is reduced.[20]

Interestingly, the reductive power of *L. fermentum* is at its greatest under optimal bacterial proliferation conditions. A correlation between the biological strength and reductive power of the bacterium is evident: the stronger the metabolic strength of the bacterium, the greater is its reducing capacity.

Furthermore, when a culture of *L. fermentum* is exposed to UV light, its capacity to reduce $[P_2Mo^{VI}_{18}O_{62}]^{6-}$ decreases with time until it practically disappears (Figure 1b). The damage and death caused by radiation have implications on the reducing capacity of the bacterial colony, measured in terms of viability. Therefore, the measurement of *L. fermentum's* capacity to reduce $[P_2Mo^{VI}_{18}O_{62}]^{6-}$ is a direct evaluation of its metabolism strength.
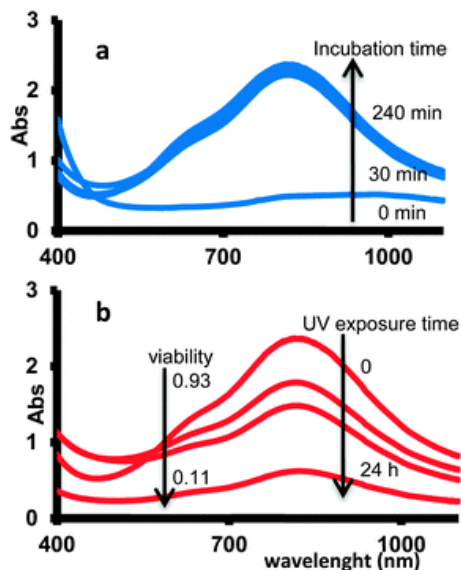
Figure 1. (a) UV-vis spectra of supernatant solution obtained after incubation of *L. fermentum* with $[P_2Mo^{VI}_{18}O_{62}]^{6-}$. The band at 800 nm increases with the incubation time. (b) UV-vis spectra of supernatant solution obtained after incubation of *L. fermentum* previously exposed to UV light with $[P_2Mo^{VI}_{18}O_{62}]^{6-}$. The band at 800 nm decreases with the UV exposure time. Likewise, values of viability, measured as the ratio between live and dead bacteria, also decrease. The weaker the metabolic strength of bacteria, the smaller is the UV-vis band at 800 nm.

On the other hand, when the reduction of $[P_2Mo^{VI}_{18}O_{62}]^{6-}$ was tested in the absence of the bacterium, but in the presence of the extracellular supernatant solution generated by the cultivated bacterium, $[P_2Mo^{VI}_{18}O_{62}]^{6-}$ was still reduced. From these observations, it can be concluded that $[P_2Mo^{VI}_{18}O_{62}]^{6-}$ is reduced with the aid of extracellular bacterial reducing agents, while the observations also suggest the existence of a chemical site for binding $[P_2Mo^{VI}_{18}O_{62}]^{6-}$ to the external surface of the bacterium, as occurs with other metalates. In this sense, Yamase *et al.*,[21] who were the first to observe the reduction of POMs by living organisms, concluded that reduction of some POMs by *Staphylococcus aureus* proceeds within cells, at the cytoplasmic

membrane. However, in contrast to this, in *L. fermentum*, the reduction takes place at the extracellular level as demonstrated by the fact that the supernatant solution, containing secreted reducing-molecules, is also capable of reducing $[P_2Mo^{VI}_{18}O_{62}]^{6-}$ and corroborated by transmission electron microscopy (TEM) images, which show reduced $[P_2Mo^{VI}_{18}O_{62}]^{6-}$ both associated and non-associated with the bacterium (Figure 2).
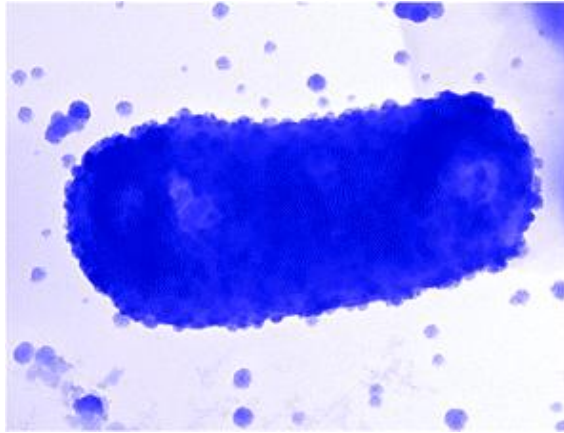
Figure 2. TEM micrograph showing the presence of POM particles on the external surface of the bacterium and outside.

TEM studies of *L. fermentum* after incubation with $[P_2Mo^{VI}_{18}O_{62}]^{6-}$ demonstrated the rod morphology typical of the *Lactobacillus* genus with large accumulations of nanoparticles on the external surface of the bacterium and outside (Figure 2).

The existence of large particles surrounding the bacterium is especially well visualized by high-angle annular dark field-scanning transmission electron microscopy (HAADF-STEM). As shown in Figure 3, the bacterium

contains bright spherical particles of heterogeneous size distributions, between 20 and 100 nm.
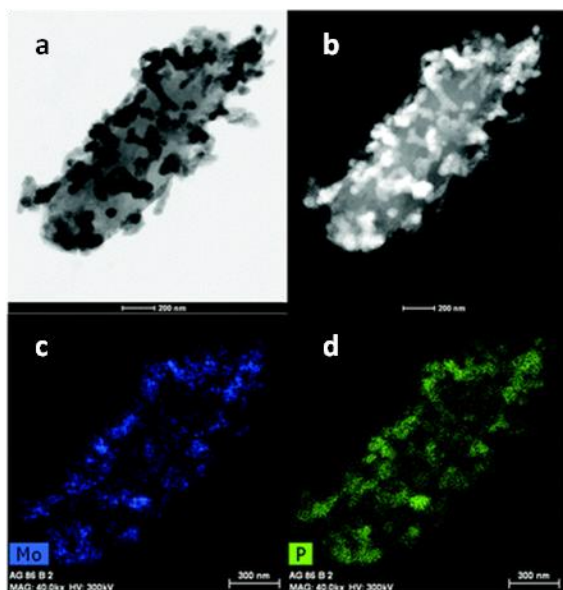
Figure 3. (a) TEM micrograph showing the presence of particles on the external surface of the bacterium. (b) The HAADF-STEM micrograph of a single bacterium. (c and d) EDX compositional maps of Mo (blue) and P (green) collected over the whole HAADF-STEM image in (b).

To confirm the presence of the reduced POM around the bacterium, energy dispersive X-ray spectroscopy (EDX) experiments were performed. The results revealed the juxtaposition of molybdenum (in blue), phosphorous (in green) and the bacterial platform (Figure 3). The particles do not seem to be confined at a specific bacterial site but associated with the broad biofilm, which is typical of *L. fermentum*.[22-23]

As the biological strength of *L. fermentum* correlates with its reducing capacity, the methodology we have developed based on the monitoring of the reduction of $[P_2Mo^{VI}_{18}O_{62}]^{6-}$ serves to analyse how specific drugs

can affect the activity of *L. fermentum*: the more damage the drug causes to the bacterium, the lower the reducing ability of the bacterium. This methodology is therefore useful for screening how some molecules impair *L. fermentum* activity. This is of interest in the context of an improved understanding of the side effects some drugs have on gut flora, of which *L. fermentum* is one of the main components.

Accordingly, we have evaluated the effect of vancomycin and omeprazole on the reducing capacity of *L. fermentum*. Both drugs are on the World Health Organization's list of essential medicines, the most important medications required by a basic health system. Vancomycin is an antibiotic used in the treatment of numerous bacterial infections. Orally administered vancomycin is indicated for intestinal infections. Omeprazole is a proton pump inhibitor used in the treatment of gastro-intestinal pathologies. There is some controversy for both vancomycin and omeprazole regarding the existence of side effects on the gut flora.

Experiments employing *L. fermentum* to reduce $[P_2Mo^{VI}_{18}O_{62}]^{6-}$ were carried out in the presence of vancomycin or omeprazole. The effect on the reductive activity of the bacterium was monitored by observing the increase or decrease in the UV-vis absorbance band centred at 800 nm corresponding to the reduced forms of $[P_2Mo^{VI}_{18}O_{62}]^{6-}$. As shown in Figure 4, the presence of vancomycin drastically affects the reducing power of *L. fermentum*. Thus, even in the presence of just millimolar concentrations of vancomycin, the reductive ability of the bacterium is almost negligible.

However, the presence of omeprazole does not seem to affect the ability of *L. fermentum* to reduce the POM $[P_2Mo^{VI}_{18}O_{62}]^{6-}$, since the large band in the UV-vis spectrum that represents the reduced forms barely changes, even at high concentrations of omeprazole (Figure 4).
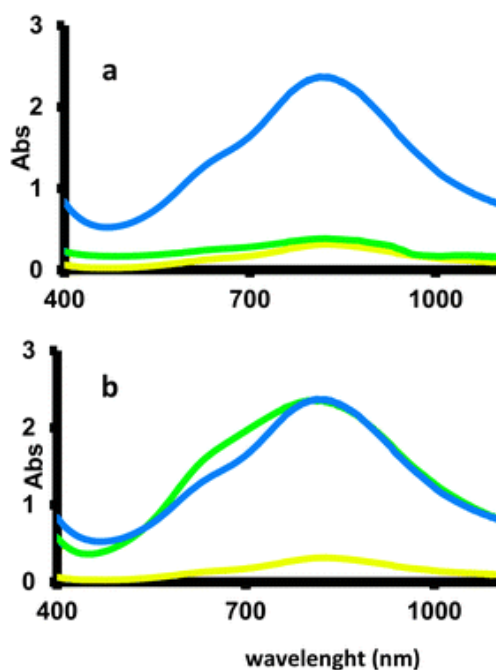
Figure 4. (a) UV-vis spectrum for the reduction of $[P_2Mo^{VI}_{18}O_{62}]^{6-}$ by *L. fermentum* in the presence of vancomycin (green spectrum). Controls for the no reduction of $[P_2Mo^{VI}_{18}O_{62}]^{6-}$ by vancomycin (yellow spectrum) as well as reduction of $[P_2Mo^{VI}_{18}O_{62}]^{6-}$ by *L. fermentum* in the absence of vancomycin (blue line) are shown for comparison. Note that in the presence of vancomycin, *L. fermentum* loses its capacity of reducing $[P_2Mo^{VI}_{18}O_{62}]^{6-}$ (green spectrum). (b) UV-vis spectra for the reduction of $[P_2Mo^{VI}_{18}O_{62}]^{6-}$ by *L. fermentum* in the presence of omeprazole (green spectrum). Controls for the no reduction of $[P_2Mo^{VI}_{18}O_{62}]^{6-}$ by omeprazole (yellow spectrum) as well as reduction of $[P_2Mo^{VI}_{18}O_{62}]^{6-}$ by *L. fermentum* in the absence of omeprazole (blue line) are shown for comparison. Note that in the presence of omeprazole, *L. fermentum* does not lose its capacity of reducing $[P_2Mo^{VI}_{18}O_{62}]^{6-}$ (green spectrum).

2.3 CONCLUSIONS

In conclusion, *L. fermentum* acts as an electron donor for the electrochromic POM $[P_2Mo^{VI}_{18}O_{62}]^{6-}$. The method developed in this study can be used to measure *L. fermentum* activity and to characterise its behaviour in the presence of certain drugs, such as the antibiotic vancomycin and the proton-pump inhibitor omeprazole. Thus, by using this method we have concluded that the antibiotic vancomycin severely affects the bacterial activity of *L. fermentum*, whereas omeprazole does not. This protocol can be extended to the characterisation of other metal-reducing bacteria (with either negative or positive effects on human health) in the field of medical analysis. In this sense, the future prospect of this work is to create new nano-devices based on the approach and methodology described in this communication for screening the *ex vivo* activity of new antibacterial materials.

2.4 EXPERIMENTAL SECTION

POM synthesis

$Na_6[P_2Mo^{VI}_{18}O_{62}]\cdot(H_2O)_{24}$ was synthesized as reported in the literature.[24] The purity of the compound was confirmed by the IR spectrum, which showed the characteristic bands of the polyanion. IR (KBr pellet, cm^{-1}): 1078 (*v* P–O, *vs.*), 941 (*v* Mo=O, *vs.*), 906 (*v* Mo–O–Mo, w), 778 (*v* Mo–O–Mo, *vs.*).

Bacteria growth

L. fermentum bacteria were grown in anaerobiosis conditions in a synthetic medium at 37 °C with orbital agitation for 24 h in an initial concentration of 1 mg bacteria in 1 mL of medium. The synthetic medium consisted of (g L^{-1}) Na_2HPO_4 – 5.0, KH_2PO_4 – 6.0, tris-ammonium citrate – 2.0, sucrose – 50.0, $MgSO_4$ – 1.0 and trace elements solution – 10 ml (consisting of (g L^{-1}): $MnSO_4$ – 2.0, $CoCl_2$ – 1.0, $ZnCl_2$ – 1.0 dissolved in 0.1 N HCl solution). The medium with an initial pH 6.7 was sterilized at 121 °C. The final *L. fermentum* cell concentration was 3.3×10^8 CFU mL^{-1}, which was used for all the experiments.

POM reduction by the bacterium

100 µL of a 10 mM stock solution of $[P_2Mo^{VI}_{18}O_{62}]^{6-}$ was added to 900 µL of *L. fermentum* culture to obtain a final concentration of 1 mM of $[P_2Mo^{VI}_{18}O_{62}]^{6-}$. Bacteria with POM were incubated for 24 h and then centrifuged. *L. fermentum's* ability to reduce the POM was measured at 30, 60, 240 and 1440 min of incubation by UV-vis spectroscopy through the apparition of a band centred at 800 nm due to reduced POM forms. A control of culture media with no bacteria reductive activity was included.

L. fermentum culture exposed to UV light

3 bacteria culture aliquots of 900 µL were exposed to UV light for 60, 240 and 1440 min before the incubation at 37 °C. After UV exposition, the cultures were incubated for 24 h at 37 °C with orbital agitation and then 100 µL of a 10 mM stock solution of [P2MoVI18O62]6- was added. After centrifugation, the reductive activity was measured by the UV-vis

absorbance band centred at 800 nm of the supernatant solution. A control of no UV light exposed culture was included.

Viability of the bacterial colony was defined as the ratio between live and dead bacteria, measured by flow cytometry. Values of 0.93, 0.70, 0.63 and 0.11 were obtained from the different UV exposed experiments at 0, 60, 240 and 1440 min.

Vancomycin and omeprazole effect on the reducing capacity

Vancomycin and omeprazole in a final concentration of 0.2 mg mL^{-1} were added to two independent cultures. The cultures were incubated for 24 h at 37 °C with orbital agitation and then 100 µL of a 10 mM stock solution of $[P_2Mo^{VI}_{18}O_{62}]^{6-}$ was added. The reductive activity in the presence of each drug was measured at 4 h by the UV-vis absorbance band centred at 800 nm at the supernatant solution obtained after centrifugation. Controls for the reduction of $[P_2Mo^{VI}_{18}O_{62}]^{6-}$ by *L. fermentum* with no drugs and reduction of $[P_2Mo^{VI}_{18}O_{62}]^{6-}$ by the drugs with no bacteria were included.

Viability values corroborated the effect of each drug of *L. fermentum*. Thus, almost null viability (0.07) was obtained for the experiment done in the presence of vancomycin whereas a value close to the control (in the absence of drug) was obtained for the experiment done in the presence of omeprazole (0.91).

Electronic microscopy

For TEM grid preparation a drop of *L. fermentum* after incubation with $[P_2Mo^{VI}_{18}O_{62}]^{6-}$ was placed onto a carbon-coated Cu grid (200 mesh) and was blotted with filter paper. Samples were observed under a FEI TITAN G2 microscope and HAADF-STEM and EDX map were done using the same equipment.

2.5 REFERENCES

1. Pope, M. T.; Müller, A., Polyoxometalate Chemistry: An Old Field with New Dimensions in Several Disciplines. Angewandte Chemie International Edition 1991, 30 (1), 34-48.

2. Mizuno, N.; Misono, M., Heterogeneous Catalysis. Chemical Reviews 1998, 98 (1), 199-218.

3. Omwoma, S.; Chen, W.; Tsunashima, R.; Song, Y.-F., Recent advances on polyoxometalates intercalated layered double hydroxides: From synthetic approaches to functional material applications. Coordination Chemistry Reviews 2014, 258, 58-71.

4. Vazylyev, M.; Sloboda-Rozner, D.; Haimov, A.; Maayan, G.; Neumann, R., Strategies for oxidation catalyzed by polyoxometalates at the interface of homogeneous and heterogeneous catalysis. Topics in Catalysis 2005, 34 (1), 93-99.

5. Yamase, T., Polyoxometalates Active Against Tumors, Viruses, and Bacteria. In Biomedical Inorganic Polymers: Bioactivity and Applications of Natural and Synthetic Polymeric Inorganic Molecules, Müller, W. E. G.; Wang, X.; Schröder, H. C., Eds. Springer Berlin Heidelberg: Berlin, Heidelberg, 2013; pp 65-116.

6. Hasenknopf, B., Polyoxometalates: introduction to a class of inorganic compounds and their biomedical applications. Frontier in Bioscience 2005, 10, 8.

7. Neumann, R., Applications of polyoxometalates in homogeneous catalysis. NATO Sci. Ser., II 2003, 98, 327.

8. Katsoulis, D. E., A Survey of Applications of Polyoxometalates. Chemical Reviews 1998, 98 (1), 359-388.

9. Clemente-Juan, J. M.; Coronado, E.; Gaita-Arino, A., Magnetic polyoxometalates: from molecular magnetism to molecular spintronics and quantum computing. Chemical Society Reviews 2012, 41 (22), 7464-7478.

10. Coronado, E.; Giménez-Saiz, C.; Gómez-García, C. J., Recent advances in polyoxometalate-containing molecular conductors. Coordination Chemistry Reviews 2005, 249 (17), 1776-1796.

11. Pope, M., Heteropoly and Isopoly Oxometalates. 1 ed.; Springer-Verlag Berlin Heidelberg: 1983.

12. Bansal, V.; Bharde, A.; Ramanathan, R.; Bhargava, S. K., Inorganic materials using 'unusual' microorganisms. Advances in Colloid and Interface Science 2012, 179, 150-168.

13. Suresh, A. K.; Pelletier, D. A.; Wang, W.; Broich, M. L.; Moon, J.-W.; Gu, B.; Allison, D. P.; Joy, D. C.; Phelps, T. J.; Doktycz, M. J., Biofabrication of discrete spherical gold nanoparticles using the metal-reducing bacterium Shewanella oneidensis. Acta Biomaterialia 2011, 7 (5), 2148-2152.

14. Mukherjee, P., Senapati, S., Mandal, D., Ahmad, A., Khan, M. I., Kumar, R. and Sastry, M., Extracellular Synthesis of Gold Nanoparticles by the Fungus Fusarium oxysporum. ChemBioChem 2002, 3, 3.

15. Das, S. K.; Das, A. R.; Guha, A. K., Gold Nanoparticles: Microbial Synthesis and Application in Water Hygiene Management. Langmuir 2009, 25 (14), 8192-8199.

16. Ramanathan, R.; Field, M. R.; O'Mullane, A. P.; Smooker, P. M.; Bhargava, S. K.; Bansal, V., Aqueous phase synthesis of copper nanoparticles: a link between heavy metal resistance and nanoparticle synthesis ability in bacterial systems. Nanoscale 2013, 5 (6), 2300-2306.

17. Mukherjee, P., Ahmad, A., Mandal, D., Senapati, S., Sainkar, S. R., Khan, M. I., Ramani, R., Parischa, R., Ajayakumar, P. V., Alam, M., Sastry, M. and Kumar, R., Bioreduction of AuCl4− Ions by the Fungus, Verticillium sp. and Surface Trapping of the Gold Nanoparticles Formed. Angewante Chemie International Edition 2001, 40 (19), 4.

18. Papaconstantinou, E., Photochemistry of polyoxometallates of molybdenum and tungsten and/or vanadium. Chemical Society Reviews 1989, 18 (0), 1-31.

19. Zhang, T. R.; Feng, W.; Lu, R.; Bao, C. Y.; Zhang, X. T.; Li, T. J.; Zhao, Y. Y.; Yao, J. N., Self-assembled 18-molybdophosphate/dioctadecyldimethylammonium composite superlattice thin films with photochromic properties. Materials Chemistry and Physics 2003, 78 (1), 116-121.

20. Papaconstantinou, E.; Pope, M. T., Heteropoly blues. III. Preparation and stabilities of reduced 18-molybdodiphosphates. Inorganic Chemistry 1967, 6 (6), 1152-1155.

21. Inoue, M.; Suzuki, T.; Fujita, Y.; Oda, M.; Matsumoto, N.; Yamase, T., Enhancement of antibacterial activity of β-lactam antibiotics by $[P_2W_{18}O_{62}]^{6-}$, $[SiMo_{12}O_{40}]^{4-}$, and $[PTi_2W_{10}O_{40}]^{7-}$ against methicillin-resistant and vancomycin-resistant *Staphylococcus aureus*. Journal of Inorganic Biochemistry 2006, 100 (7), 1225-1233.

22. Martín, M.; Carmona, F.; Cuesta, R.; Rondón, D.; Gálvez, N.; Domínguez-Vera, J. M., Artificial Magnetic Bacteria: Living Magnets at Room Temperature. Advanced Functional Materials 2014, 24 (23), 3489-3493.

23. Carmona, F.; Martín, M.; Gálvez, N.; Dominguez-Vera, J. M., Bioinspired Magneto-optical Bacteria. Inorganic Chemistry 2014, 53 (16), 8565-8569.

Lactic Acid (LA)

hv

(365nm)

SCFAs: Acetic (AA), propionic, butiric and succinic acids
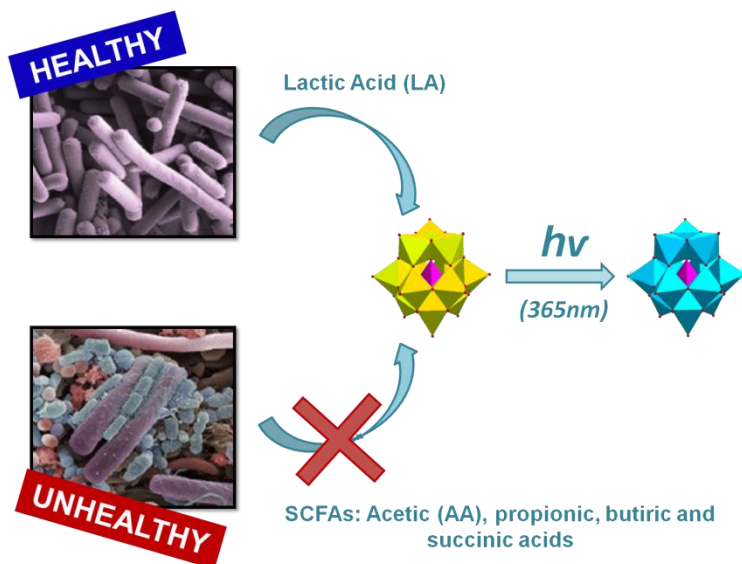
CHAPTER 3.

RAPID COLOUR-BASED DIAGNOSIS OF VAGINAL HEALTH USING ELECTROCHROMIC POLYOXOMETALATES

3.1 INTRODUCTION

Almost every woman suffers from vaginal infections in her lifetime, which not only leads to physical and psychological distress, but if not timely managed, may cause major health complications.[1-2] Bacterial vaginosis (BV or bacterial dysbiosis), a condition caused by the imbalance of natural bacterial population in the lower female reproductive tract (FRT), remains the most frequent cause of vaginal infections among reproductive-aged women.[3] BV during pregnancy causes preterm labour, premature birth and postpartum uterine infections.[4] BV also increases the risks of subsequently acquiring many other infections, including the pelvic inflammatory disease and sexually transmitted diseases (STDs).[5-6] A close association of BV with increased incidences of HIV transmission during unprotected sexual activities has become a topic of major scrutiny in recent years.[7-8]

Although the use of broad-spectrum antibiotics offers effective therapy against BV; the lack of user-friendly, low-cost, fast and reliable diagnosis of BV remains a major bottleneck in its timely management.[9-10] The situation is worsened as more than half of the women with BV do not have any symptoms.[11] A major challenge with BV diagnosis is that multiple species of bacteria can cause BV through disrupting the natural vaginal microenvironment. A healthy FRT is typically dominated by *Lactobacillus* family of bacteria that produce lactic acid, a molecule that provides natural immunity against infections and transmission of STDs.[12] During BV, *Lactobacilli* are suppressed by the overgrowth of a number of other infectious bacteria, such as *Gardnerella vaginalis*, *Bacteroides spp*.

and *Mobiluncus spp.*[13] Microbiological assays are not only inherently time consuming, it is challenging to employ them for reliably detecting BV, as the vaginal microenvironment is highly complex. For instance, the causative agents of BV may vary depending upon race, demography, culinary habit and lifestyle.[14-15] Further, small populations of some of these pathogenic bacteria may still be present in healthy individuals; whereas in a woman with BV, the small populations of multiple unhealthy bacterial species may interact in a complex manner causing the disease.

The complexity of this disease has led to alternative strategies for BV detection, including the Amsel and Spiegel criteria[16-17] and the Nugent score.[18] The Amsel criteria determine BV by fulfilling three of the following four conditions: (i) presence of abnormal vaginal discharge, (ii) elevated vaginal pH (> 4.5), (iii) positive amine odour test, and (iv) presence of clue cells on vaginal Gram smear. Spiegel completed this test by making an interpretation of Gram-stained vaginal smears from pregnant women. Another approach is based on the Nugent score that classifies the vaginal fluid from 0 to 10 based on the number of large Gram- positive rods (*Lactobacillus morphotypes*), small Gram-negative to Gram-variable rods (*G. vaginalis* and *Bacteroides spp. Morphotypes*), and curved Gram-negative rods (*Mobiluncus spp. Morphotypes*), such that a score of ≥7 indicates BV infection. Notably, due to the lack of a more suitable diagnostic tool, these methods are currently used for BV detection in clinics. However, it is well-recognised that these methods are far from ideal, as they are time-consuming and rely on highly qualified medical personnel, leading to expensive, non-quantitative, and at times, unreliable diagnosis of BV depending on the experience of the personnel.

As an alternative, BVBlue® test offers simple and rapid chromogenic analysis of the enhanced sialidase enzyme activity observed in infected vaginal fluids.[19-20] However, enhanced sialidase production is also common with other vaginal inflammations, including yeast and fungal infections (e.g. Trichoderma vaginalis), thereby restricting BVBlue® as a tool for presumptive diagnosis of BV.[21]

There is no doubt that the high complexity of BV makes it very challenging to employ conventional microbiology and molecular biology approaches to develop a reliable diagnostic tool. Therefore, there remains an unmet need to develop innovative approaches for rapid, simple and low-cost, and reliable diagnosis of BV.

In this study, we propose and validate a conceptual advance that does not attempt to detect the complex microbiome responsible for BV, but instead detects the overall bacterial metabolites produced during BV progression. It is well known that the high concentration of lactic acid (~100 mM) produced predominantly by Lactobacilli in the vaginal fluid keeps the lower FRT of women healthy, whereas the other short chain fatty acids (SCFAs), such as acetic, propionic, butyric, and succinic acids, produced by other bacteria are present in relatively smaller concentration (~2 mM).[22] When BV occurs, with decreasing population of Lactobacillus and the overgrowth of anaerobes, the metabolic profile of vaginal fluids significantly changes, leading to a dramatic loss of lactic acid (~20 mM) along with concomitant increase in concentration of mixed SCFAs (~100 mM).[23] An approach that allows the relative profiling of lactic acid vs. SCFAs offers a promising avenue to detect BV. The subtle

differences in the molecular structures of lactic acid and other SCFAs present next level of challenge in BV diagnosis, and as such, we utilise polyoxometalates (POMs) for this purpose.

POMs are heteropoly acids consisting of three or more transition metal oxyanions linked together by shared oxygen atoms to form a closed 3-dimensional framework.[24] With their high structural, chemical and electronic versatility[25], POMs are often employed as redox catalysts for a variety of reactions.[26-28] Our previous studies[29-32] have shown that POMs are promising electrochromic materials with the ability to be reduced by the addition of various number of electrons, leading to a family of mixed-valence species with a characteristic deep blue colour ('heteropoly blues'). These reduced forms of POMs can be easily detected by UV–visible absorbance spectroscopy or even with naked eye.[32-33] UV light irradiation can be used to easily reduce POMs into 'heteropoly blues' in the presence of a suitable sacrificial electron donor.[34-35] Notably, different chemical species may have remarkably different abilities to donate electrons to a particular POM, and it is this differential ability of lactic acid vs. other SCFAs that we utilise to detect BV.

Therefore, we demonstrate here a novel strategy to diagnosis BV using a kind of POMs phosphomolybdic acid (PMA) to detect changes in the vaginal acid profiles. By the aid of UV light irradiation, a simple colour change (colourless to blue) will be observed within 5-10 min in healthy non-BV samples as in the presence of the dominant metabolite lactic acid, which is produced by lactobacillus bacteria, PMA reduces. In contrast, no colour change could be detected in unhealthy BV samples since in the presence of SFCAs, which are produced by the BV associated

bacteria, PMA is not reduced. Moreover, the colour intensity directly correlates with the vaginal lactic acid concentration, allowing the diagnosis of a variety of healthy or BV conditions.

Our approach offers a simple qualitative measure of the vaginal health by naked-eye detection, similar to that observed in pregnancy strips. Using simple spectroscopy, a quantitative profile of level of BV infection can also be generated, adding additional value if required for clinical interventions. It is also convenient to use this approach as an easy to perform screening test for diagnosis of BV before the samples are sent to a microbiology lab for further evaluation.

3.2 RESULTS AND DISCUSSION

Studies investigating the metabolites have shown the lactobacillus-dominated microbiota in eubiosis vaginal environment produces high levels of lactic acid, which range from 0.72% to 1.48% (w/v, 80-164 mM) with an average of 1.0±0.2% (w/v, 111 mM).[36] When BV occurs, lactic acid undergoes a striking loss to less than 20 mM[22] along with an increasing concentration of mixed SCFAs.[37] Therefore, a broad working range of 0 to 180mM acids was chosen in this study to cover all possible eubiosis and dysbiosis conditions.

A series of concentrations (0 to 180mM) of lactic acid, acetic acid, propionic acid, butyric acid, and succinic acid were mixed with 5 mM PMA solution (1:1, v/v), respectively. Upon incubating PMA and lactic acid, a concentration-dependent wide band centred at 700 nm gradually developed after UV irradiation (see Supporting information; Figure S1A).

In contrast, there is no change in the UV spectra upon incubating PMA and the other SCFAs after same time UV irradiation (see Supporting information; Figure S1BCDE), indicating that PMA has not been reduced by these SCFAs.

The related mechanism is proposed in Scheme 1. PMA is photoreduced under UV irradiation accompanying with the oxidation of lactic acid. It can be reversibly reduced in one- or-multiple electron step,[38] allowing the generation of escalating blue colour appearance with increasing lactic acid concentration.

PMA   Reduced PMA

$$PMo^{VI}_{12}O_{40}{}^{3-} + 4\,e^- \rightleftharpoons PMo^{V}_{4}Mo^{VI}_{8}O_{40}{}^{7-}$$
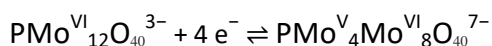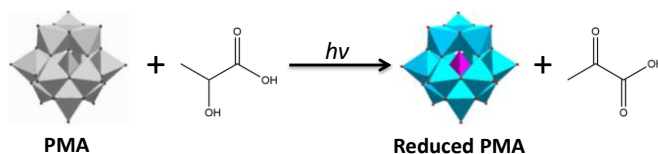
Scheme 1. PMA is reduced under UV irradiation with the oxidation of lactic acid.

Therefore, by the aid of PMA, lactic acid can be distinguished from the other SCFAs in the vaginal fluids, and the concentration of lactic acid, which reflects the health condition of women's vaginal environment, can be monitored by observing the UV-vis absorbance band centred at 700 nm corresponding to the reduced forms of PMA (Figure 1).

Figure 1. UV-vis absorption band centred at 700 nm of different concentrations of lactic, acetic, succinic, propionic and butyric acids with 5 mM PMA after 30 min UV irradiation.

Given that the vaginal fluid is more complex than a mixture of few acids, it's of great importance to ensure the diagnosis of BV is not affected by the other components in the vaginal fluid. Therefore, a vaginal fluid simulant (VFS)[39] was made with fluid representatives to test the ability of PMA as a sensor to detect BV in analogous conditions. In the typical scenario, when BV occurs, with the vaginal levels of lactic acid being depleted from approx. 120 mM to 2-20 mM, the levels of SCFAs, particularly acetic acid, increase from 0-4 mM to 120 mM. The other SCFAs such as propionic, butyric and succinic acids also increase from 1 mM to 2-20 mM.[22-23, 40] However, there might be several intermediate and extreme conditions as well. In these conditions, there should be a balance between lactic acid and the other SCFAs, particularly, acetic acid. Once *Lactobacillus* bacteria get supressed by the overgrowth of the unhealthy bacteria, acetic acid concentration increases along with the decreasing lactic acid. Hence, we calculated the corresponding acetic acid

concentrations at a series of fixed lactic acid concentrations (0, 5, 10, 20, 40, 60, 80, 100, 120, 140, 160 and 180 mM) and prepared VFS samples according to these lactic acid-acetic acid combinations to simulate a variety of eubiosis and dysbiosis conditions.

After incubating these samples with PMA solution (5 mM) under UV irradiation, the mixture remained colourless when lactic acid concentration was lower than 20 mM, whereas a gradually deepen blue colour can be seen by the naked eye with increasing lactic acid concentration. The intensity of colour directly corresponds to the concentration of lactic acid, meaning that the darker the blue colour, the more lactic acid is present, the less possibility of getting BV. As can be seen in Figure 2, the UV- vis absorbance at 700 nm has a good correlation with lactic acid concentration. The exponential fit (see Supporting information; Figure S2) obtained by the data offers a potential of quantification of vaginal lactic acid by using simple spectroscopy with good precision of 95.40% and accuracy of 70% on 10% contingency or 100% on 15% contingency. As lactic acid 20 mM with acetic acid 120 mM and lactic acid 120 mM with acetic acid 2 mM, which represent the typical unhealthy (BV) and healthy (non-BV) scenarios, respectively, have significant difference (p=0.01) after the incubation with PMA, we then used these two representatives in the following studies.

Given that the BV and non-BV samples can be differentiated after UV irradiation, a time dependent study was carried out to investigate their sensitivity to UV irradiation. The difference started to occur even after 1min, and became increasing as extending UV exposure time (Figure 3).

Figure 2. Lactic acid and acetic acid combinations with 5mM PMA after 30 min UV irradiation.

Figure 3. Increasing response of non-BV (120 mM LA+2 mM AA) and BV (120 mM AA+20 mM LA) samples with 5 mM PMA under UV irradiation.

Moreover, adding the other SCFAs (propionic acid, butyric acid, succinic acid) to the lactic acid and acetic acid mixture did not affect their response (see Supporting information; Figure S3).

According to the Amsel criteria, BV occurs when the pH is greater than 4.5. When using PMA to diagnosis BV, the detection is not only correlated

with lactic acid concentration, but also pH sensitive. To explore the pH effect on our method, a series of samples made of 120 mM lactic acid and 2 mM acetic acid, or 20 mM lactic acid and 120 mM acetic acid were prepared as non-BV simulant and BV simulant, respectively. The pH of these samples was adjusted to 3.5 and 5.5, which are in the range of healthy and unhealthy vaginal pH, respectively. Upon 30 min incubation with 5 mM PMA under UV irradiation, only non-BV samples with pH 3.5 changed to blue. By contrast, in the non-BV samples with pH 5.5 and all BV samples did not appear any colour. This response can also be quantified by the UV-vis absorbance at 700 nm (Figure 4). The colour change and increase in the UV-vis absorbance will only occur within the healthy pH range, which is in good accordance with the Amsel criteria.

Figure 4. Effect of different pH on non-BV sample(120 mM lactic acid +2 mM acetic acid) and BV sample (120 mM acetic acid +20 mM lactic acid) with 5 mM PMA after 30 min UV irradiation.

The reduction potential of PMA depends on pH as a result of protonation.[34, 41] The reduction potential may shift to more negative

values with increasing pH. Lactic acid can exist as protonated lactic acid or the unprotonated lactate anion, which is determined by the acid dissociation constant (pKa=3.9).[23] In non-BV conditions with low pH, lactic acid predominates, which has more potential to reduce PMA. Given that both lactic acid concentration and vaginal pH contribute to the BV diagnosis using PMA, it is further confirmed that this method is a reliable diagnostic approach with high specificity.

This method could also be applied on diluted real samples. According to a set of clinical data, representative BV and non-BV samples were prepared with the following conditions: 21.2 mM lactic acid and 120 mM acetic acid with the pH of 4.9; and 88.2 mM lactic acid and 15 mM acetic acid with the pH of 3.9, respectively. These samples were diluted up to 30 times to simulate the actual detection conditions. After incubation with PMA under UV irradiation, there is a clear difference between the BV and non-BV samples (Figure 5).

A   **B**

Figure 5. (A) Undiluted samples: BV (21.2 mM lactic acid and 120 mM acetic acid) and Non-BV (88.2 mM lactic acid and 15 mM) with 5 mM PMA after UV irradiation; (B) 30 times diluted of (A).

3.3 CONCLUSION

In this work we present a rapid and easy to use bacterial vaginosis diagnosis with good precision and high specificity. It deals with a new approach, based on the use of the electrochromic PMA as a colour-based sensor to detect the unbalance of bacterial metabolites occurring during BV. By the aid of UV irradiation, PMA is photo-reduced by lactic acid, the predominant metabolite of healthy vaginal bacteria, to generate a clear blue colour, which can be easily observed by naked eye. However, no change colour occurs with SCFAs, the predominant metabolites of unhealthy vaginal bacteria. Since intensity of blue colour correlates with the ratio lactic acid (healthy)/acetic acid (unhealthy), this spectroscopic method allows determining the infection level and therefore serves to monitor the efficacy of antibiotic treatments by tracking whether lactic acid production has increased during and after antibiotic use.

3.4 EXPERIMENTAL SECTION

Phosphomolybdic acid (PMA), lactic acid, propionic acid, butyric acid, succinic acid, sodium chloride (NaCl), potassium hydroxide (KOH), calcium hydroxide (Ca(OH)$_2$), urea, glucose, bovine serum albumin and sodium hydroxide (NaOH) were purchased from Sigma-Aldrich. Acetic acid and hydrogen chloride (HCl) were from VMR International S.A.S and Rowe scientific PTY LTD, respectively.

UV irradiation experiments were performed using a UV light source which was comprised of four 9 Watt halogen tubes, delivering a total power of 36 Watt at λmax of 361 nm at the source (Nail curing lamp, eBay). The working distance between the source and the centre of the

samples for the UV irradiation process was fixed at 4.5 cm. UV-vis spectra were recorded in 96-well plate using a Perkin Elmer EnVisionTM 2104 Multilable Plate Reader.

Vaginal fluid simulant (VFS)

VFS base (without lactic acid and acetic acid) was made following the recipe previously published by Owen[39] with some changes. Compounds needed for 1 L of VFS are as follows: NaCl, 3.51 g; KOH, 1.40 g; $Ca(OH)_2$, 0.222 g; bovine serum albumin, 0.018 g; and urea, 0.4 g. This VFS base was completed to healthy VFS and unhealthy VFS by adding different amount of lactic acid and acetic acid and adjusting pH with HCl.

3.5 SUPPORTING INFORMATION

A

B   C

D   E
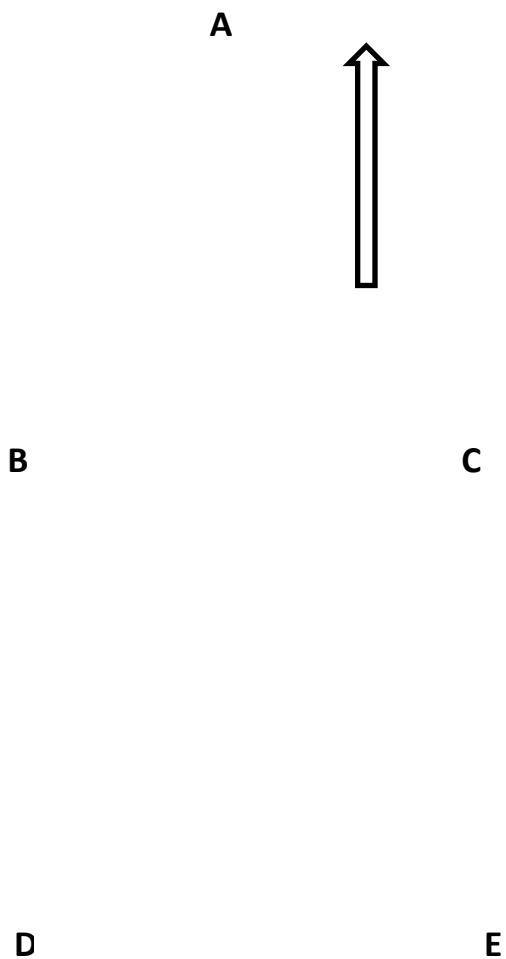
Figure S1. Concentration dependent response of Lactic acid (A), Acetic acid (B), Succinic acid (C), Propionic acid (D) and Butyric acid (E) (0-180 mM) to PMA (5mM) after 30min UV exposure.

Figure S2. The calibration curve of the absorbance at 700 nm versus the concentration of lactic acid in a mixture of lactic acid and acetic acid.
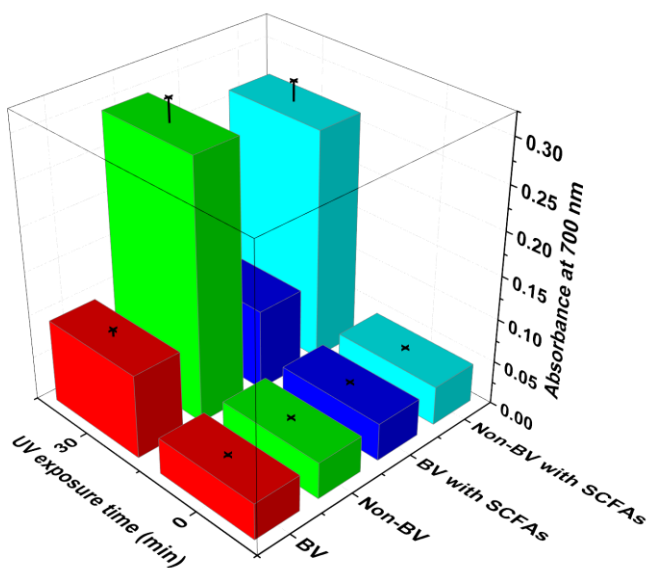
Figure S3. Response of BV (120 mM LA+2 mM AA) and Non-BV (120 mM AA+20 mM LA) samples and these samples in presence of the other SCFAs with 5 mM PMA to UV exposure.

3.6 REFERENCES

1. Jade E. Bilardi , S. W., Meredith Temple-Smith, Ruth McNair, Julie Mooney-Somers, Clare Bellhouse, Christopher K. Fairley, Marcus Y. Chen, Catriona Bradshaw, The Burden of Bacterial Vaginosis: Women's Experience of the Physical, Emotional, Sexual and Social Impact of Living with Recurrent Bacterial Vaginosis. *PloS one* **2013,** *8* (9).

2. Martin, D. H., The microbiota of the vagina and its influence on women's health and disease. *The American journal of the medical sciences* **2012,** *343* (1), 2.

3. Sobel, J. D., Bacterial Vaginosis. *Annual Review of Medicine* **2000,** *51* (1), 349-356.

4. McGregor, J. A., Bacterial Vaginosis in Pregnancy. *Obstetrical & Gynecological Survey* **2000,** *55* (5), 1-19.

5. Taylor, B. D.; Darville, T.; Haggerty, C. L., Does Bacterial Vaginosis Cause Pelvic Inflammatory Disease? *Sexually Transmitted Diseases* **2013,** *40* (2), 117-122.

6. Fethers, K. A.; Fairley, C. K.; Hocking, J. S.; Gurrin, L. C.; Bradshaw, C. S., Sexual Risk Factors and Bacterial Vaginosis: A Systematic Review and Meta-Analysis. *Clinical Infectious Diseases* **2008,** *47* (11), 1426-1435.

7. Cohen, C. R.; Lingappa, J. R.; Baeten, J. M.; Ngayo, M. O.; Spiegel, C. A.; Hong, T.; Donnell, D.; Celum, C.; Kapiga, S.; Delany, S.; Bukusi, E. A., Bacterial Vaginosis Associated with Increased Risk of Female-to-Male HIV-1 Transmission: A Prospective Cohort Analysis among African Couples. *PLoS Med* **2012,** *9* (6), e1001251.

8. Alcaide, M. L.; Strbo, N.; Romero, L.; Jones, D. L.; Rodriguez, V. J.; Arheart, K.; Martinez, O.; Bolivar, H.; Podack, E. R.; Fischl, M. A., Bacterial Vaginosis Is Associated with Loss of Gamma Delta T Cells in the Female Reproductive Tract in Women in the Miami Women Interagency HIV Study (WIHS): A Cross Sectional Study. *PloS one* **2016,** *11* (4), e0153045.

9. Sha, B. E.; Chen, H. Y.; Wang, Q. J.; Zariffard, M. R.; Cohen, M. H.; Spear, G. T., Utility of Amsel Criteria, Nugent Score, and Quantitative PCR for Gardnerella vaginalis, Mycoplasma hominis, and Lactobacillus spp. for Diagnosis of Bacterial Vaginosis in Human Immunodeficiency Virus-Infected Women. *Journal of clinical microbiology* **2005,** *43* (9), 4607-4612.

10. Bradshaw, C. S.; Sobel, J. D., Current Treatment of Bacterial Vaginosis—Limitations and Need for Innovation. *The Journal of Infectious Diseases* **2016,** *214* (suppl_1), S14-S20.

11. Koumans, E. H.; Sternberg, M.; Bruce, C.; McQuillan, G.; Kendrick, J.; Sutton, M.; Markowitz, L. E., The Prevalence of Bacterial Vaginosis in the United States, 2001–2004; Associations With Symptoms, Sexual Behaviors, and Reproductive Health. *Sexually Transmitted Diseases* **2007,** *34* (11), 864-869.

12. O'Hanlon, D. E.; Moench, T. R.; Cone, R. A., In vaginal fluid, bacteria associated with bacterial vaginosis can be suppressed with lactic acid but not hydrogen peroxide. *BMC Infectious Diseases* **2011,** *11* (1), 200.

13. Fredricks , D. N.; Fiedler , T. L.; Marrazzo , J. M., Molecular Identification of Bacteria Associated with Bacterial Vaginosis. *New England Journal of Medicine* **2005,** *353* (18), 1899-1911.

14. Zhou, X.; Brown, C. J.; Abdo, Z.; Davis, C. C.; Hansmann, M. A.; Joyce, P.; Foster, J. A.; Forney, L. J., Differences in the composition of vaginal microbial communities found in healthy Caucasian and black women. *ISME J* **2007,** *1* (2), 121-133.

15. Ravel, J.; Gajer, P.; Abdo, Z.; Schneider, G. M.; Koenig, S. S. K.; McCulle, S. L.; Karlebach, S.; Gorle, R.; Russell, J.; Tacket, C. O.; Brotman, R. M.; Davis, C. C.; Ault, K.; Peralta, L.; Forney, L. J., Vaginal microbiome of reproductive-age women. *Proceedings of the National Academy of Sciences of the United States of America* **2011,** *108* (Suppl 1), 4680-4687.

16. Amsel, R.; Totten, P. A.; Spiegel, C. A.; Chen, K. C. S.; Eschenbach, D.; Holmes, K. K., Nonspecific vaginitis. *The American Journal of Medicine* **1983,** *74* (1), 14-22.

17. Spiegel, C. A.; Amsel, R.; Holmes, K. K., Diagnosis of bacterial vaginosis by direct gram stain of vaginal fluid. *Journal of clinical microbiology* **1983,** *18* (1), 170-177.

18. Nugent, R. P.; Krohn, M. A.; Hillier, S. L., Reliability of diagnosing bacterial vaginosis is improved by a standardized method of gram stain interpretation. *Journal of clinical microbiology* **1991,** *29* (2), 297-301.

19. Myziuk, L.; Romanowski, B.; Johnson, S. C., BVBlue Test for Diagnosis of Bacterial Vaginosis. *Journal of clinical microbiology* **2003,** *41* (5), 1925-1928.

20. Bradshaw, C. S.; Morton, A. N.; Garland, S. M.; Horvath, L. B.; Kuzevska, I.; Fairley, C. K., Evaluation of a Point-of-Care Test, BVBlue, and Clinical and Laboratory Criteria for Diagnosis of Bacterial Vaginosis. *Journal of clinical microbiology* **2005,** *43* (3), 1304-1308.

21. Wiggins, R.; Hicks, S. J.; Soothill, P. W.; Millar, M. R.; Corfield, A. P., Mucinases and sialidases: their role in the pathogenesis of sexually transmitted infections in the female genital tract. *Sexually Transmitted Infections* **2001,** *77* (6), 402-408.

22. S. Al-Mushrif, A. E. a. B. M. J., Inhibition of chemotaxis by organic acids from from anaerobes may prevent a purulent response in bacterial vaginosis. *The Patological Sociaty of Great Britain and Ireland* **2000,** *49*, 1023-1030.

23. Aldunate, M.; Srbinovski, D.; Hearps, A. C.; Latham, C. F.; Ramsland, P. A.; Gugasyan, R.; Cone, R. A.; Tachedjian, G., Antimicrobial and immune modulatory effects of lactic acid and short chain fatty acids produced by vaginal microbiota associated with eubiosis and bacterial vaginosis. *Frontiers in physiology* **2015,** *6* (164).

24. Coronado, E.; Giménez-Saiz, C.; Gómez-García, C. J., Recent advances in polyoxometalate-containing molecular conductors. *Coordination Chemistry Reviews* **2005,** *249* (17), 1776-1796.

25. Clemente-Juan, J. M.; Coronado, E.; Gaita-Arino, A., Magnetic polyoxometalates: from molecular magnetism to molecular spintronics and quantum computing. *Chemical Society Reviews* **2012,** *41* (22), 7464-7478.

26. Chen, J.; Liu, S.; Feng, W.; Zhang, G.; Yang, F., Fabrication phosphomolybdic acid–reduced graphene oxide nanocomposite by UV photo-reduction and its electrochemical properties. *Physical Chemistry Chemical Physics* **2013,** *15* (15), 5664-5669.

27. Lv, H.; Song, J.; Zhu, H.; Geletii, Y. V.; Bacsa, J.; Zhao, C.; Lian, T.; Musaev, D. G.; Hill, C. L., Visible-light-driven hydrogen evolution from water using a noble-metal-free polyoxometalate catalyst. *Journal of Catalysis* **2013,** *307* (Supplement C), 48-54.

28. Li, H.; Pang, S.; Feng, X.; Mullen, K.; Bubeck, C., Polyoxometalate assisted photoreduction of graphene oxide and its nanocomposite formation. *Chemical Communications* **2010,** *46* (34), 6243-6245.

29. Pearson, A.; Bhargava, S. K.; Bansal, V., UV-Switchable Polyoxometalate Sandwiched between TiO2 and Metal Nanoparticles for Enhanced Visible and Solar Light Photococatalysis. *Langmuir* **2011,** *27* (15), 9245-9252.

30. Pearson, A.; Zheng, H.; Kalantar-zadeh, K.; Bhargava, S. K.; Bansal, V., Decoration of TiO2 Nanotubes with Metal Nanoparticles Using Polyoxometalate as a UV-Switchable Reducing Agent for Enhanced Visible and Solar Light Photocatalysis. *Langmuir* **2012,** *28* (40), 14470-14475.

31. Pearson, A.; Bhosale, S.; Bhargava, S. K.; Bansal, V., Combining the UV-Switchability of Keggin Ions with a Galvanic Replacement Process to Fabricate TiO2–Polyoxometalate–Bimetal Nanocomposites for Improved Surface Enhanced Raman Scattering and Solar Light Photocatalysis. *ACS Applied Materials & Interfaces* **2013,** *5* (15), 7007-7013.

32. Gonzalez, A.; Galvez, N.; Clemente-Leon, M.; Dominguez-Vera, J. M., Electrochromic polyoxometalate material as a sensor of bacterial activity. *Chemical Communications* **2015,** *51* (50), 10119-10122.

33. Papaconstantinou, E., Photochemistry of polyoxometallates of molybdenum and tungsten and/or vanadium. *Chemical Society Reviews* **1989,** *18* (0), 1-31.

34. Papaconstantinou, E.; Dimotikali, D.; Politou, A., Photochemistry of heteropoly electrolytes. The 18-molybdodiphosphate. *Inorganica Chimica Acta* **1980,** *43* (Supplement C), 155-158.

35. Troupis, A., Hiskia, A. and Papaconstantinou, E., Synthesis of Metal Nanoparticles by Using Polyoxometalates as Photocatalysts and Stabilizers. *Angewandte Chemie International Edition* **2002,** *41*, 4.

36. O'Hanlon, D. E.; Moench, T. R.; Cone, R. A., Vaginal pH and microbicidal lactic acid when lactobacilli dominate the microbiota. *PloS one* **2013,** *8* (11), e80074.

37. Chaudry, A. N.; Travers, P. J.; Yuenger, J.; Colletta, L.; Evans, P.; Zenilman, J. M.; Tummon, A., Analysis of vaginal acetic acid in patients undergoing treatment for bacterial vaginosis. *Journal of clinical microbiology* **2004,** *42*.

38. Okuhara, T.; Mizuno, N.; Misono, M., Catalytic Chemistry of Heteropoly Compounds. In *Advances in Catalysis*, Eley, D. D.; Haag, W. O.; Gates, B., Eds. Academic Press: 1996; Vol. 41, pp 113-252.

39. Katz, D. H. O. a. D. F., A Vaginal Fluid Simulant. *Elsevier Science Inc.* **1999,** *59*, 91–95.

40. Mirmonsef, P.; Zariffard, M. R.; Gilbert, D.; Makinde, H.; Landay, A. L.; Spear, G. T., Short-chain fatty acids induce pro-inflammatory cytokine production alone and in combination with toll-like receptor ligands. *American journal of reproductive immunology* **2012,** *67* (5), 391-400.

41. Sadakane, M.; Steckhan, E., Electrochemical Properties of Polyoxometalates as Electrocatalysts. *Chemical Reviews* **1998,** *98* (1), 219-238.
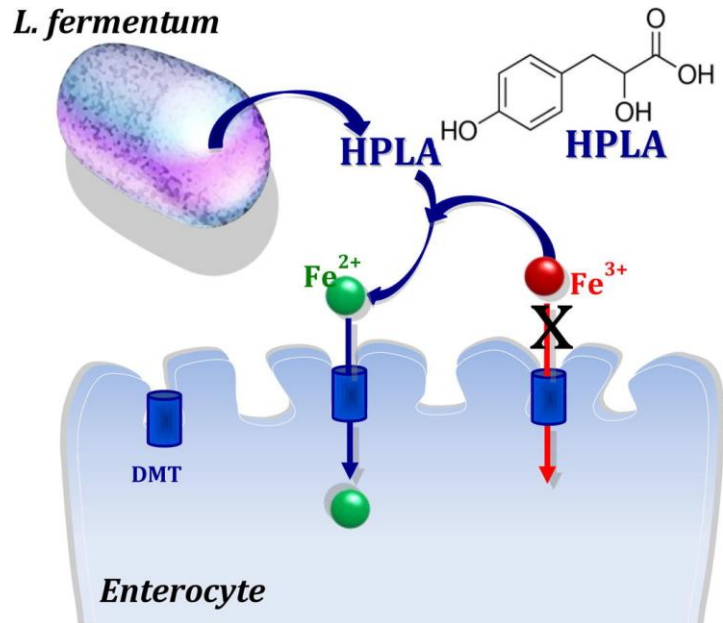
CHAPTER 4.

IDENTIFICATION OF THE KEY EXCRETED MOLECULE BY *LACTOBACILLUS FERMENTUM* RELATED TO HOST IRON ABSORPTION

4.1 INTRODUCTION

Iron is an indispensable element for humans due to its involvement in essential biochemical processes, including energy production, biosynthesis, replication, and locomotion.[1-2] Iron deficiency is the most common and widespread nutritional disorder in the world. Besides affecting many children and women in developing countries, it is the only nutrient deficiency prevalent in industrialized countries. The human body receives iron from food. Though the daily requirement is 20–25 mg, no more than 2 mg are really absorbed.[3] Adequate iron levels in the blood are partially maintained by recycling the iron released upon the degradation of iron-containing proteins, especially hemoglobin.

Heme-iron, present in hemoglobin and myoglobin, has high bioavailability[4]; however, the majority of iron in food (>90%) is in non-heme forms, either as free iron or bound to low molecular-weight biomolecules[5]. Iron from food is mainly absorbed by the duodenum enterocytes (90%). The stomach does not play a significant role in the assimilation of iron, as its absorption is no more than 2% of the total.[6]

Iron transfer through the enterocyte membrane occurs by the combined activities of two proteins: DMT1 and DcytB. The coupled work of DcytB/DTM1 is required for iron absorption since iron enters the small intestine lumen mainly as Fe(III), the result of Fe(II) oxidation by gastric juice components. Free Fe(III) is not able to enter into the enterocyte and must be reduced.[7-8] The iron-regulated ferrireductase protein, DcytB, is highly expressed at duodenal enterocytes and reduces Fe(III) to Fe(II). Upon reduction, Fe(II) is transferred across the apical membrane of

enterocytes by divalent metal transporters, mainly DMT1. Once inside the enterocytes, Fe(II) can be used for synthesis of iron-containing proteins, transported to plasma by the membrane protein ferroportin, or stored inside ferritin for later use when needed by cells.[7-8]

Interestingly, the bioavailability of iron is influenced by a series of chemical species in the gastrointestinal tract. Whereas oxalates, phytates, phenolates and phosphates suppress iron absorption, ascorbic and citric acids, increase it.[9] For this reason commercial iron supplements are usually accompanied by ascorbic or citric acid. Strategies to increase the intake of iron-rich foods, as well as dietary factors that enhance iron absorption, are therefore extremely important for human health.

Probiotic bacteria constitute an important part of natural microbiota. Bacteria produce many different metabolic substances that can act as antioxidants, bioflocculants or even immune activators.[10-12] They survive the harsh stomach conditions and nest in different areas of intestines. Though the European Food Safety Authority (EFSA) has recently concluded that there is insufficient evidence to claim that a probiotic can help boost iron absorption,[13] other studies have shown that the probiotic bacteria of the human gut microbiota facilitate iron absorption.[14-16] For example, it has been observed that the amount of probiotic bacteria in gut flora is significantly lower in anemic patients than in healthy people.

The mechanisms of this influence are not entirely understood. As of yet no compound excreted by bacteria has been shown to be related to iron absorption. Some have proposed that bacterial fermentation in intestines decreases the pH due to the production of lactic acid, which

can increase iron solubility, leading to higher iron absorption.[15] No published study has evaluated the effect of the ferric-reducing activity of probiotic bacteria on iron absorption. We show that *Lactobacillus fermentum*, one of the main components of the microbiota, exhibits considerable extracellular ferric-reducing activity. We have isolated and identified the excreted molecule that produces the ferric-reducing activity of *Lactobacillus fermentum*: *p*-hydroxyphenyllactic acid (HPLA). This molecule efficiently reduces Fe(III) to Fe(II) at acidic pH.

From the results described here, we propose that the increase of iron absorption in humans, due to the presence of probiotic bacteria in gut flora, could be related, not only to the decrease of pH caused by these lactic acid bacteria,[15] but also to the ferric-reducing activity of the excreted HPLA. We have performed an *in vitro* experiment on iron uptake by enterocytes to confirm that HPLA promotes iron absorption. These results shed light on the reason why probiotic bacteria increase iron absorption in humans and can lead to more efficient strategies to increase iron absorption in humans.

4.2 RESULTS AND DISCUSSION

Lactobacillus fermentum shows a high ferric-reducing activity. The ability to reduce Fe(III) to Fe(II) is usually related to the antioxidant properties of a chemical species. In the context of iron metabolism, this redox reaction is essential for iron absorption since non-heme iron is usually in the form of Fe(III), which cannot be absorbed by enterocytes until it has been reduced to Fe(II).

The ferric-reducing activity of *L. fermentum* was measured through its incubation with Fe(III) and ferrozine by monitoring the formation of the Fe(II) complex with the chelator, $[Fe^{II}(fz)_3]$, through the appearance and increase of its characteristic UV–vis band at 562 nm. The supernatant liquid isolated after centrifugation of the bacteria exhibits activity similar to that of the bacterial broth after 6 and 24 h (Figure 1). This evidence indicates that the ferric-reducing ability of *L. fermentum* is due to the molecule(s) excreted by the bacteria, However, the patterns of ferric-reducing activity of the supernatant and the bacterial culture differ. Whereas the former is able to reduce a specific amount of Fe(III) and then is rendered inactive, the latter exhibits prolonged activity. The bacterial culture can reduce additional amounts of Fe(III) after reducing the same amount of Fe(III) as reduced by the supernatant. This could be explained if the bacterium continuously excreted or regenerated the molecule responsible for its ferric-reducing activity.

The characterization of excreted active molecules by living organisms is of great interest in the biomedical field. In fact, some of these molecules are in the pharmaceutical market for different medical purposes. We addressed the challenge of isolating and characterizing the molecule responsible for the ferric-reducing activity of *L. fermentum* because no such study has been thus far done.
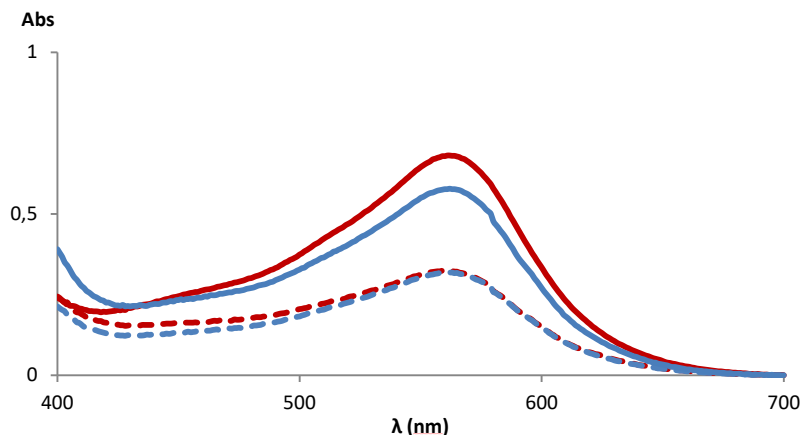
Figure 1. Ferric-reducing activity *of L. Fermentum* (red) and the supernatant liquid (blue) after 6 (dashed lines) and 24 h. Development of the UV-vis band centered at 562 nm due to [FeII(fz)3] informs of the ferric-reducing activity.

An assay-guided fractionation approach was implemented. First, an extract of the culture supernatant was prepared. A brominated polystyrenic resin (SP207ss), with the capacity to retain both polar and non-polar compounds, was used for the solid-phase. After confirming the ferric-reducing activity of the extract obtained by elution from the resin with methanol, the extract was subjected to semipreparative HPLC fractionation. After passing through a C8 reversed-phase column, the fractions with the reducing ability were pooled and further fractionated with a C18 column. The two fractions showing ferric-reducing activity were pooled and analyzed by NMR and LC-DAD-ESI-TOFMS. The ^{1}H NMR spectrum (Figure 2) revealed a mixture of a few compounds. The signals of a *para*-hydroxyphenyl group, corresponding to one of the major components, could easily be identified. Additional 2D NMR experiments, including COSY, HSQC and HMBC (see supporting information; Figure S1–S8), were employed to elucidate the connectivity of the compound

containing this structural moiety, which turned out to correspond to *p*-hydroxyphenyllactic acid (HPLA, Chart 1).
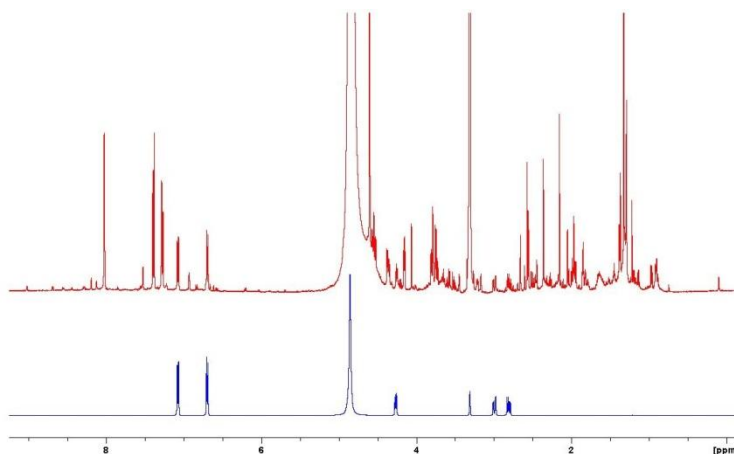
Figure 2. ^{1}H NMR spectra (500 MHz, CD3OD) of the final pooled fractions displaying ferric reducing activity (red) and *p*-hydroxyphenyllactic acid standard, HPLA (blue).
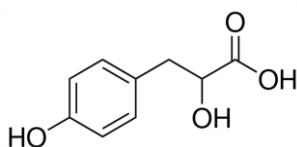
Chart 1. Chemical structure of *p*-hydroxyphenyllactic acid HPLA.

The molecular formula of HPLA, $C_9H_{10}O_4$, was a major component detected in the corresponding LC–HRMS analysis (see supporting information; Table S1).

Further confirmation of the identity of the compound was obtained by direct comparison of the NMR spectra of the final pooled active fractions with the spectrum of a commercial HPLA standard (Fig. 2). When the standard was evaluated for its ferric-reducing activity, it showed the

same reducing power. Thus, HPLA is the compound excreted by *L. fermentum*, responsible for the bacterial ferric-reducing activity.

Interestingly, HPLA has already been identified as an antioxidant compound, in a radical-scavenging assay, produced by the sister species *Lactobacillus plantarum*.[17] The production of HPLA by lactic acid bacteria (LAB) was first reported from *L. plantarum* 21B.[18] This compound has shown antifungal activity and contributes to the biopreservative properties claimed for LAB.[19] HPLA has been isolated as its L-enantiomer in *L. plantarum*.[17] The same chirality is expected for the HPLA produced by the *L. fermentum* strain employed in this work, assuming a common pathway for HPLA production among lactobacilli. The biosynthesis of HPLA in LAB likewise explains the apparent regeneration of the ferric-reducing activity observed for *L. fermentum* in reduction experiments with increasing amounts of Fe(III). In these bacteria, tyrosine is transformed by transamination into 4-hydroxyphenylpyruvate, which is further reduced to HPLA by a hydroxyacid dehydrogenase.[18, 20-21] Transamination is the rate-limiting step in such biosynthesis. It has been demonstrated that HPLA production dramatically increases in fermentations of *Lactobacillus sp. SK007* supplemented with 4-hydroxyphenylpyruvate (tyrosine as supplement renders just a moderate increase in production).[22] These results indicate that the bacterium is very efficient in reducing 4-hydroxyphenylpyruvate to HPLA. Such efficiency would help to recycle the HPLA consumed in the reduction of Fe(III). In this ferrireduction HPLA gets oxidized to 4-hydroxyphenylpyruvate which would get back to HPLA via the corresponding *Lactobacillus* hydroxyacid dehydrogenase, that way

explaining the apparent regeneration of the ferric-reducing activity already mentioned.

Once HPLA was identified as the molecule responsible for the ferric-reducing activity of *L. fermentum*, a study of its ability to reduce Fe(III) to Fe(II) as a function of pH was carried out. As shown in Figure 3, HPLA exhibits a ferric-reducing activity extremely dependent on pH. At pH above 6, HPLA hardly reduces Fe(III) to Fe(II) but, at pH 3.8, this reduction is practically complete.
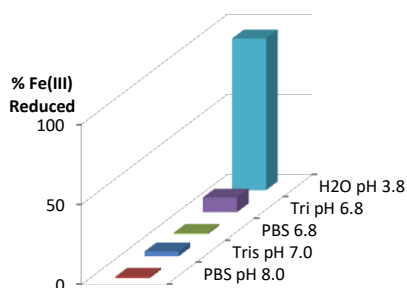
Figure 3. Ferric-reducing activity of HPLA at different pHs and buffers. The % of Fe(III) reduction was calculated as the ratio between concentrations of [Fe^{II}(fz)$_3$] and the initial Fe(III).

To further verify that HPLA is the principal factor in the ferric-reducing activity of *L. fermentum*, we performed an experiment in which HPLA was directly added to a 6 h bacterial culture. The resulting ferric-reducing activity of the mixture was compared to that of the 24 h bacterial culture. As shown in Figure 4, the addition of HPLA to the culture media leads to an increase in the ferric-reducing activity (Figure 4, green bar). The activity of this mixture is close to the sum of that of *L. fermentum* (Figure 4, blue bar) and the HPLA control (Figure 4, red bar). Likewise, the

addition of HPLA to the 6 h culture medium gives rise to a ferric-reducing activity close to that of the 24 h culture medium, indicating that HPLA is continuously excreted during the bacterial growth from 6 to 24 h and that this molecule is responsible for the ferric-reducing activity of *L. fermentum*.
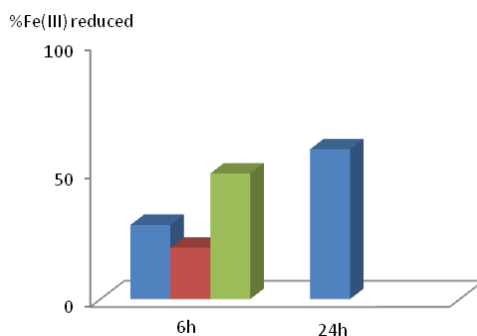
Figure 4. Ferric-reducing activity, as a percentage of Fe(III) reduction, of a 6 and 24 h culture *L. fermentum* (blue), the addition of HPLA (3,6 μM) to the culture medium (green), and HPLA at the same concentration in the growth medium (red).

Interestingly, HPLA seems to be a specific reductant of Fe(III). It does not reduce other chemical species, such as Au(III) or the polyoxometalate $[P_2Mo^{VI}_{18}O_{62}]^{6-}$, which are quite reduced in the presence of *L. fermentum.*[23-24] This result indicates that the chemical reducing mechanism of *L. fermentum* does not solely contain HPLA but also other reducing molecules. Our work has reached a milestone in unravelling such a reducing mechanism after having being able to identify one of the molecules excreted by *L. fermentum* and label its functionality for future applications.

The characterization of HPLA as the main agent of the pH-dependent ferric-reducing activity of *L. fermentum* and its strong reducing ability

dependence on pH, provokes us to hypothesise that excreted HPLA could reduce Fe(III) under acid stomach conditions and facilitate Fe(II) absorption in the duodenum, as occurs for ascorbic and citric acids. Related studies report that low molecular weight fractions exhibiting ferric-reducing activity in human milk enhance iron absorption in newborns.[25]

HPLA contains two chemical moieties with potential reducing Fe(III) activity: the terminal lactic acid and the phenol group. To get insight into the mechanism of the ferric-reducing activity of HPLA, we compared the HPLA ability to reduce Fe(III) at acidic pH with that of its pure chemical moieties, namely lactic acid (LA) and *p*-methylphenol (*p*-mPh), and the mixture of both (LA + *p*-mPh). Both an excess of reducing molecules with respect to Fe(III) and a slight excess of Fe(III) with respect to the active molecules were examined. The first was to understand the kinetics of Fe(III) reduction and the second was to evaluate the ferric-reducing activity of the individual chemical moieties.

The most interesting result of these experiments is that HPLA reduces Fe(III) to the same extent as the mixture of lactic acid and *p*-mPh, practically doubling the reducing capacity of separated LA and *p*-mPh (Figure 5). Thus, both HPLA chemical moieties are effective for Fe(III) reduction and exhibit ferric-reducing activity. When the experiment was done in excess of Fe(III) towards the reducing molecules, the ferric-reducing activity vs. time revealed that HPLA seems to reduce Fe(III), first by the LA moiety and then by *p*-mPh (Figure 5A). Fe(III) reduction versus time shows that the reduction by HPLA follows the same pattern as LA in the initial steps. The %Fe(III) reduction was about 20% by HPLA and 15%

by LA after 2 h, whereas that of *p*-mPh was 90%. This indicates that pure *p*-mPh has faster Fe(III) reduction mechanisms than LA and HPLA. However, over a prolonged period of time (24 h), the % Fe(III) reductions of HPLA, *p*-mPh, and the mixture, LA – *p*-mPh, are similar and close to 100%, whereas that of LA is about 80%.
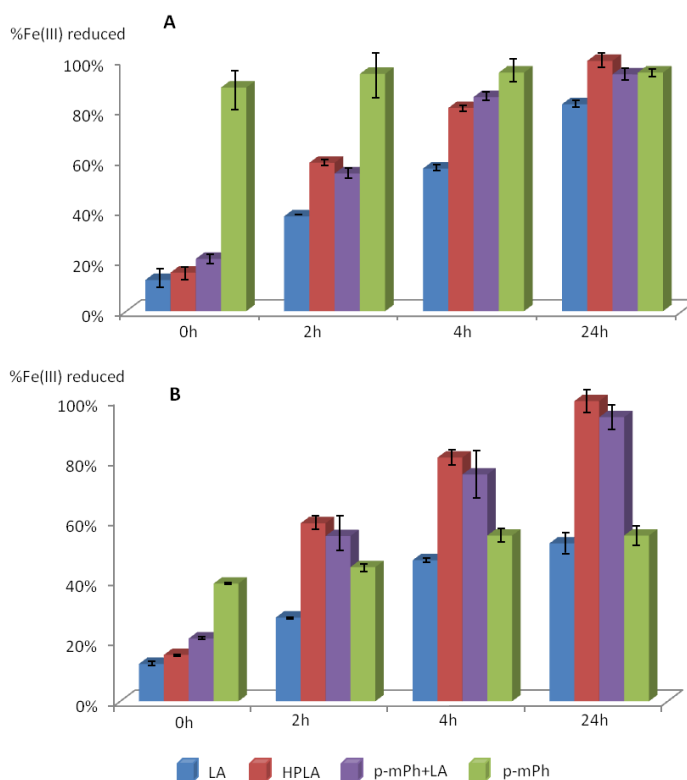

Figure 5. Ferric-reducing activity at pH 3.5 of HPLA, lactic acid (LA), *p*-methylphenol (*p*-mPh) and the mixture of LA and *p*-mPh at different times. A: Fe(III) is in default with respect to reducing molecules. B: Fe(III) is in excess with respect to the reducing molecules. The %Fe(III) reduction is referred to the concentration of Fe(III) (A) or the reducing molecules (B). Error bars, ±SD.

In the second experiment, Fe(III) was in excess with respect to the reducing molecules. The results clearly indicate that the capacity of HPLA

to reduce Fe(III) is double than that of LA and of *p*-mPh and is close to the capacity of the mixture of both (Figure 5B). Therefore, the combination of both chemical moieties (lactic acid and phenol) makes HPLA an extraordinary Fe(III) reducing molecule.

An *in vitro* experiment of iron uptake by enterocytes in the presence of HPLA was performed to test whether HPLA could be related to the effect on iron absorption by probiotic bacteria (Figure 6). HPLA was incubated at two concentrations (36 and 360 µM) with enterocytes (IEC-6 cells) in the presence of Fe(III). *L. fermentum*, and its supernatant liquid obtained after bacterial centrifugation, were also incubated with IEC-6 enterocytes and Fe(III). The concentration of total iron (Fe(II) and Fe(III)) of the solutions was measured at two different times (30 and 300 min), by ICP-OES, to evaluate the amount of iron internalized into the cells.
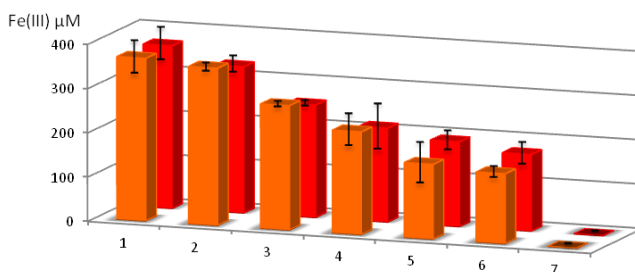
Figure 6. Fe(III) (367 µM) was incubated with enterocyte cells IEC-6 in the presence of HPLA at 36 µM (columns 3), 360 µM (columns 4), *L. fermentum* (columns 5) and the supernatant liquid obtained after centrifugation of *L. fermentum* (columns 6). Fe concentrations in the solutions were measured by ICP-OES after 30 (orange) and 300 min (red). Columns 1 corresponds to the initial Fe(III) solutions; columns 2 corresponds to Fe(III) after incubation with IEC-6 (control) and columns 7 data to the plates only containing cells (control). Error bars, ±SD.

The first conclusion drawn from these data is that *L. fermentum* and its supernatant liquid significantly increased iron absorption by enterocytes. Values for Fe(III) absorption after incubation with enterocytes are very close to initial values, meaning that enterocytes hardly absorb Fe(III) (Figure 6). In contrast, both enterocytes with *L. fermentum* and enterocytes with the supernatant (the excreted molecules) reduce iron concentrations to less than half those of the controls. Thus, the bacteria and excreted molecules facilitate enterocyte iron uptake. Moreover, enterocyte iron absorption by bacteria and by supernatant liquid obtained after centrifugation are similar, which substantiates that the effect of probiotic bacteria on iron absorption is due to the molecules excreted by these bacteria.

HPLA is less effective in assisting enterocytes with iron absorption than the bacterial broth or its supernatant liquid. However, higher HPLA concentrations (360 µM) result in more absorption. Iron concentrations decrease from approximately 350 µM (Figure 6, columns 2) to 231 and 211 µM after 30 and 300 min of incubation, respectively. While the higher concentration of HPLA (360 µM) increases enterocyte iron uptake by about 40%, the increase for the lower HPLA concentration (36 µM) is only about 30%.

Though HPLA clearly increases enterocyte iron absorption, the higher quantities of enterocyte iron absorption by *L. fermentum* and its supernatant liquid with respect to HPLA suggest that other molecules excreted by the probiotic bacteria must also be involved in this complex

process. Lactic acid is a likely candidate, since *L. fermentum* is defined as a lactic bacterium that excretes this molecule while proliferating.

Therefore, HPLA exhibits extraordinary ferric-reducing activity and increases enterocyte iron uptake. Taking into account enterocytes in the duodenum and the participation of the ferric-reducing protein DcytB,[7-8] our results point to a mechanism of iron absorption in which HPLA would act similarly to DcytB by facilitating Fe(III) reduction in the stomach and ultimately promoting Fe(II) uptake by DMT1 channels.

4.3 CONCLUSIONS

L. fermentum, one of the main probiotics of the microbiota, exhibits an extraordinary ferric-reducing activity. This activity is mainly due to one of the molecules excreted by this bacterium: *p*-hydroxyphenyllactic acid (HPLA). HPLA effectively reduces Fe(III) to Fe(II) and in the gastroinstestinal tract can mimic the functionality of the DcytB ferric-reducing protein by promoting iron uptake by enterocytes. We have demonstrated that the increase of iron absorption in the presence of probiotic bacteria is related to the ferric-reducing activity of excreted molecules. These results are a huge step towards solving the enigma of why probiotic bacteria increase iron absorption. This discovery opens new avenues for the treatment of human iron deficiency, one of the most common and widespread nutritional disorders in the world.

4.4 EXPERIMENTAL SECTION

Lactobacillus fermentum culture

L. fermentum CECT5716 was grown in anaerobic conditions in a synthetic medium at 37 °C with orbital agitation for 24 h at an initial concentration of 1 mg of bacteria per ml of medium. The synthetic medium consisted of (g l^{-1}) Na_2HPO_4 – 5.0, KH_2PO_4 – 6.0, trisammonium citrate – 2.0, sucrose – 50.0, $MgSO_4$ – 1.0 and trace elements solution – 10 ml (consisting of (g l^{-1}): $MnSO_4$ – 2.0, $CoCl_2$ – 1.0, $ZnCl_2$ – 1.0 dissolved in 0.1 N HCl solution). The medium with an initial pH 6.7 was sterilized at 121 °C. The final *L. fermentum* cell concentration was 3.3×10^8 CFU ml^{-1}.

Ferric-reducing activity of L. fermentum

1 ml of bacterial culture was mixed with 3.6 µl of a 10 mM $Fe(NO_3)_3 \cdot 9H_2O$ water solution and 7 µl of a 70 mM 3-(2-pyridiyl)-5,6-diphenyl-1,2,4-triazine-*p,p'*-disulfonic acid monosodium salt hydrate (ferrozine, fz) water solution and the resulting mixture was incubated for 6 and 24 h and then centrifuged. The ferric-reducing capacity of *L. fermentum* was measured by UV–vis spectroscopy through the apparition of a band centred at 562 nm due to the formation of the complex [Fe^{II}(fz)$_3$] (ε^{562} = 27,900 M^{-1}). A control of the ferric-reducing activity of the culture media, without bacteria, showed no UV–vis band at 562 nm. Similar ferric-reducing activity was exhibited by the corresponding supernatant solution (1 ml) from the bacterial culture.

Isolation of excreted bacterial compound/s with ferric-reducing activity

Bacteria were removed by centrifugation at 3000g for 10 min and then the supernatant was filtered, using EMD Millipore Steritop™ Sterile Vacuum Bottle-Top Filters. 2 l of the filtered supernatant solution were subjected to solid-phase extraction on a column packed with SP-207ss brominated polystyrenic resin (65 g to render a column bed of 3.5 cm diameter and 11 cm height) previously equilibrated with water. The column was washed with water (1 l) and afterwards eluted with 200 ml of methanol. The solvent was evaporated under a nitrogen stream and the resulting extract dissolved in 500 µl of DMSO and further purified by reversed phase semi-preparative HPLC (Agilent Zorbax SB-C8, 9.4 × 250 mm, 7 µm; 3.6 ml/min, UV detection at 210 and 280 nm) with a linear gradient of water-CH3CN (5%–50%) over 40 min to yield 80 fractions of 1.8 ml. The ferric-reducing activity of each fraction was tested, using a 96-well microtiter plate containing 2 µl of each fraction diluted with 198 µl of water. 1.08 µl of a 10 mM $Fe(NO_3)_3$ stock solution and 2.1 µl of a 70 mM fz stock solution were added to each well. The presence of the complex $[Fe^{II}(fz)_3]$, determined by measuring the absorbance at 570 nm, using a microplate reader (Envision 2104 multilabel reader. Perkin Elmer), was detected only in fractions 8–11. These fractions were pooled, evaporated and then dissolved in 1 ml of distilled water. The resulting water solution was further purified by reversed phase semi-preparative HPLC (Waters Atlantis C18, 9.4 × 250 mm, 7 µm; 3.6 ml/min, UV detection at 210 and 280 nm) with a linear gradient of water-CH_3CN (0–25%) over 40 min to yield 80 fractions of 1.8 ml. The ferric-reducing activity of these fractions was tested as

before. Only fractions 28 and 29 exhibited ferric-reducing activity. These fractions were pooled, evaporated and analyzed by LC–ESI-TOFMS and NMR spectroscopy.

Structure elucidation of the excreted bacterial compound with ferric-reducing activity

For NMR analysis, the sample (pooled dry fractions or the HPLA standard) was dissolved in deuterated methanol, CD_3OD. NMR spectra, including ^{1}H, COSY, HSQC and HMBC, were recorded on a Bruker Avance III spectrometer (500 and 125 MHz for 1H and 13C NMR, respectively) equipped with a 1.7 mm TCI MicroCryoProbeTM, using the signal of the residual deuterated solvent as internal reference (δ_H 3.31 and δ_C 49.0 ppm). LC–DAD-ESI-HRMS analysis of an aliquot of the final pooled fractions was performed on an Agilent 1200 rapid resolution HPLC system hyphenated with a Bruker maXis QTOF mass spectrometer, using a Zorbax SB-C8 column (2.1 × 30 mm, 5 µm), maintained at 40 °C and with a flow rate of 300 µl min^{-1}. Solvent A consisted of 10% acetronitrile and 90% water with 1.3 mM trifluoroacetic acid and ammonium formate, and solvent B was 90% acetronitrile and 10% water with 1.3 mM trifluoroacetic acid and ammonium formate. The gradient started at 10% B and went to 100% B in 6 min, kept at 100% B for 2 min and returned to 10% B for 2 min to initialize the system. Full diode array UV scans from 100 to 900 nm were collected in 4 nm steps at 0.25 s/scan. The mass spectrometer was operated in positive ESI mode. The instrumental parameters were: 4 kV capillary voltage, drying gas flow of 11 l min^{-1} at 200 °C, nebulizer pressure at 2.8 bars. TFA-Na cluster ions were used for

mass calibration of the instrument prior to sample injection. Pre-run calibration was by infusion with the same TFA-Na calibrant. The structure of the target compound was established, using the NMR data. Its molecular formula was corroborated by the HRMS results. Further confirmation on the identity was obtained by direct comparison with the ^{1}H and HSQC NMR spectra of an HPLA standard prepared in CD_3OD. The corresponding test of ferric-reducing activity of the HPLA standard unequivocally determined this molecule as the target excreted compound responsible for such reducing power displayed by the *L. fermentum* culture.

Ferric-reducing activity of HPLA vs pH

Racemic HPLA was acquired from Sigma-Aldrich. Solutions of HPLA (144 µM) were prepared in different buffers with pH ranging from 3.0 to 7.4 and mixed with solutions of 10 mM $Fe(NO_3)_3 \cdot 9H_2O$ and 70 mM of fz. Ferric-reducing activity of HPLA at these different pH values was measured by UV–vis spectroscopy through the appearance of a band centred at 562 nm, due the formation of the complex $[Fe^{II}(fz)_3]$ ($\varepsilon^{562} = 27{,}900$ M^{-1}). The results showed that HPLA exhibits high ferric-reducing activity only at low pH.

Ferric-reducing activity of L. fermentum after HPLA addition

The ferric-reducing capacity of *L. fermentum* was measured, as indicated above, after incubation for 6 and 24 h. HPLA (3.6 µM) was added to the supernatant obtained after centrifugation of the 6 h culture and the ferric-reducing activity of the resulting mixture was measured.

The ferric-reducing activity of HPLA (3.6 µM) in the medium grown was used as control.

Ferric-reducing activity of HPLA versus lactic acid (LA), p-methylphenol (p-mPh) and the mixture p-methylphenol and lactic acid (LA + p-mPh)

Two different experimental conditions were assayed, excess and deficiency of Fe(III) with respect to the reducing molecules. The ferric-reducing activity was referred to the initial concentrations of Fe(III) or the chemical reductant, respectively.

A 50 mM stock solution of HPLA was prepared by dissolving 9.1 mg in 1 ml of Mili-Q water. Solutions of LA and *p*-mPh at the same 50 mM concentration were prepared, as well as a mixture solution of both (LA + *p*-mPh) containing 50 mM of each reducing molecule. Lactic acid and *p*-methylphenol were also purchased from Sigma-Aldrich.

110 µl of each stock solution were added to 879 µl of Mili-Q water containing 3.6 µl of a 10 mM solution of $Fe(NO_3)_3 \cdot 9H_2O$ and 7 µl of a ferrozine solution (70 mM). The *p*-methylphenol and lactic acid mixture was preparing by adding 110 µl of the *p*-methylphenol stock solution and 110 µl of the lactic acid stock solution to 769 µl of Mili-Q water containing 3.6 µl of a 10 mM $Fe(NO_3)_3 \cdot 9H_2O$ solution and 7 l of a 70 mM fz solution. The final concentrations of the reducing molecules and Fe(III) were 5.5 mM and 36 µM. The ferric-reducing activity of each sample was determined at 0, 2, 4 and 24 h by monitoring the UV–vis band at 562 nm of the complex $[[FeII(fz)_3]$. In a second experiment a 25 µM concentration of each reducing molecule was used.

*In vitro experiment on iron internalization in enterocyte cells*

IEC6 epithelial rat small intestine cells were provided by the Scientific Instrumentation Centre (University of Granada, Spain). Cell line was grown adherently and maintained in DMEM + 2 mM glutamine + 0.1 IU/ml of insulin + 5% of foetal bovine serum (FBS) at 37 °C in 5% CO_2. All experiments were performed in 12-well plates. Cells were seeded onto the plates at a density of 5×10^4 cells per well and incubated for 48 h prior to the experiments.

The wells were filled up to a final volume of 1 ml with a water solution of $Fe(NO_3)_3 \cdot 9H_2O$ (360 µM), the grown medium and HPLA, at two different concentrations, 360 and 36 µM. Two more wells with a blank sample containing only cells were also prepared. Plates were incubated at 37 °C for 0.5 or 5 h. Samples were filtered, using a 0.2 µm Minisart RC filter and the total iron concentration (Fe(II) and Fe(III)) measured by ICP-OES.

Statistical analysis

The ferric-reducing activity of HPLA versus LA, *p*-mPh and the mixture LA + *p*-mPh and the *in vitro* experiment on iron internalization in enterocyte cells were conducted in triplicates. Descriptive error bars represent the standard deviation (SD) of the triplicates and it was calculated using the n − 1 method.
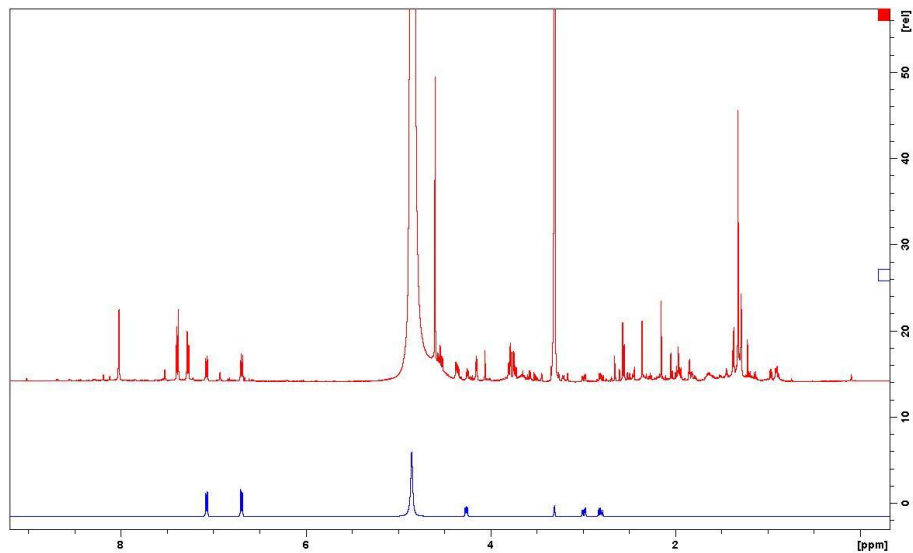
4.5 SUPPORTING INFORMATION
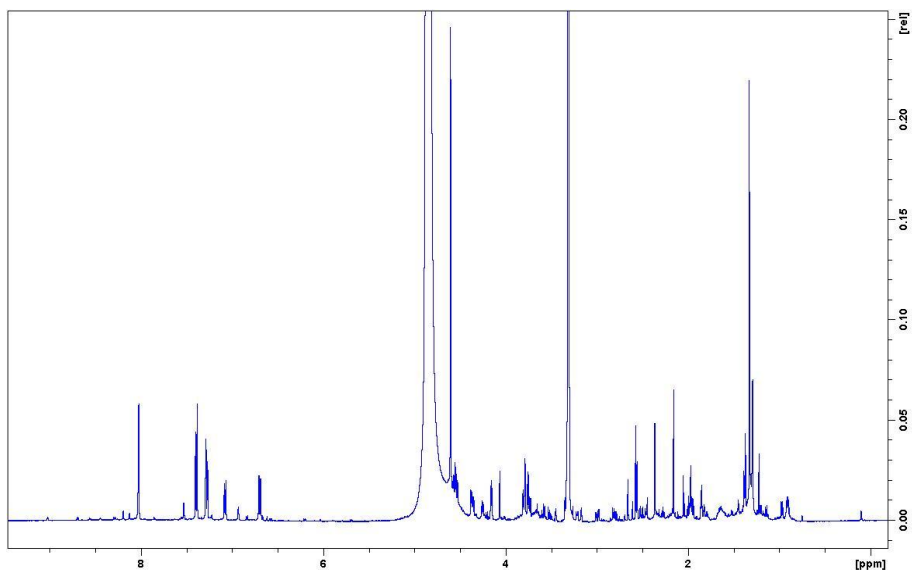
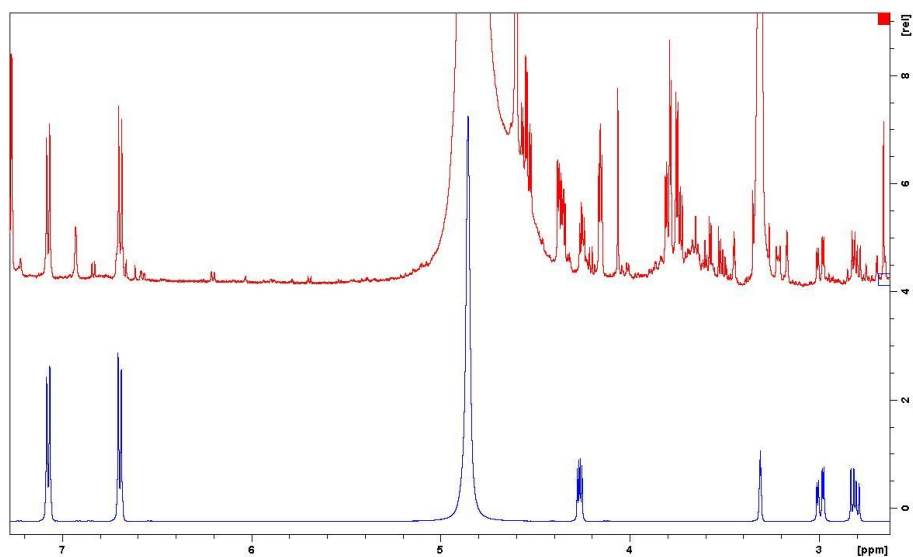**Figure S1**. ^{1}H NMR spectrum (500 MHz, CD$_3$OD) of the final pooled fractions displaying ferric-reducing activity.
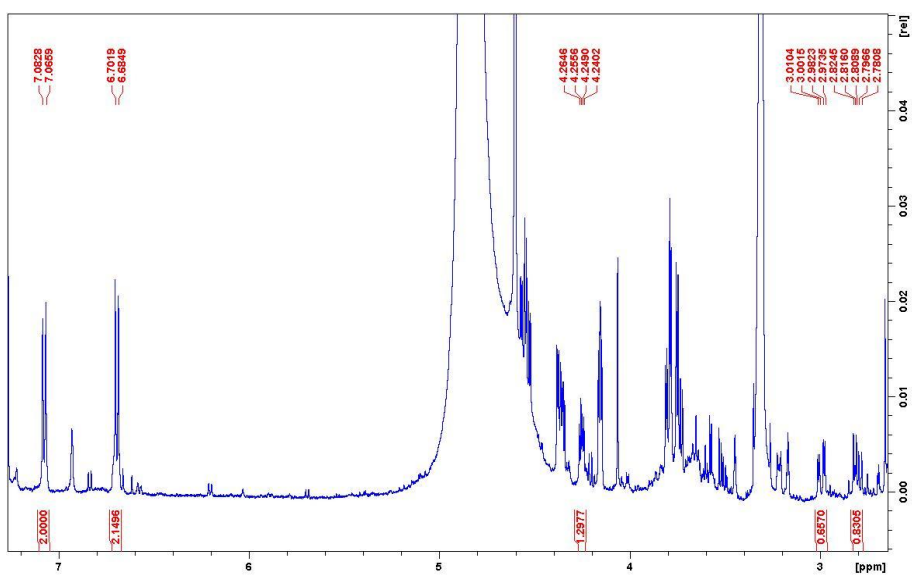
Figure S2. Expansion of the ^{1}H NMR spectrum of the final pooled fractions displaying ferric-reducing activity, highlighting the signals of HPLA.
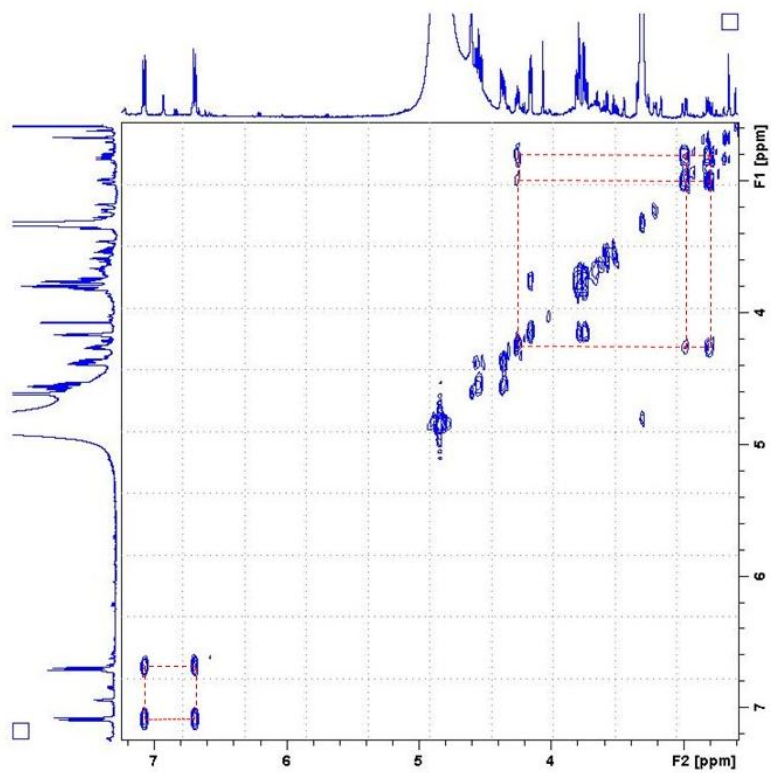
Figure S3. Comparison of the ^{1}H NMR spectra of the final pooled fractions displaying ferric-reducing activity (red) and the HPLA standard (blue).
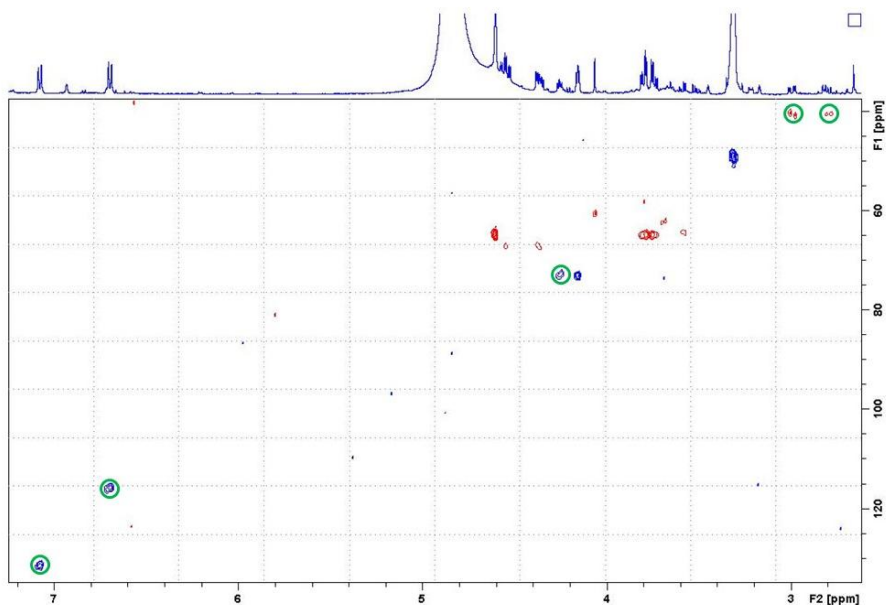

Figure S4. Expansion of the ^{1}H NMR spectra of the final pooled fractions displaying ferric-reducing activity (red) and the HPLA standard (blue).
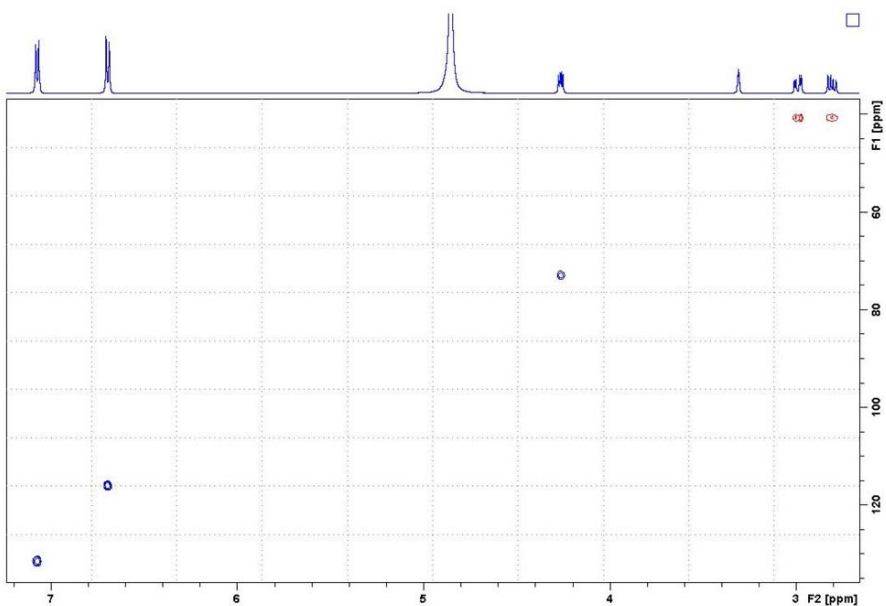
Figure S5. Expansion of the COSY spectrum of the final pooled fractions displaying ferric-reducing activity showing the key correlations for HPLA.
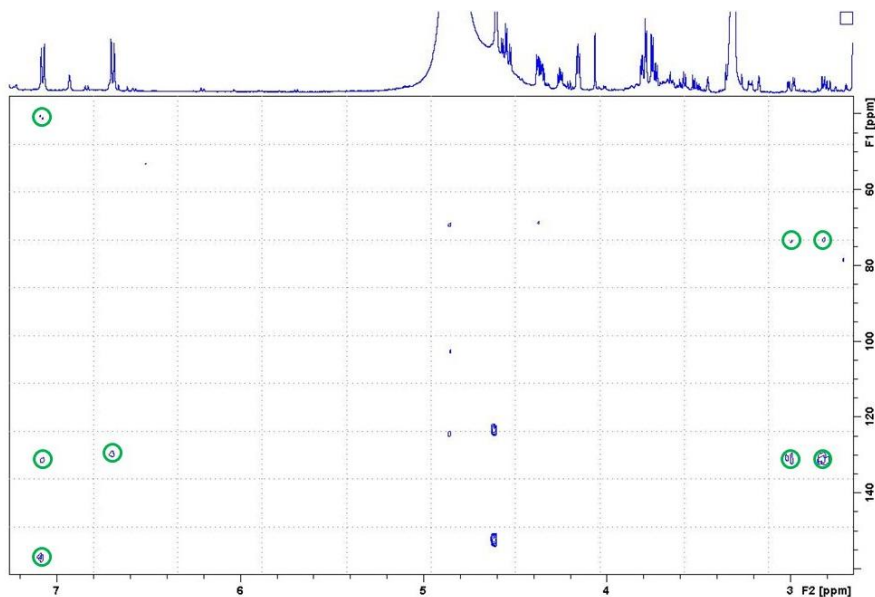
Figure S6. Expansion of the HSQC spectrum of the final pooled fractions displaying ferric-reducing activity showing the cross peaks of HPLA.
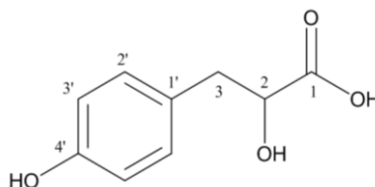

**Figure S7**. HSQC spectrum of the HPLA standard.

Figure S8. Expansion of the HMBC spectrum of the final pooled fractions displaying ferric-reducing activity showing key correlations for HPLA.

position	δ_H (*J* in Hz)	δ_C , type
1	-	n. d. , C
2	4.25, dd (7.7, 4.5)	72.7, CH
3	a 2.99, dd (14.0, 4.4) b 2.80, dd (14.0, 7.8)	40.4, CH$_2$
1'	-	129.8, C
2'	7.07, d (8.5)	131.3, CH
3'	6.69, d (8.5)	115.7, CH
4'	-	156.8, C

Table S1. NMR Spectroscopic Data (500 MHz, CD$_3$OD, at 24 ºC) for HPLA
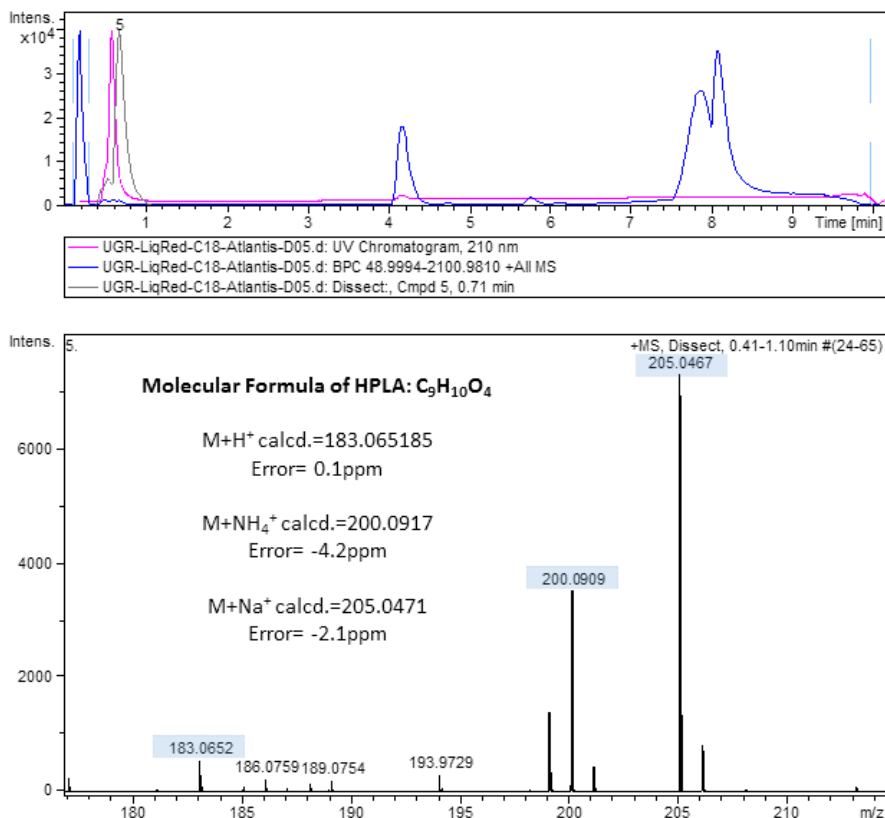
Figure S8. LC-UV-HRMS analysis of the final pooled fractions displaying ferric-reducing activity showing detection of a major component matching the molecular formula of HPLA.

4.6 REFERENCES

1. Crichton, R., *Inorganic biochemistry of iron metabolism: From molecular mechanisms to clinical consequences*. John Wiley & Sons: England, 2001.

2. Silva, B.; Faustino, P., An overview of molecular basis of iron metabolism regulation and the associated pathologies. *Biochimica et Biophysica Acta (BBA) - Molecular Basis of Disease* **2015,** *1852* (7), 1347-1359.

3. Milto, I. V. S., I. V.; Prokopieva,V. D.; Klimenteva,T. K. , Molecular and cellular bases of iron metabolism in humans. *Organic Chemistry and Pharmaceutical Substances Lab* **2016,** *81*.

4. R. Huch, R. S., *Iron deficiency and iron deficiency anaemia. Pocket Atl.* Thieme Medical Publishers: New York, 2006.
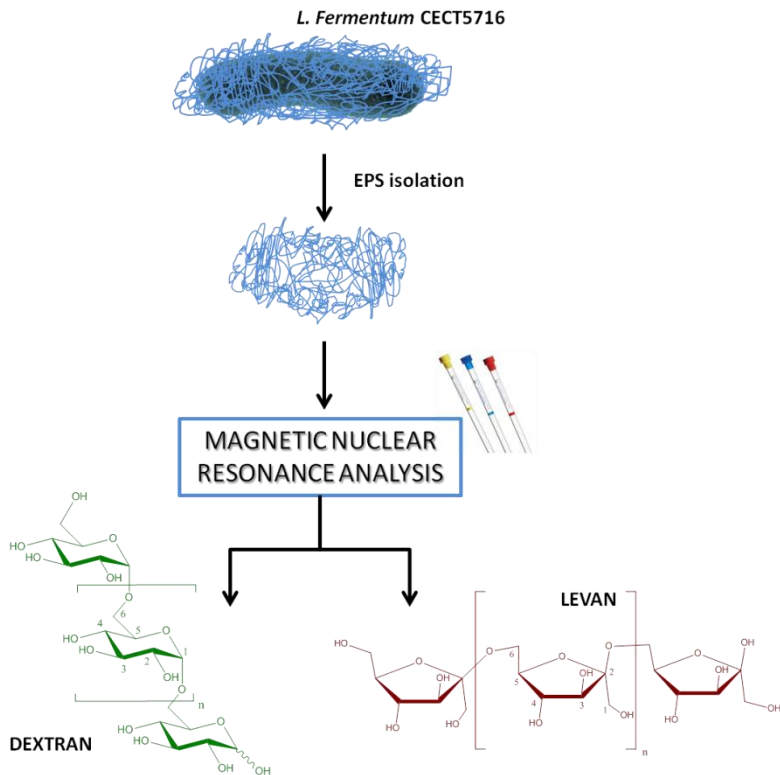
5. Robert R. Crichton, B. G. D., Peter Geisser, *Iron therapy - With Special Emphasis on Intravenous Administration*. 4th ed.; UNI-MED Science: 2008; p 128.

6. Shayeghi, M.; Latunde-Dada, G. O.; Oakhill, J. S.; Laftah, A. H.; Takeuchi, K.; Halliday, N.; Khan, Y.; Warley, A.; McCann, F. E.; Hider, R. C.; Frazer, D. M.; Anderson, G. J.; Vulpe, C. D.; Simpson, R. J.; McKie, A. T., Identification of an intestinal heme transporter. *Cell* **2005,** *122* (5), 789-801.

7. Lane, D. J.; Bae, D. H.; Merlot, A. M.; Sahni, S.; Richardson, D. R., Duodenal cytochrome b (DCYTB) in iron metabolism: an update on function and regulation. *Nutrients* **2015,** *7* (4), 2274-96.

8. McKie, A. T., The role of Dcytb in iron metabolism: an update. *Biochemical Society transactions* **2008,** *36* (Pt 6), 1239-41.

9. Conrad, M. E.; Umbreit, J. N., Pathways of Iron Absorption. *Blood Cells, Molecules, and Diseases* **2002,** *29* (3), 336-355.

10. Lin, C. S.; Chang, C. J.; Lu, C. C.; Martel, J.; Ojcius, D. M.; Ko, Y. F.; Young, J. D.; Lai, H. C., Impact of the gut microbiota, prebiotics, and probiotics on human health and disease. *Biomedical journal* **2014,** *37* (5), 259-68.

11. Peccia, J.; Kwan, S. E., Buildings, Beneficial Microbes, and Health. *Trends in microbiology* **2016,** *24* (8), 595-7.

12. Sommer, F.; Backhed, F., The gut microbiota--masters of host development and physiology. *Nature reviews. Microbiology* **2013,** *11* (4), 227-38.

13. EFSA Panel on Dietetic Products, N., and Allergies (NDA), Scientific Opinion on Dietary Reference Values for vitamin D1. *European Food Safety Authority (EFSA)* **2016**, 179.

14. Bering, S.; Suchdev, S.; Sjøltov, L.; Berggren, A.; Tetens, I.; Bukhave, K., A lactic acid-fermented oat gruel increases non-haem iron absorption from a phytate-rich meal in healthy women of childbearing age. *British Journal of Nutrition* **2007,** *96* (1), 80-85.

15. Hoppe, M.; Onning, G.; Berggren, A.; Hulthen, L., Probiotic strain Lactobacillus plantarum 299v increases iron absorption from an iron-supplemented fruit drink: a double-isotope cross-over single-blind study in women of reproductive age. *The British journal of nutrition* **2015,** *114* (8), 1195-202.

16. Perez-Conesa, D.; Lopez, G.; Ros, G., Effect of Probiotic, Prebiotic and Synbiotic Follow-up Infant Formulas on Iron Bioavailability in Rats. *Food Science and Technology International* **2007,** *13* (1), 69-77.

17. Suzuki, Y.; Kosaka, M.; Shindo, K.; Kawasumi, T.; Kimoto-Nira, H.; Suzuki, C., Identification of antioxidants produced by Lactobacillus plantarum. *Bioscience, biotechnology, and biochemistry* **2013,** *77* (6), 1299-302.

18. Lavermicocca, P.; Valerio, F.; Evidente, A.; Lazzaroni, S.; Corsetti, A.; Gobbetti, M., Purification and Characterization of Novel Antifungal Compounds from the Sourdough Lactobacillus plantarum Strain 21B. *APPLIED AND ENVIRONMENTAL MICROBIOLOGY* **2000,** *66* (9), 6.

19. Crowley, S.; Mahony, J.; van Sinderen, D., Current perspectives on antifungal lactic acid bacteria as natural bio-preservatives. *Trends in Food Science & Technology* **2013,** *33* (2), 93-109.

20. Li, X.; Jiang, B.; Pan, B., Biotransformation of phenylpyruvic acid to phenyllactic acid by growing and resting cells of a Lactobacillus sp. *Biotechnology letters* **2007,** *29* (4), 593-7.

21. Valerio, F.; Lavermicocca, P.; Pascale, M.; Visconti, A., Production of phenyllactic acid by lactic acid bacteria: an approach to the selection of strains contributing to food quality and preservation. *FEMS microbiology letters* **2004,** *233* (2), 289-95.

22. Mu, W.; Yang, Y.; Jia, J.; Zhang, T.; Jiang, B., Production of 4-hydroxyphenyllactic acid by Lactobacillus sp. SK007 fermentation. *Journal of bioscience and bioengineering* **2010,** *109* (4), 369-71.

23. Carmona, F.; Martin, M.; Galvez, N.; Dominguez-Vera, J. M., Bioinspired magneto-optical bacteria. *Inorganic chemistry* **2014,** *53* (16), 8565-9.

24. Ana Gonzalez, N. G., Miguel Clemente-Leon, Jose Manuel Dominguez-Vera, Electrochromic polyoxometalate material as a sensor of bacterial activity. *Chemical Communications* **2015,** *51*, 4.

25. Pullakhandam, R.; Nair, M. K.; Kasula, S.; Kilari, S.; Thippande, T. G., Ferric reductase activity of low molecular weight human milk fraction is associated with enhanced iron solubility and uptake in Caco-2 cells. *Biochemical and Biophysical Research Communications* **2008,** *374* (2), 369-372.

L. Fermentum CECT5716

EPS isolation

MAGNETIC NUCLEAR RESONANCE ANALYSIS

DEXTRAN

LEVAN

CHAPTER 5.

ISOLATION, PURIFICATION AND CHARACTERIZATION OF *L. FERMENTUM* CECT5716 EPS

5.1 INTRODUCTION

As mention in the Introduction chapter, a biofilm is constituted by bacteria and a matrix of substances that are excreted out by them. Among all these extracellular polymeric substances, the most abundant are the exopolysaccharides (EPS).[1]

Composition and structure of EPS vary depending on many physical factors such as the environment in which the biofilm is formed or the type and amount of bacteria absorbed on it. For this reason, biofilms are considered unique for each environment and microbiota.[2] Nutrients' gradient between the carbon source and other limiting nutrients (nitrogen, potassium, phosphate, etc.) also influence the EPS composition but more specifically the amount of EPS formed.[3]

Despite the complexity of the characterization of EPS due to all of these physical parameters, some data, related with the structure, are known. The primary configuration is directly determined by the composition. Then, polymers acquire a secondary conformation, in form of aggregated helices, in which the typical backbones for rigid structures correspond with β-(1,4) or β-(1,3) linkages and for the more flexible ones with α-(1,2) or α-(1,6) linkages. Normally, helices are very long chains with a molecular mass of the order of 10^6 and aspect of floc or gel.[3] Finally, a tertiary structure results by interactions of secondary helices such as London forces, electrostatic interactions and hydrogen bonds.[4]

The characterization of the composition and structure of biofilm's EPS is a good strategy to understand the mechanism by which several

functions of them are carried out. For example, EPS from lactic acid bacteria (LAB), which are well known beneficial microorganisms for humans' health, are related with the adhesion and colonization of these organisms to the gastrointestinal tract.[5] Moreover, these EPS are industrially implied in the development of functional food products as yoghurt, cheese or cereal-based products[6-9] and some biological functions such as the possibility of acting as prebiotics have been reported.[10-12]

Two different types or EPS can be synthesized from LAB: Heteropolysaccharides (HePS) and homopolysaccharides (HoPS). HePS are produced by mesophilic and thermophilic LAB intracellularly and then the repeating units translocate the membrane polymerizing extracellularly to form polymers with repeating units of three to eight monosaccharides, derivatives of monosaccharides or substituted monosaccharides. On the other hand, HoPS are directly extracellularly synthesized from sucrose degradation by LAB producing glucansucrases and fructansucrases enzymes, obtaining α-glucans or β-fructans, respectively. Regarding to the linkage type and the position of the carbon involved in the bond, HoPS are classify in α-D-glucans (dextran, mutan, reuteran, and alternan), β-D-glucans and fructans (levan and inulin-type).[13] Figure 1 summarize a classification of the HoPs produced by LAB bacteria, indicating the linkage type and branching linkage.
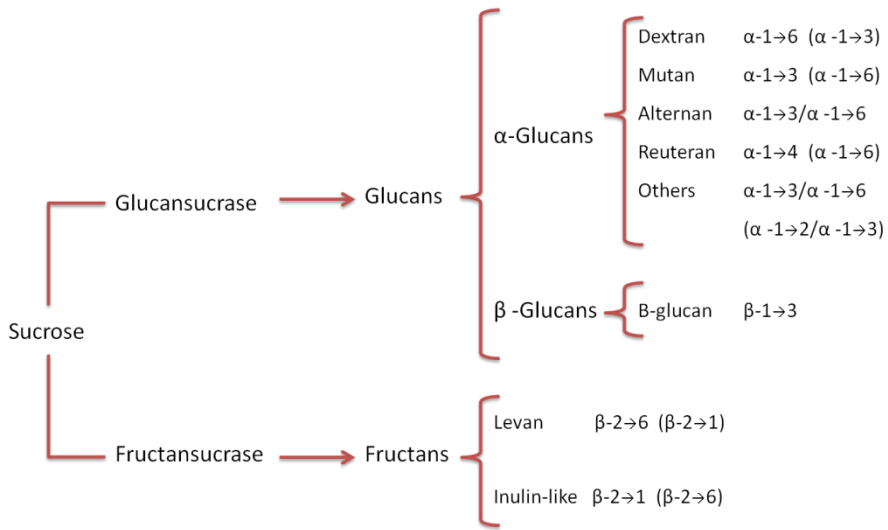
Figure 1. Homopolysaccharides (HoPS) classification and their typical linkages. The bond in parenthesis represents the branching linkage.

A destructive or non-destructive approach can be follow for the isolation and characterization of the EPS. In the first one, chemical methods, such as centrifugation, filtration, heating, blending and sonication, followed by microscopy and spectroscopic techniques, are used to find the monosaccharide units composing the EPS. On the other hand, the non-destructive methods apply the same kind of techniques to obtain information of the whole structure and composition of the EPS.[14-15]

Following the destructive approach, monosaccharide units from many different strains of LAB have been isolated and characterized. In the case of *Lactobacillus plantarum* strains, EPS composed of mannose, fructose, galactose and glucose for YW32 strain,[16] glucose and mannose for RJF$_4$ strain,[17] and glucose and galactose for YW11 strain[18] have been reported.

Other characterized EPS composition for LAB which have been characterized are: i) rhamnose, raffinose and maltose for *L. fermentum* CFR 2195;[19] ii) two fractions of different molecular mass for *Lactobacillus rhamnosus* KF5, one of 1.36×10^4 Da, composed of glucose, arabinose, glucosamine, galactosamine and galactose and other of 1.23×106 Da, contained rhamnose, glucose and galactose;[20] and iii) glucose, galactose, N-acetylglucosamine and phosphate for *Lactobacillus suebicus*.[21]

In the case of the whole composition of the EPS by the use of non-destructive approaches several polymers have been found in LAB cultures. Dextran, mutan, reuteran, β-glucan, levan and inulin have been reported as EPS produced by *Lactobacillus* strains by the use of high performance size exclusion chromatography (HPSEC).[9, 22] In the case of *Leuconostoc* strains, dextran, alternan, levan and inulin EPS have been found. Finally, *Streptococcus* ability to synthesize dextran, mutan, levan and inulin have been determined.[7, 13]

In this chapter it will be described the isolation, purification and characterization of the EPS from a probiotic bacteria, *L. fermentum* CECT5716, by the use of a non-destructive approach which uses nuclear magnetic resonance.

5.2 RESULTS AND DISCUSSION

The native EPS were analyzed by NMR spectroscopy. 0.8 mg of the EPS sample was dissolved in 100 μL of D_2O. Some material remained insoluble and the sample was centrifuged, transferring the clear supernatant to the NMR tube.

The 1D 1H NM spectrum (Figure 2) shows two types of carbohydrate signals. On the one hand, a set of sharp signals corresponding to sucrose are clearly observed, indicating that the native EPS sample would require further dialysis to get rid of sucrose. On the other hand, broad signals overlapping with those of sucrose are also clearly observed. Their broad appearance immediately associates them to the polysaccharide.[23]
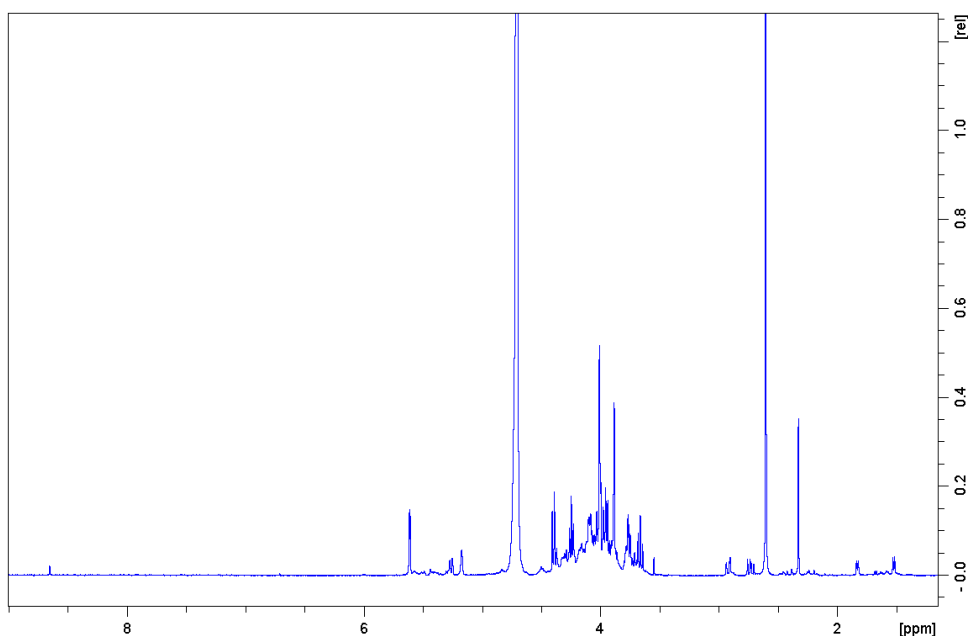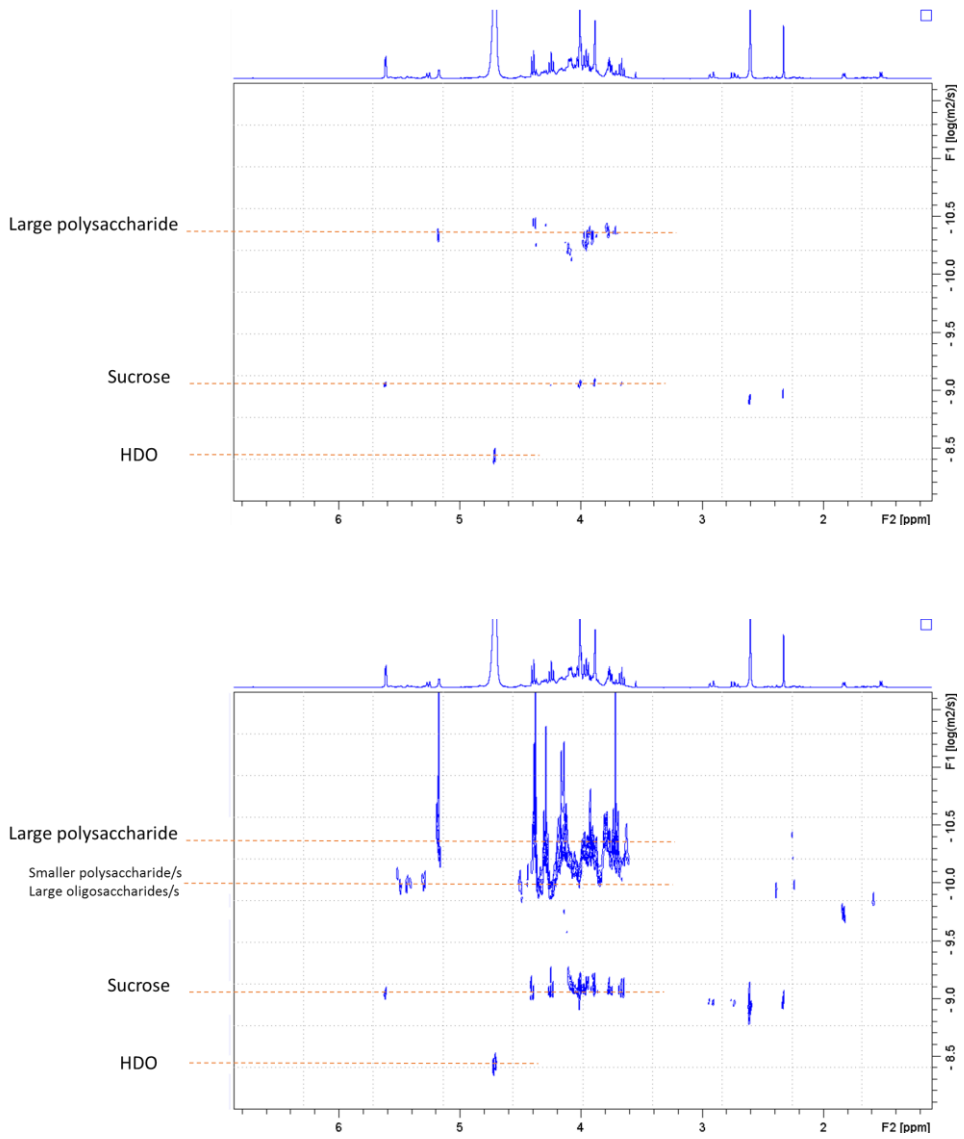

Figure 2. ^{1}H NMR spectrum of native EPS sample (recorded in D_2O at 297 K, 500 MHz)

To obtain a virtual spectrum of the polysaccharide, a pulsed field gradient (PFG) diffusion NMR experiment was carried out taking advantage of the huge difference in molecular size between sucrose and EPS. Diffusion-ordered spectroscopy has already proved to be a very appropriate technique for studying polysaccharides.[24-25] The diffusion encoded spectrum was acquired by varying the gradient strength while

keeping the diffusion time constant.[26] The raw data was processed first by biexponential fitting to get a DOSY (diffusion-ordered spectroscopy) plot or pseudospectrum (chemical shift vs. log Diffusion coefficient)[27] and also by the multivariate curve resolution method DECRA (direct exponential curve resolution algotirhm) to get virtual spectra associated to different diffusion coefficients.[28-29]

A DOSY plot can be compared to a virtual size exclusion chromatography separation since the higher the molecular size the smaller the diffusion coefficient. The DOSY pseudospectrum of the native EPS sample clearly identifies signals corresponding to sucrose, a large polysaccharide and smaller polysaccharides species (Figure 3). A very rough estimation, in the absence of a proper calibration curve with polysaccharide standards, of the MW for the large polysaccharide would be around 2.5×10^6 Da and for the smaller polysaccharide around 180 kDa.[24-25]

The traces at different diffusion coefficient corresponding to those molecular species can be extracted directly from the DOSY plot, however, such traces display low resolution and an alternative and better approach to obtain the virtual subspectra of those species is provided by the DECRA processing of the same PFG diffusion NMR raw data. Not surprisingly, this approach provided very clean virtual subspectra of the molecular species which are very different in molecular size (Figure 4). The DECRA subspectrum of the large polysaccharide is equivalent to that which could be obtained with a fully dialized sample free from sucrose. This polysaccharide subspectrum show the typical proton resonances observed for dextran and levan.[30]

Figure 3. DOSY pseudospectrum of native EPS sample. The diffusion coefficient of the identified molecular species are highlighted with red dashed lines. The upper and lower plots display different threshold of the contour levels.
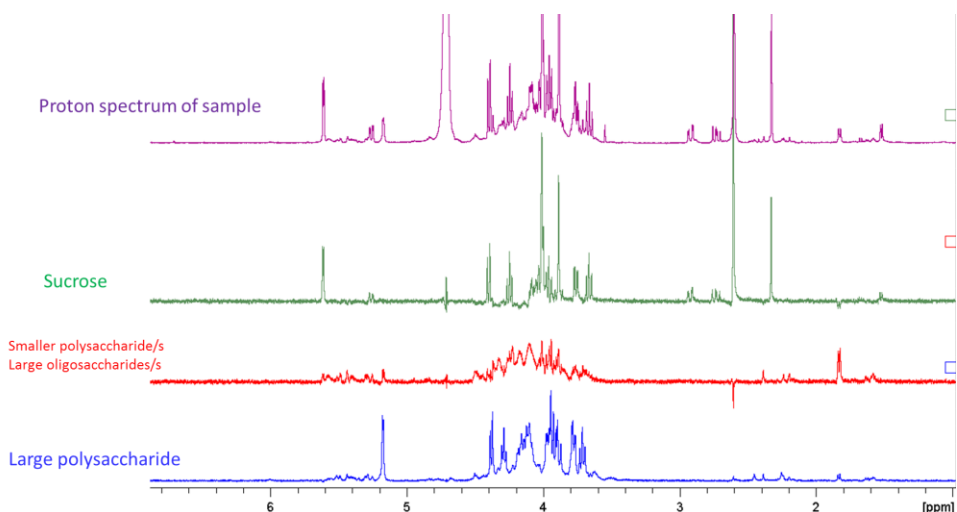
Figure 4. DECRA subspectra of the different molecular species (corresponding to different diffusion coefficients) found in the native EPS sample. The identified molecular species are indicated in each subspectrum.

Both dextran and levan are archetypical EPS from lactic acid bacteria obtained from sucrose by the action of dextransucrases and levansucrases.[13] Interestingly, a direct comparison of the DECRA subspectrum of the polysaccharide with the proton spectra of the EPS isolated from *Leuconostoc mesenteroides* bacteria (strains K24 and G15)[31] provides an unequivocal identification of the chemical nature of the EPS we have isolated from *Lactobacillus fermentum* CECT5716 (Figure 5).

Additionally, an HSQC spectrum was also acquired (Figure 6). The sucrose signals are easily identified and the signals of both dextran and levan could likewise be assigned unambiguously, providing a further evidence on the chemical nature of the polysaccharides produced by *Lactobacillus fermentum* CECT5716.
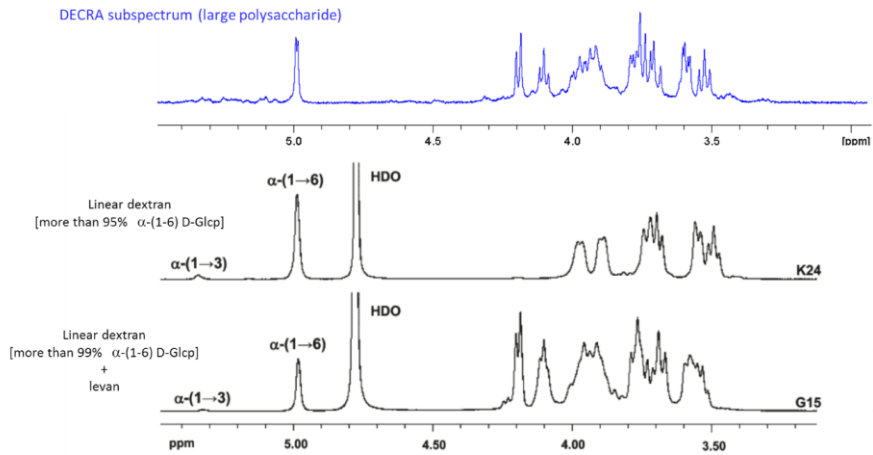
Figure 5. DECRA subspectrum of the large polysaccharide from *Lactobacillus fermentum* CECT5716 compared with the spectra of the EPS obtained from *Leuconostoc mesenteroides* strains K24 and G15 (from Bounaix, M. *et al.*[31]). The chemical shift scale of the DECRA subspectrum has been recalibrated (compared to Figures. 1-3) to facilitate the comparison.
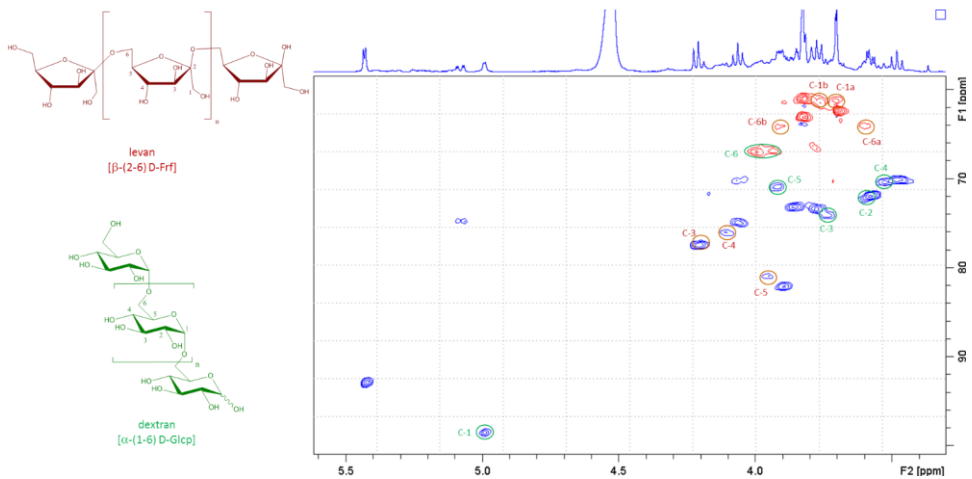
Figure 6. Edited HSQC spectrum (methylene signals in red, methyl and methine signals in blue) of native EPS sample from *Lactobacillus fermentum* CECT5716. The signals of dextran and levan are unambiguously identified and highlighted in the spectrum.

5.3 CONCLUSIONS

A new isolation and characterization of EPS from a probiotic bacteria such as *L. fermentum* CECT5716 have been carried out. The EPS from this bacterium displays an estimated size around 2.5 x 10^6 Da and are comprised by two homopolysaccharides. On the one hand, a linear dextran essentially displaying α-(1-6) D-glucopyranose linkages as indicated by the presence in the DECRA subspectrum of basically just one anomeric glucopyranose proton. On the other hand, levan, a polysaccharide comprised by fructofuranose monomers displaying β-(2-6) D-fructoranose linkages. The direct comparison with the EPS spectrum of *L. mesenteroides* strain G15[31] (Figure 4), suggests that *L. fermentum* CECT5716 synthesizes both dextran and levan, approximately in a 1:3 ratio.

An accurate determination of the actual dextran:levan ratio and the molecular weight of these homopolysaccharides produced by *L. fermentum* CECT5716 will be carried out in the future using commercial standards of dextran and levan of known molecular weight. In addition, their biological activity and implication in the probiotic role of *L. fermentum* CECT5716 will be tested.

5.4 EXPERIMENTAL SECTION

Bacterial growth

L. fermentum CECT5716 was grown in anaerobic conditions in a synthetic growth medium at 37 $^{\circ}$C on an orbital shaker for 24 h with an initial concentration of 1mg bacteria in 1mL of medium. The synthetic

growth medium consisted of (g L^{-1}) Na_2HPO_4 – 5.0, KH_2PO_4 – 6.0, trisammonium citrate – 2.0, sucrose – 50.0, $MgSO_4$ – 1.0 and trace elements solution – 10 ml (consisting of (g L^{-1}): $MnSO_4$ – 2.0, $CoCl_2$ – 1.0, $ZnCl_2$ – 1.0 dissolved in 0.1 N HCl solution). The medium had an initial pH 6.7 and was sterilized at 121ºC. The final *L. fermentum* cell concentration was 3.3·108 CFU mL^{-1}.

EPS of L. fermentum isolation

Bacteria were removed by centrifugation at 3000 g for 10 min. The supernatant was again centrifuged to guarantee that all the cells were removed. Ice-cold ethanol (2 vol) was added to the cell-free supernatant (1 vol) under continuous stirring, and kept overnight for precipitation in the refrigerator. The alcoholic supernatant was centrifuged at 22,000 g for 35 min and the EPS precipitated were washed with acetone and again centrifuged. The solid obtained was dissolved in distilled water (100 mL) and dialyzed against distilled water for 24h (MWCO 12,000 to 14,000). The dialyzed solution was frozen and then lyophilized.

NMR Spectroscopy

Native EPS sample (0.8 mg) was dissolved in 100 µL of D2O and transferred to a 1.7 mm NMR tube. 1H and 13C chemical shifts are referenced to external sucrose. The NMR spectra were acquired on an Avance III (Bruker) 500 MHz spectrometer (500 MHz for 1H NMR and 125 MHz for 13C NMR) using a 1.7 mm MicroCryoprobe™. Acquisition and spectral processing was carried with TopSpin 3.2 software. The temperature was 297 K. 1D 1H NMR and HSQC spectra were acquired

using standard pulse sequences (zg30 and hsqcedetgpsp.3 respectively) from the spectrometer library The Diffusion NMR experiment was recorded using a stimulated echo sequence incorporating bipolar gradients (pulse program stegpbp1s from the spectrometer library). The gradient strength was exponentially incremented in 12 steps from 5% up to 95% of the maximum gradient strength provided by the probe. Diffusion time was set to 175 ms and gradient pulse durations to 1.2 ms. Spectral acquisition and processing was carried out with Topspin 3.2 software.

5.5 REFERENCES

1. Wingender, J.; Neu, T. R.; Flemming, H.-C., What are Bacterial Extracellular Polymeric Substances? In *Microbial Extracellular Polymeric Substances: Characterization, Structure and Function*, Wingender, J.; Neu, T. R.; Flemming, H.-C., Eds. Springer Berlin Heidelberg: Berlin, Heidelberg, 1999; pp 1-19.

2. Hans-Curt Flemming, T. R. N., Daniel J Wozniak, The EPS Matrix: The "House of Biofilm Cells". *Journal of Bacteriology* **2007,** *189* (22), 3.

3. Sutherland, I. W., Biofilm exopolysaccharides: a strong and sticky framework. *Microbiology* **2001,** *147* (1), 3-9.

4. Mayer, C.; Moritz, R.; Kirschner, C.; Borchard, W.; Maibaum, R.; Wingender, J.; Flemming, H.-C., The role of intermolecular interactions: studies on model systems for bacterial biofilms. *International Journal of Biological Macromolecules* **1999,** *26* (1), 3-16.

5. Ruas-Madiedo, P.; Gueimonde, M.; Margolles, A.; de los Reyes-Gavilan, C. G.; Salminen, S., Exopolysaccharides produced by probiotic strains modify the adhesion of probiotics and enteropathogens to human intestinal mucus. *J Food Prot* **2006,** *69* (8), 2011-5.

6. Badel, S.; Bernardi, T.; Michaud, P., New perspectives for Lactobacilli exopolysaccharides. *Biotechnology Advances* **2011,** *29* (1), 54-66.

7. Ruas-Madiedo, P.; Hugenholtz, J.; Zoon, P., An overview of the functionality of exopolysaccharides produced by lactic acid bacteria. *International Dairy Journal* **2002,** *12* (2), 163-171.

8. Jolly, L.; Vincent, S. J. F.; Duboc, P.; Neeser, J.-R., Exploiting exopolysaccharides from lactic acid bacteria. *Antonie van Leeuwenhoek* **2002,** *82* (1), 367-374.

9. Tieking, M.; Korakli, M.; Ehrmann, M. A.; Gänzle, M. G.; Vogel, R. F., In Situ Production of Exopolysaccharides during Sourdough Fermentation by Cereal and Intestinal Isolates of Lactic Acid Bacteria. *Applied and Environmental Microbiology* **2003,** *69* (2), 945-952.

10. Liu, C.; Lu, J.; Lu, L.; Liu, Y.; Wang, F.; Xiao, M., Isolation, structural characterization and immunological activity of an exopolysaccharide produced by Bacillus licheniformis 8-37-0-1. *Bioresource Technology* **2010,** *101* (14), 5528-5533.

11. Patel, S.; Majumder, A.; Goyal, A., Potentials of Exopolysaccharides from Lactic Acid Bacteria. *Indian Journal of Microbiology* **2012,** *52* (1), 3-12.

12. Salazar, N.; Gueimonde, M.; de los Reyes-Gavilán, C. G.; Ruas-Madiedo, P., Exopolysaccharides Produced by Lactic Acid Bacteria and Bifidobacteria as Fermentable Substrates by the Intestinal Microbiota. *Critical Reviews in Food Science and Nutrition* **2016,** *56* (9), 1440-1453.

13. Zannini, E.; Waters, D. M.; Coffey, A.; Arendt, E. K., Production, properties, and industrial food application of lactic acid bacteria-derived exopolysaccharides. *Appl Microbiol Biotechnol* **2016,** *100* (3), 1121-35.

14. Neu, T. R.; Lawrence, J. R., In Situ Characterization of Extracellular Polymeric Substances (EPS) in Biofilm Systems. In *Microbial Extracellular Polymeric Substances: Characterization, Structure and Function*, Wingender, J.; Neu, T. R.; Flemming, H.-C., Eds. Springer Berlin Heidelberg: Berlin, Heidelberg, 1999; pp 21-47.

15. Pan, M.; Zhu, L.; Chen, L.; Qiu, Y.; Wang, J., *Detection Techniques for Extracellular Polymeric Substances in Biofilms: A Review*. 2016; Vol. 11.

16. Wang, J.; Zhao, X.; Yang, Y.; Zhao, A.; Yang, Z., Characterization and bioactivities of an exopolysaccharide produced by Lactobacillus plantarum YW32. *International Journal of Biological Macromolecules* **2015,** *74* (Supplement C), 119-126.

17. Dilna, S. V.; Surya, H.; Aswathy, R. G.; Varsha, K. K.; Sakthikumar, D. N.; Pandey, A.; Nampoothiri, K. M., Characterization of an exopolysaccharide with potential health-benefit properties from a probiotic Lactobacillus plantarum RJF4. *LWT - Food Science and Technology* **2015,** *64* (2), 1179-1186.

18. Wang, J.; Zhao, X.; Tian, Z.; Yang, Y.; Yang, Z., Characterization of an exopolysaccharide produced by Lactobacillus plantarum YW11 isolated from Tibet Kefir. *Carbohydrate Polymers* **2015,** *125* (Supplement C), 16-25.

19. Yadav, V.; Prappulla, S. G.; Jha, A.; Poonia, A., A novel exopolysaccharide from probiotic Lactobacillus fermentum CFR 2195: Production, purification and characterization. *Biotechnol. Bioinf. Bioeng.* **2011,** *1* (4), 6.

20. Shao, L.; Wu, Z.; Zhang, H.; Chen, W.; Ai, L.; Guo, B., Partial characterization and immunostimulatory activity of exopolysaccharides from Lactobacillus rhamnosus KF5. *Carbohydrate Polymers* **2014,** *107* (Supplement C), 51-56.

21. Ibarburu, I.; Puertas, A. I.; Berregi, I.; Rodríguez-Carvajal, M. A.; Prieto, A.; Dueñas, M. T., Production and partial characterization of exopolysaccharides produced by two Lactobacillus suebicus strains isolated from cider. *International Journal of Food Microbiology* **2015,** *214* (Supplement C), 54-62.

22. Kralj, S.; van Geel-Schutten, G. H.; Dondorff, M. M. G.; Kirsanovs, S.; van der Maarel, M. J. E. C.; Dijkhuizen, L., Glucan synthesis in the genus Lactobacillus: isolation and characterization of glucansucrase genes, enzymes and glucan products from six different strains. *Microbiology* **2004,** *150* (11), 3681-3690.

23. Cheng, H. N.; Neiss, T. G., Solution NMR Spectroscopy of Food Polysaccharides. *Polymer Reviews* **2012,** *52* (2), 81-114.

24. Viel, S.; Capitani, D.; Mannina, L.; Segre, A., Diffusion-Ordered NMR Spectroscopy: A Versatile Tool for the Molecular Weight Determination of Uncharged Polysaccharides. *Biomacromolecules* **2003,** *4* (6), 1843-1847.

25. Maina, N. H.; Pitkänen, L.; Heikkinen, S.; Tuomainen, P.; Virkki, L.; Tenkanen, M., Challenges in analysis of high-molar mass dextrans: Comparison of HPSEC, AsFlFFF and DOSY NMR spectroscopy. *Carbohydrate Polymers* **2014,** *99* (Supplement C), 199-207.

26. Pages, G.; Gilard, V.; Martino, R.; Malet-Martino, M., Pulsed-field gradient nuclear magnetic resonance measurements (PFG NMR) for diffusion ordered spectroscopy (DOSY) mapping. *Analyst* **2017,** *142* (20), 3771-3796.

27. Nilsson, M.; Connell, M. A.; Davis, A. L.; Morris, G. A., Biexponential Fitting of Diffusion-Ordered NMR Data: Practicalities and Limitations. *Analytical Chemistry* **2006,** *78* (9), 3040-3045.

28. Windig, W.; Antalek, B., Direct exponential curve resolution algorithm (DECRA): A novel application of the generalized rank annihilation method for a single spectral mixture data set with exponentially decaying contribution profiles. *Chemometrics and Intelligent Laboratory Systems* **1997,** *37* (2), 241-254.

29. Antalek, B.; Hewitt, J. M.; Windig, W.; Yacobucci, P. D.; Mourey, T.; Le, K., The use of PGSE NMR and DECRA for determining polymer composition. *Magnetic Resonance in Chemistry* **2002,** *40* (13), S60-S71.

30. McIntyre, D. D.; Vogel, H. J., Nuclear Magnetic Resonance Studies of Homopolysaccharides Related to Starch. *Starch - Stärke* **1991,** *43* (2), 69-76.

31. Bounaix, M.-S.; Gabriel, V.; Morel, S.; Robert, H.; Rabier, P.; Remaud-Siméon, M.; Gabriel, B.; Fontagné-Faucher, C., Biodiversity of Exopolysaccharides Produced from Sucrose by Sourdough Lactic Acid Bacteria. *Journal of Agricultural and Food Chemistry* **2009,** *57* (22), 10889-10897.
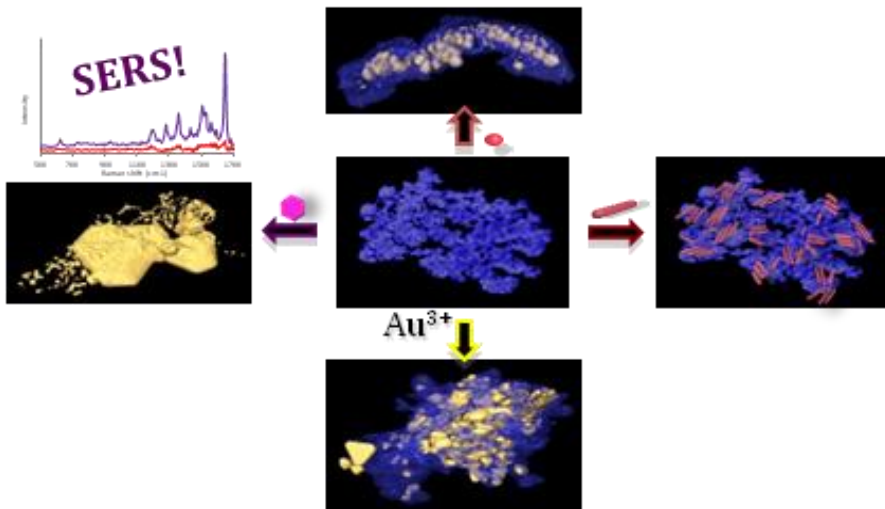
CHAPTER 6.

OPTICAL AND TOMOGRAPHY STUDIES OF GOLD NANOPARTICLES ASSEMBLY ON BACTERIAL EPS

6.1 INTRODUCTION

Gold nanoparticles (AuNPs) have attracted considerable attention because of their extraordinary properties, especially optical properties.[1-4] Furthermore, gold is one of few metals that survive as nanoparticles under atmospheric conditions. The combination of optical properties and stability in aerobic environments has enabled AuNPs to become one of the most important materials in nanotechnology.[5-10]

AuNPs exhibit a strong absorption band in the visible region, due to a small particle effect absent in individual atoms and bulk materials. This absorption results when the incident photon frequency is resonant with the collective oscillation of the conduction band electrons (the so-called plasmons).[1-4] The phenomenon is known as surface plasmon resonance (SPR). SPR is the key to optical properties of AuNPs and is strongly dependent upon the size, shape, chemical environment, and aggregation of nanoparticles.[1-4] Fine-tuning these parameters enables the production of AuNPs with desired optical properties for specific applications.

Spherical gold nanoparticles (AuNSs) have a SPR centered in the range of 500-600 nm. The absorptions at these wavelengths limit the use of AuNSs in biomedicine since blood and soft tissues absorb at these wavelengths. However, when SPR of AuNPs occurs at lower energies such as the near-infrared (NIR), the clinical use of AuNPs can extend beyond superficial applications, since NIR light can penetrate much deeper to reach AuNPs inside the body.

Two frequent approaches to shift the SPR of AuNPs to lower energies are the production of anisotropically-shaped AuNPs[11] and the aggregation of nanoparticles.[12] The first method of shifting AuNP SPR involves synthesizing nanoparticles with anisotropic geometries. When particles are not spherical, two plasma resonances appear. In gold nanorods (AuNRs) for instance, the SPR splits into two bands: the transverse mode shows a resonance at about 500 nm, which is co-incident with the SPR of spherical particles, while the resonance of the longitudinal mode is red-shifted to wavelengths depending on the length to width ratio of the nanorods. In shapes with even greater anisotropy, such as gold nanoprisms (AuNPrs), the low-energy SPR falls in the near-infrared region with wavelengths reaching values of 1100 nm.

A second approach to shifting AuNP SPR to NIR wavelengths is using the formation of nanoparticle aggregates. The SPR changes drastically if particles are densely packed such that individual particles are electronically coupled to each other. The SPR of the aggregate is red-shifted depending on coordination number and interparticle distances.[12]

The SPR shift is not the only consequence produced by aggregation of AuNPs. In comparison to isolated nanoparticles, AuNP aggregates increase the surface-enhanced Raman spectroscopy (SERS) effect due to the formation of hot spot in the interparticle region. AuNPs act as antennas for incident light with the same frequency that the collective oscillation of plasmons. The AuNPs therefore concentrate the oscillating electric fields at their surfaces, with the same frequency as the incident light but with several orders of magnitude higher intensities. The electric field enhancement excite the Raman modes of the molecule being

studied, therefore increasing the signal of the Raman scattering.[13-17] SERS is currently one of the most powerful spectroscopic methods for ultrasensitive detection of molecules.

Therefore, aggregation can both improve optical properties and lead to additional applications. With this in mind, different approaches to synthesizing AuNP aggregates have arisen: hydrogen bonding, electrostatic forces, layer-by-layer techniques, substrates template, etc.[1-4] In the present work, AuNPs aggregates were produced using exopolysaccharides (EPS) of *Lactobacillus fermentum* (*L. fermentum*), a probiotic that constitutes an important part of the natural healthy microbiota.

EPS are natural polysaccharides secreted by some bacteria. They play a crucial role in bacterial surface adhesion, an essential step for colonization.[18] In particular, *L. fermentum* EPS allows colonization of these healthy bacteria in intestines by facilitating adhesion to enterocyte cells. Furthermore, *L. fermentum* EPS is digestible, biocompatible, and approved by governmental health agencies (e.g. Food and Drug Administration).[19-20]

We produced AuNP aggregates using EPS of *L. fermentum* with two different approaches: i) EPS as a surface for deposition of previously prepared AuNPs with defined size and shape and ii) EPS as a combined reducing and stabilizing agent. The resulting AuNP aggregates obtained differ in size and shape and thus in optical properties and SERS effects. To rationalize the huge differences found in SERS effects, we carried out an electronic microscopy tomography study on the nanostructures. These

studies allowed us to conclude that improving optical properties and SERS effects largely depends on the access of the analyte to the hot spot generated by gold nanoparticles aggregation.

## 6.2 RESULTS AND DISCUSSION

Deposition of AuNPs onto EPS

First, following well-documented procedures we prepared AuNPs with the three more representative shapes: spheres (AuNSs),[21] rods (AuNRs)[22-23] and prisms (AuNPrs).[24] The expected shapes, sizes, and SPR values were confirmed by Transmission Electron Microscopy (TEM) and UV-vis spectroscopy (Figure 1). Next, we incubated gold samples with EPS isolated from *L. fermentum*[25] to produce AuNSs-EPS, AuNRs-EPS and AuNPrs-EPS. In the three samples, large aggregates of nanoparticles on the EPS were revealed by TEM (Figure 1). The deposition of AuNPs did not result in any changes of shape or size, which is an advantage since other coating often results in reshaping the particles.

The aggregates were also examined using High Annular Dark Field-Scanning Transmission Electron Microscopy HAADF-STEM (Figure 2). To confirm the presence of the AuNPs on the EPS, energy dispersive X-ray spectroscopy (EDX) experiments were performed, which showed that Au (in violet) is associated to EPS. The spatial distribution of gold, which was barely detectable outside the EPS region, indicates that the AuNPs were glued to the EPS.
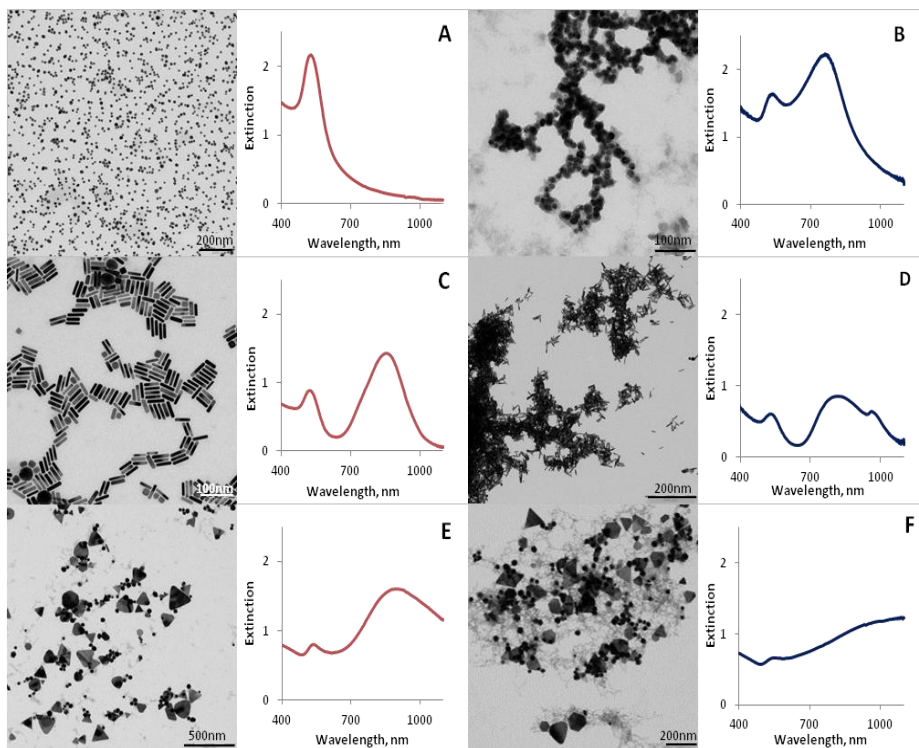
Figure 1. TEM images and UV-vis spectra of AuNSs, AuNRs and AuNPrs before (a, c, e) and after incubation with EPS to give AuNSs-EPS, AuNRs-EPS and AuNPrs-EPS (b, d, f).

As shown in Figure 1, once the AuNPs were deposited onto EPS, their UV-vis spectra showed additional absorbance peaks at lower energies, which indicate that the particles were assembled into aggregates with strong interparticle interactions.[12] For AuNSs-EPS, a second, more intense peak appeared at 760 nm. AuNRs-EPS produces two new bands at 815 and 960 nm. The AuNPrs-EPS exhibits a new broad band centered around 1100 nm. These UV-vis spectra are consistent with some AuNP assemblies previously reported and with theoretical predictions that take into account the effect of plasmon-plasmon interactions between AuNPs in the UV-vis spectrum.[12]

163
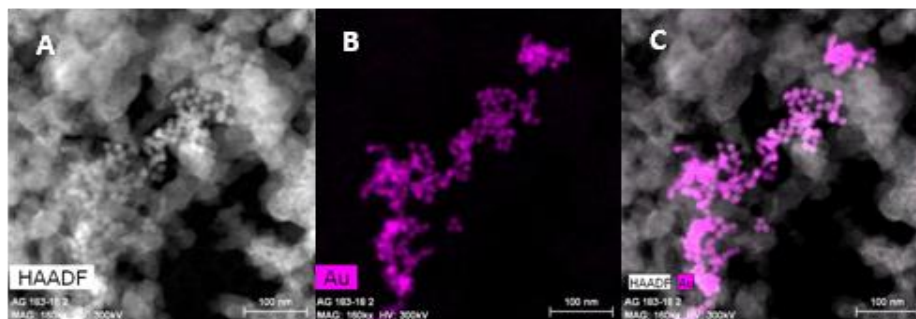
Figure 2. (a) HAADF micrograph of AuNSs after incubation with EPS (AuNSs-EPS). (b) EDX compositional map of gold (violet) collected over the whole HAADF-STEM image in (a). (c) Compositional map of (a) and (b) images. Similar images were obtained for AuNRs-EPS and AuNPrs-EPS.

Synthesis of gold nanoparticles using EPS as reductant (Au-EPS)

In a second phase, we addressed the possibility of producing AuNPs aggregate by EPS and gold cations in one step. Carbohydrates in general and EPS in particular have been used as reducing and stabilizing agents for AuNPs formation.[26-28]

We used EPS of *L. fermentum* as a reducing agent by adding it to a boiling aqueous solution of Au(III). The resulting mixture (Au-EPS) was analyzed by TEM. As shown in Figure 3, AuNPs were formed on EPS. The contrast of the darker, electron-dense gold enhances the visualization of the lighter EPS material. A range of different sizes and shapes of nanoparticles was seen: spheres, rods, and prisms of different sizes (2-80 nm) are clearly noticeable from the TEM image. The aggregates were visualized by HAADF-STEM (Figure 3). To confirm the presence of the AuNPs on the EPS, energy dispersive X-ray spectroscopy (EDX) experiments were performed, which showed that Au (in violet) is linked

to EPS (Figure 3C and D). The spatial distribution of gold, which was barely detectable outside the EPS region, demonstrates that the AuNPs were produced and incorporated onto the EPS. In these experimental conditions, EPS of *L. fermentum* produced heterogeneous gold particles without preferred size and shapes. In accordance with this result, the UV-vis spectrum of Au-EPS consists of a broad band with a peak maximum centered at 570 nm and a tail absorbing up to 1000 nm (Figure 3B). Since band position is dependent on both the number of coupled nanoparticles and their relative position with respect to each other and to the incident light, this broad band is the result of the contribution of differently shaped AuNPs and a lack of uniform distribution.
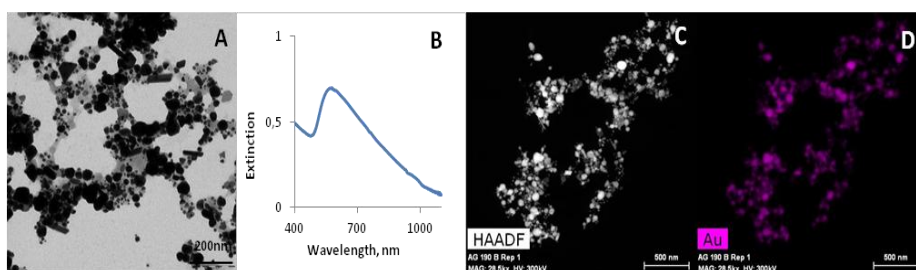
Figure 3. (a) TEM image of Au-EPS and (b) its UV-vis spectrum. (c) HAADF micrograph of Au-EPS and (d) EDX compositional map of gold (violet) collected over the whole HAADF-STEM image in (c).

It should be noted the lower absorbance values in the UV-visible spectrum of the sample Au-EPS (Figure 3B) with respect to those of AuNSs-EPS, AuNRs-EPS and AuNPrs-EPS (Figure 1). The concentration of Au(III) incubated with EPS to form Au-EPS was the same (0.25 mM) as that used in gold nanoparticle synthesis for the samples AuNSs-EPS, AuNRs-EPS and AuNPrs-EPS. Therefore, the low absorbance values found

for Au-EPS indicates that the EPS does not reduce all gold cations but just a fraction, which leads to a lower concentration of gold nanoparticles.

SERS experiments

We have applied these AuNPs materials to improve the SERS signals of an analyte. As shown by TEM, EPS efficiently glues AuNPs together. The short distances between AuNPs generate hot spots where if an analyte deposits it can improve their SERS signals.[13-17]

We tested the SERS performance of all gold aggregates for the detection of the model analyte rhodamine B (RhB). We analyzed the SERS performance of four samples: the three AuNPs morphologies deposited onto EPS (AuNSs, AuNRs and AuNPrs) and the AuNPs made by the EPS themselves (Au-EPS). We incubated RhB (1 μM) with gold samples (0.25 mM in Au) in water, and the mixtures were analyzed by SEM and Raman spectroscopy.

A total of 10 Raman spectra were collected on 10 different regions of the SEM grid. Representative Raman spectra obtained for each sample are shown in Figure 4. SEM images of sample sections used for SERS are included in the supporting information (see supporting information; Figure S1). Interestingly, the SERS results differed dramatically depending on the gold sample. A marginal increase of the Raman signal intensity of RhB was observed for the aggregated samples AuNSs-EPS and AuNRs-EPS with respect to the isolated samples, AuNSs and AuNRs, respectively (Figure 4B and C). However, the intensity of Raman signals of RhB in the presence of AuNPrs-EPS (Figure 3A, violet spectrum) was two orders of magnitude higher than that of AuNPrs (Figure 4A, red spectrum).

166
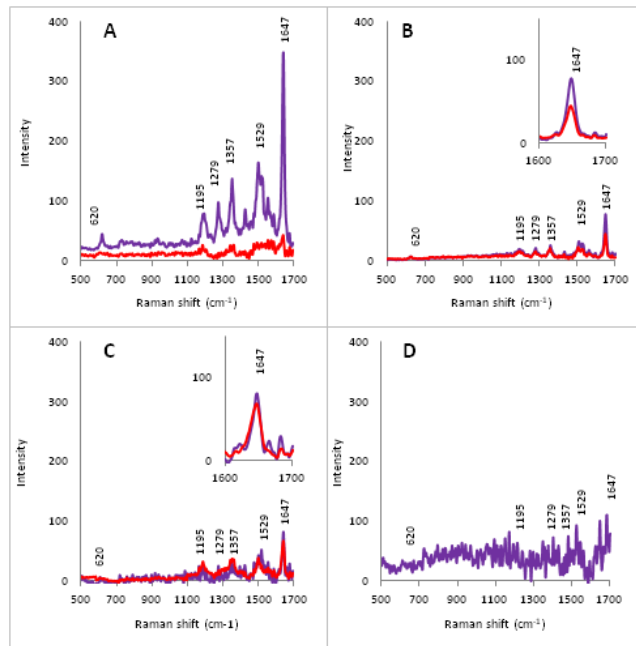
Figure 4. Raman spectra of RhB (red) in the presence of isolated AuNPrs (a), AuNSs (b) and AuNRs (c). In violet the RhB Raman spectra in the presence of aggregated samples: AuNPrs-EPS (a), AuNSs-EPS (b), AuNRs-EPS (c), and Au-EPS (d).

The dramatic increase in the Raman signal intensity of RhB in the presence of AuNPrs-EPS is not related to the prism shape of gold nanoparticles, since isolated AuNPrs did not exhibit a significant SERS effect (Figure 4A red). The increase does correspond to the aggregated state of the nanoparticles.

In order to understand the size of the SERS effect of AuNPrs-EPS in comparison to the rest of samples, we point out that although EPS glues the gold nanoparticles together, RhB access to the regions in between individual nanoparticles is not the same in all samples. As the SERS effect depends on RhB reaching the hot spots, this difference in accessibility

results in the different SERS effects. To evaluate this hypothesis, we carried out a tomography study of all samples.

Electron Tomography (ET)

This study revealed clear differences between the samples in terms of nanoparticle spatial distribution with respect to the EPS layer between the samples. As is evident from Figure 5a, in the AuNPSs-EPS sample, the gold appears in aggregates of spherical-like nanoparticles mostly embedded within EPS. Note that yellow and blue colours represent gold and EPS, respectively. Although some of these AuNPSs partially expose EPS-free surfaces (Figure 5a, very few yellow sections), most of them are located at positions where they are fully embedded in the EPS shell which averages a thickness of 24 nm (see supporting information, Figure S2).
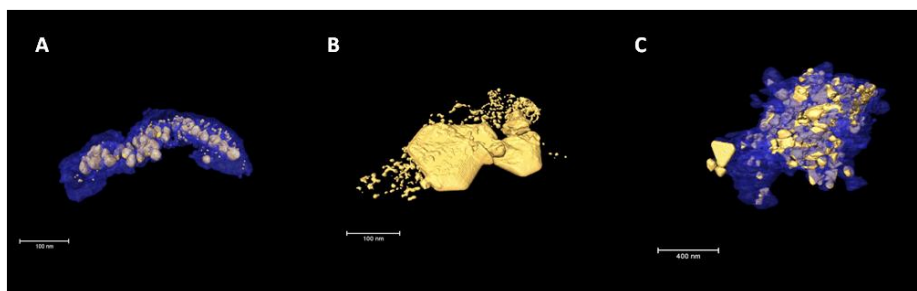
Figure 5. Electron Tomography results (rendered 3D volumes) of AuNSs (a); AuNPrs-EPS (b) and Au-EPS (c).

The situation is different for AuNPrs–EPS, the sample that exhibits the highest SERS effect. In this case, groups of prismatic-like Au nanoparticles of largely varying size, and in close proximity to each other, depict mostly clean surfaces (Figure 5b). Although a very small number of polymer filamentary structures attached to the nanoparticles are visible, most of

their surface remains free from EPS (the yellow colour of gold, it clearly predominant, Figure 5b). This spatial distribution of the two components favors the access of external molecules, such as RhB, to the hot spot locations between gold nanoprisms. This difference in exposed nanoparticle surface explains the drastic increase of intensity in the SERS spectrum and the improvement of the Raman spectrum of RhB with well-resolved and intense peaks.[29] Finally, the Au-EPS sample showed a mixture of heterogeneously sized and shaped gold nanoparticles (Figure 5c), which appear much more agglomerated than in AuNPrs-EPS. In contrast with the latter, particles are partially embedded within EPS, similar to what occurs in AuNPSs-EPS. A more compact EPS layer with an average thickness of 87 nm (see supporting information, Figure S3) in direct contact with a significant fraction of the Au nanoparticles is present in this sample. In this case, the EPS layer limits RhB access to the Au surfaces.

6.3 CONCLUSIONS

EPS of *L. fermentum,* a healthy bacteria present in our microbiota, is an extraordinarily effective bioplatform for aggregating gold nanoparticles of different sizes and shapes as well as for directly producing gold aggregates from a Au(III) solution. All gold aggregates were water-soluble and could be lyophilized and safely stored as a powder.

The gold aggregates on EPS improved the optical properties of isolated gold nanoparticles and showed additional absorptions at lower energies.

SERS effects of gold aggregates were significantly different than isolated nanoparticles. An electronic tomography study confirmed that efficiency as a RhB SERS probe directly correlates with the extension of EPS-coating of hot spots of gold aggregates. In particular, the sample AuNPrs-EPS, consisting of aggregated gold prisms onto the EPS, displayed RhB Raman spectra with intensities two orders of magnitude higher than free RhB.

6.4 EXPERIMENTAL SECTION

Materials

All reagents were purchased at Sigma Aldrich. UV-vis spectra were recorded at a Unicam UV 300 Thermo Spectronic spectrophotometer.

Bacterial growth

L. fermentum was grown in anaerobic conditions in a synthetic growth medium at 37 $^{\circ}$C on an orbital shaker for 24 h with an initial concentration of 1mg bacteria in 1mL of medium. The synthetic growth medium consisted of (g L^{-1}) Na_2HPO_4 – 5.0, KH_2PO_4 – 6.0, trisammonium citrate – 2.0, sucrose – 50.0, $MgSO_4$ – 1.0 and trace elements solution – 10 ml (consisting of (g L^{-1}): $MnSO_4$ – 2.0, $CoCl_2$ – 1.0, $ZnCl_2$ – 1.0 dissolved in 0.1 N HCl solution). The medium had an initial pH 6.7 and was sterilized at 121ºC. The final *L. fermentum* cell concentration was 3.3·108 CFU mL^{-1}.

EPS of L. fermentum isolation[25]

Bacteria were removed by centrifugation at 3000 g for 10 min. The supernatant was filtered using EMD Millipore Steritop™ Sterile Vacuum Bottle-Top Filters. Ice-cold ethanol (2 vol) was added to the cell-free

supernatant (1 vol) under continuous stirring, and kept overnight for precipitation in the refrigerator. The alcoholic supernatant was centrifuged at 22,000 g for 35 min and the EPS precipitated were washed with acetone and again centrifuged. The solid obtained was dissolved in water (20 mL), filtered again and lyophilized.

Synthesis of spherical gold nanoparticles (AuNSs)[21]

5 mL of a 1.0 mM $HAuCl_4$ solution in water was stirred and heated to boiling on a hot plate. After the solution began to boil, 500 µL of a 38.8 mM $Na_3C_6H_5O_7$ solution in water was added. The mixture was boiled and stirred continuously for about 10 min until it was a deep red color. The solution was cooled to room temperature. The AuNSs were characterized by UV-vis spectroscopy and transmission electron microscopy (TEM).

Synthesis of gold nanorods (AuNRs)

To prepare AuNRs, a seed-mediated growth method was carried out.[22] Solutions of $HAuCl_4$ 1 mM, $AgNO_3$ 8 mM, Ascorbic Acid 78.8 mM and $NaBH_4$ 10 mM were prepared at room temperature. The $NaBH_4$ solution was ice-cooled after preparation. Solutions of Cetyl trimethylammonium bromide (CTAB) 0.2 M and (11-Mercaptoundecyl)-N, N, N-trimethylammonium bromide 92 mM, were separately prepared by heating at 50 ºC and stirring until dissolved and then cooled to room temperature. All the solutions were prepared in Mili-Q ultrapure water. Gold seed synthesis: 5 mL of CTAB 0.2 M, 2.5 mL $HAuCl_4$ 1 mM and 0.6 mL of ice-cold $NaBH_4$ 10 mM were mixed and stirred for 2 min at 25 ºC. When seeds were formed, the solution color changed from yellow to

slightly brown. NRs synthesis: 5 mL of the 0.2 M CTAB solution were placed in a flask previously set in an oil bath at 30 ºC under stirring at 180 rpm. 5 mL of $HAuCl_4$ 1 mM, 70 μL of Ascorbic Acid 78.8 mM and 100 μL of $AgNO_3$ 8 mM were added in this order to the CTAB solution. The mixture was completed with 160 μL of the seed solution. The completed mixture was kept stirring at 180 rpm and 30 ºC for 48 h. Due to CTAB antibacterial activity[23] CTAB excess was removed. AuNRs were collected twice by high-speed centrifugation at 13,000 rpm for 10 min, the supernatant was removed and the collected nanorods were dissolved in 1 mL of Mili-Q ultrapure water and 1 mL of (11-Mercaptoundecyl)-N, N, N-trimethylammonium bromide 92 mM and stirred mildly. AuNRs were collected again by high-speed centrifugation at 13,000 rpm for 10 min 48 h later and the pellet was dissolved in 1 mL of Mili-Q ultrapure water. The AuNRs were characterized by UV-vis spectroscopy and transmission electron microscopy (TEM).

Synthesis of gold nanoprisms (AuNPrs)[24]

100 mL of $HAuCl_4$ 2 mM and 120 mL of fresh $Na_2S_2O_3$ 0.5 mM, both prepared in Mili-Q ultrapure water, were mixed and stirred gently at 15 ºC. After 9 min ("seed" formation) an extra 50 mL of fresh $Na_2S_2O_3$ 0.5 mM was added. Growth mixture was left overnight at 15 ºC under mild stirring conditions. The AuNPrs were characterized by UV-vis spectroscopy and TEM.

Deposition of AuNPs onto EPS

A 10 mg mL^{-1} EPS solution in water was adjusted to pH 2 using HCl 1 M. The EPS solution was heated for 24 h at 80 ºC under continuous

stirring at 200 rpm. The solution was cooled to room temperature. AuNSs, AuNRs and AuNPrs (1vol) were added to three different aliquots of the cooled EPS pH2 solution (1vol). The Au nanoparticle aggregation onto EPS was characterized by UV-vis spectroscopy, TEM and EDX compositional maps collected with HAADF-STEM images. All EPS- samples were lyophilized and stored as powders. Redissolution of powders in water gave unchanged UV-vis spectra.

Synthesis of gold nanoparticles using EPS as reductant (Au-EPS)

A 2.5 mL 1.0 mM $HAuCl_4$ solution was stirred and heated to boiling on a stir/hot plate. After the solution began to boil, 2.5 mL of a 10 mg mL^{-1} EPS aqueous solution (pH 2) was added. The mixture was boiled and stirred for 30 min until it was a purple/blue color and then cooled to room temperature. The samples were characterized by UV-vis spectroscopy, TEM, and EDX compositional maps collected with HAADF-STEM images.

Electronic microscopy sample preparation

TEM samples were prepared by placing a drop of each sample onto a FCF200-Cu (Formvar/Carbon 200 Mesh, Copper) grid and blotting with filter paper. Samples were observed under a LIBRA 120 PLUS from Carl Zeiss SMT and EDX maps were done using a HAADF-STEM system.

SERS experiments

A 10 µM solution of RhB in water was prepared. A 5 µL solution was added to three different solutions each containing 25 µL of the isolated

gold nanoparticles (AuNSs, AuNRs and AuNPrs) and 25µL of H_2O. The same volume of RhB 10 µM was added to 50 µL of the AuNSs, AuNRs and AuNPrs onto EPS samples and to 50 µL of AuNPs synthesized by EPS at pH 2.

Gold nanoparticles on EPS samples were prepared as described above. An aluminum adhesive was fixed on stubs of metal. A 20 µL drop of each sample was placed over a stub and dried overnight at room temperature. Samples were observed under a Zeiss SUPRA40VP microscope and Raman spectrums were collected using a Structural Chemical Analyzer (SCA) with excitation at 532 nm (intensity of 35% and 3 acquisitions). A study on the stability of SERS effect was carried out by incubation of gold aggregates and RhB for different times (30 min, 1 and 4 h). The intensity of Raman signals were practically the same, pointing out a permanent SERS effect of the gold nanostructures on the RhB.
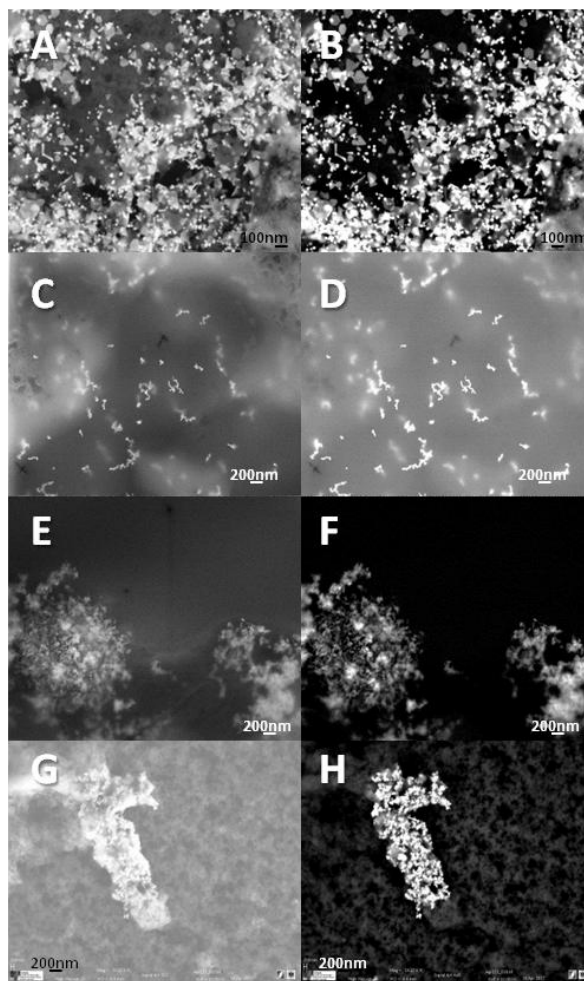
Electron Tomography (ET)

Electron Tomography (ET) experiments were performed in a FEI Titan3 Themis 60-300 Double Aberration Corrected microscope operated at 80kV. A convergence angle of 9 mrad was selected in order to improve the depth of focus. HAADF and DF detectors were used to image the EPS and nanoparticles signals, respectively. In particular, a camera length of 185 mm was used for AuNSs and AuNPrs-EPS and 56 mm for Au-EPS. Then, a series of STEM-HAADF/DF images at different tilts were recorded using the software FEI Explore3D v.4.1. The tracking, focusing and tilting were carried out automatically. The samples were tilted from -70º to +70º and images acquired every 5º. Then, the whole set of images were

aligned combining cross-correlation method, using FEI Inspect3D, and the landmark-based alignment implemented in TomoJ. The tilt series images were also background-subtracted, normalized and binned to 512x512 pixels. Afterwards, they were reconstructed into a 3D volume using a Compressed Sensing algorithm based on Minimization of the Total Variation (TVM) of the individual STEM-HAADF images. In particular, a 3D implementation of the TVAL3 routine, using AstraToolBox, was employed. For visualization and further nanometrological analysis of the reconstructed volumes, the FEI Avizo Software was used. The resolution in electron tomography is anisotropic. In the XY direction, which is that of the projections, the scale bars of the figures are real. In the XZ direction, the resolution depends on the number of projections and the reconstruction algorithm used. In this work, the advanced algorithm used eliminates elongation artefacts, and the spatial resolution is below 1 nm.
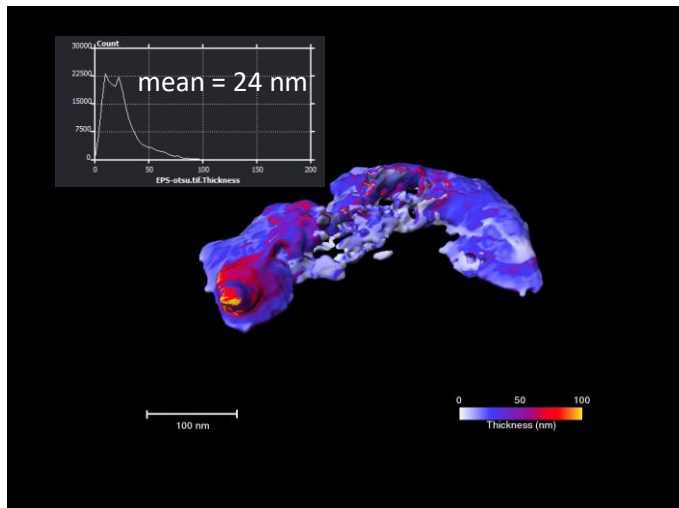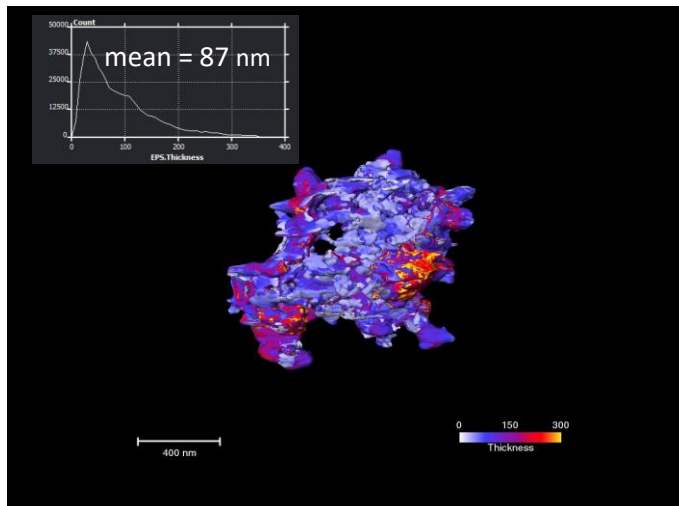
6.5 SUPPORTING INFORMATION

Figure S1. SEM images (A, C, E and G) of sections analyzed by Raman spectroscopy. Contrasted images to highlight the presence of gold nanoparticles (B, D, F and H).

Figure S2. Electron tomography thickness map of the EPS shell in the sample AuNPSs-EPS.

Figure S3. Electron tomography thickness map of the EPS shell in the sample AuNPSs-EPS.

6.6 REFERENCES

1. Li, N.; Zhao, P.; Astruc, D., Anisotropic Gold Nanoparticles: Synthesis, Properties, Applications, and Toxicity. *Angew. Chem., Int. Ed.* **2014,** *53* (7), 1756-1789.

2. Saha, K.; Agasti, S. S.; Kim, C.; Li, X.; Rotello, V. M., Gold Nanoparticles in Chemical and Biological Sensing. *Chem. Rev.* **2012,** *112* (5), 2739-2779.

3. Jans, H.; Huo, Q., Gold nanoparticle-enabled biological and chemical detection and analysis. *Chem. Soc. Rev.* **2012,** *41* (7), 2849-2866.

4. Dykman, L.; Khlebtsov, N., Gold nanoparticles in biomedical applications: recent advances and perspectives. *Chem. Soc. Rev.* **2012,** *41* (6), 2256-2282.

5. Kennedy, L. C.; Bickford, L. R.; Lewinski, N. A.; Coughlin, A. J.; Hu, Y.; Day, E. S.; West, J. L.; Drezek, R. A., A New Era for Cancer Treatment: Gold-Nanoparticle-Mediated Thermal Therapies. *Small* **2011,** *7* (2), 169-183.

6. Cao-Milán, R.; Liz-Marzán, L. M., Gold nanoparticle conjugates: recent advances toward clinical applications. *Expert Opin. Drug Delivery* **2014,** *11* (5), 741-752.

7. Abadeer, N. S.; Murphy, C. J., Recent Progress in Cancer Thermal Therapy Using Gold Nanoparticles. *J. Phys. Chem. C* **2016,** *120* (9), 4691-4716.

8. Pérez-Juste, J.; Pastoriza-Santos, I.; Liz-Marzán, L. M.; Mulvaney, P., Gold nanorods: Synthesis, characterization and applications. *Coord. Chem. Rev.* **2005,** *249* (17–18), 1870-1901.

9. Yeh, Y.-C.; Creran, B.; Rotello, V. M., Gold nanoparticles: preparation, properties, and applications in bionanotechnology. *Nanoscale* **2012,** *4* (6), 1871-1880.

10. Carnovale, C.; Bryant, G.; Shukla, R.; Bansal, V., Size, shape and surface chemistry of nano-gold dictate its cellular interactions, uptake and toxicity. *Prog. Mater. Sci.* **2016,** *83*, 152-190.

11. Reguera, J.; Langer, J.; Jimenez de Aberasturi, D.; Liz-Marzan, L. M., Anisotropic metal nanoparticles for surface enhanced Raman scattering. *Chem. Soc. Rev* **2017,** *46* (13), 3866-3885.

12. Ghosh, S. K.; Pal, T., Interparticle Coupling Effect on the Surface Plasmon Resonance of Gold Nanoparticles: From Theory to Applications. *Chem. Rev.* **2007,** *107* (11), 4797-4862.

13. Li, K.; Stockman, M. I.; Bergman, D. J., Self-Similar Chain of Metal Nanospheres as an Efficient Nanolens. *Phys. Rev. Lett.* **2003,** *91* (22), 227402.

14. Alvarez-Puebla, R. A.; Agarwal, A.; Manna, P.; Khanal, B. P.; Aldeanueva-Potel, P.; Carbó-Argibay, E.; Pazos-Pérez, N.; Vigderman, L.; Zubarev, E. R.; Kotov, N. A.; Liz-Marzán, L. M., Gold nanorods 3D-supercrystals as surface enhanced Raman scattering

spectroscopy substrates for the rapid detection of scrambled prions. *Proc. Natl. Acad. Sci. U. S. A.* **2011,** *108* (20), 8157-8161.

15. Pazos-Perez, N.; Wagner, C. S.; Romo-Herrera, J. M.; Liz-Marzán, L. M.; García de Abajo, F. J.; Wittemann, A.; Fery, A.; Alvarez-Puebla, R. A., Organized Plasmonic Clusters with High Coordination Number and Extraordinary Enhancement in Surface-Enhanced Raman Scattering (SERS). *Angew. Chem., Int. Ed.* **2012,** *51* (51), 12688-12693.

16. Xu, J.; Zhang, L.; Gong, H.; Homola, J. í.; Yu, Q., Tailoring Plasmonic Nanostructures for Optimal SERS Sensing of Small Molecules and Large Microorganisms. *Small* **2011,** *7* (3), 371-376.

17. Barbosa, S.; Agrawal, A.; Rodríguez-Lorenzo, L.; Pastoriza-Santos, I.; Alvarez-Puebla, R. A.; Kornowski, A.; Weller, H.; Liz-Marzán, L. M., Tuning Size and Sensing Properties in Colloidal Gold Nanostars. *Langmuir* **2010,** *26* (18), 14943-14950.

18. Gunn, J. S.; Bakaletz, L. O.; Wozniak, D. J., What's on the Outside Matters: The Role of the Extracellular Polymeric Substance of Gram-negative Biofilms in Evading Host Immunity and as a Target for Therapeutic Intervention. *J. Biol. Chem.* **2016,** *291* (24), 12538-12546.

19. Zannini, E.; Waters, D. M.; Coffey, A.; Arendt, E. K., Production, properties, and industrial food application of lactic acid bacteria-derived exopolysaccharides. *Appl. Microbiol. Biotechnol.* **2016,** *100* (3), 1121-1135.

20. Patel, A. K. M., Philippe; Singhania, Reeta Rani; Soccol, Carlos Ricardo; Pandey, Ashok, Polysaccharides from Probiotics: New Developments as Food Additives. *Food Technol. Biotechnol.* **2010,** *48* (4), 451.

21. McFarland, A. D.; Haynes, C. L.; Mirkin, C. A.; Van Duyne, R. P.; Godwin, H. A., Color My Nanoworld. *J. Chem. Educ.* **2004,** *81* (4), 544A.

22. Nikoobakht, B.; El-Sayed, M. A., Preparation and Growth Mechanism of Gold Nanorods (NRs) Using Seed-Mediated Growth Method. *Chem. Mater.* **2003,** *15*, 1957.

23. Jin, Y.; Deng, J.; Liang, J.; Shan, C.; Tong, M., Efficient bacteria capture and inactivation by cetyltrimethylammonium bromide modified magnetic nanoparticles. *Colloids Surf.* **2015,** *136*, 659-665.

24. Pelaz, B.; Grazu, V.; Ibarra, A.; Magen, C.; del Pino, P.; de la Fuente, J. M., Tailoring the synthesis and heating ability of gold nanoprisms for bioapplications. *Langmuir* **2012,** *28* (24), 8965-70.

25. Vijayendra, S. V. N.; Palanivel, G.; Mahadevamma, S.; Tharanathan, R. N., Physico-chemical characterization of an exopolysaccharide produced by a non-ropy strain of Leuconostoc sp. CFR 2181 isolated from dahi, an Indian traditional lactic fermented milk product. *Carbohydr. Polym.* **2008,** *72* (2), 300-307.

26. Pradeepa; Vidya, S. M.; Mutalik, S.; Udaya Bhat, K.; Huilgol, P.; Avadhani, K., Preparation of gold nanoparticles by novel bacterial exopolysaccharide for antibiotic delivery. *Life Sci.* **2016,** *153*, 171-179.

27. Sathiyanarayanan, G.; Vignesh, V.; Saibaba, G.; Vinothkanna, A.; Dineshkumar, K.; Viswanathan, M. B.; Selvin, J., Synthesis of carbohydrate polymer encrusted gold nanoparticles using bacterial exopolysaccharide: a novel and greener approach. *RSC Adv.* **2014,** *4* (43), 22817-22827.

28. Das, S. K.; Das, A. R.; Guha, A. K., Microbial Synthesis of Multishaped Gold Nanostructures. *Small* **2010,** *6* (9), 1012-1021.

29. Alvarez-Puebla, R. A.; Liz-Marzán, L. M., SERS Detection of Small Inorganic Molecules and Ions. *Angew. Chem., Int. Ed.* **2012,** *51* (45), 11214-11223.

CAPÍTULO 7.
CONCLUSIONES

1. *Lactobacillus fermentum* tiene un comportamiento reductor como consecuencia de la excreción de moléculas con capacidad reductora. Este comportamiento reductor correlaciona con su fortaleza metabólica.

2. Hemos desarrollado un test simple para cuantificar la fortaleza metabólica de *L. fermentum*. El polyoxometalato electrocrómico $Na_6[P_2Mo^{VI}_{18}O_{62}]$ (POM) sirve como sensor de la actividad reductora de *L. fermentum*. El seguimiento por espectroscopía UV-vis de *L. fermentum* en presencia de POM permite evaluar su actividad reductora y por ende su fortaleza metabólica.

3. Esta metodología anterior permite evaluar el efecto químico de fármacos sobre *L. fermentum*. Así, se puede concluir que mientras que omeprazol no afecta al metabolismo de *L. fermentum*, la vancomicina (un antibiótico de amplio rango muy habitual) le provoca daños irreparables. Esta metodología puede ser extensible a otros fármacos y otros probióticos componentes de la flora bacteriana.

4. Hemos desarrollado una metodología simple que puede servir para diagnosticar de forma rápida y sencilla la infección vaginal conocida como vaginosis bacteriana. Esta metodología está basada en las propiedades electrocrómicas de un segundo polyoxometalato, phosphomolybdic acid (PMA) y en la influencia de la luz UV en su comportamiento redox. Mientras que PMA en presencia de luz UV es reducido por ácido láctico, excretado por lactobacilos saludables que habitan en la vagina, no es reducido sin embargo por ácido acético, excretado por la bacterias patógenas responsables de la infección

vaginal. Así con un simple método colorimétrico puede diferenciarse una situación sana (azul) de una infecciosa (incolora).

5. Hemos desvelado el mecanismo por el cual las bacterias probióticas facilitan la absorción de hierro a nivel digestivo, un hecho que se conoce desde hace décadas pero que no había sido interpretado. Dicho mecanismo radica en la excreción de una molécula, ácido *p*-hidroxifeniloláctico que posee capacidad ferrireductasa. Puesto que la reducción de Fe(III) a Fe(II) en el duodeno es un proceso necesario para su absorción en el enterocito vía DMT1, la presencia de HPLA favorece esta absorción. De hecho, el enterocito contiene una proteína de membrana, DcytB, encargada precisamente de llevar a cabo esta función. En este sentido, por tanto, HPLA asistiría o sustituiría a DcytB, favoreciendo por así la absorción de hierro.

6. Hemos logrado aislar y caracterizar los EPS de *L. fermentum*. Dada la importancia de los EPS en el proceso de colonización y proliferación de bacterias (saludables o patológicas) en un tejido, hay un enorme interés en su caracterización. Sin embargo, los ejemplos existentes son relativamente escasos. Mediante métodos químicos hemos logrado aislar los EPS de *L. fermentum*. El estudio de RMN mostró que se trata de una mezcla de polímeros, dextran (polímero de glucosa) y levan (polímero de fructosa).

7. Los EPS naturales de *L. fermentum* sirven como plataforma para la agregación de nanopartículas de oro de diferentes morfologías,

esféricas, cilíndricas o prismáticas. Producto de esta agregación, las propiedades ópticas de las nanopartículas de oro cambian, apareciendo una nueva banda de absorción a más bajas energías en el espectro visible.

8. Los EPS en sí mismos muestran capacidad reductora y son capaces de formar, en ausencia de un reductor adicional, agregados de nanopartículas de oro con tamaño y formas heterogéneas.

CHAPTER 7.
CONCLUSIONS

1. *Lactobacillus fermentum* acts as a reducing agent due to the excretion of molecules with reducing capacity. This reducing behaviour is correlated with its metabolic strength.

2. We have developed a simple test to quantify the metabolic strength of *L. fermentum*. The electrochromic polyoxometalate $Na_6[P_2Mo^{VI}_{18}O_{62}]$ (POM) acts as a sensor of the reducing activity of *L. fermentum*. The evaluation of *L. fermentum* reducing activity, and in consequence its metabolic strength, is accomplished by monitoring UV-vis spectra.

3. This previous methodology allows the evaluation of the chemical effect of some drugs on *L. fermentum*. Then, it is possible to conclude that while omeprazole does not affect the *L. fermentum* metabolism, vancomicine (a very common antibiotic) provokes irreparable damages over it. This methodology can be applied to other drugs and other probiotics of the bacterial flora.

4. We have developed a simple methodology that allows a rapid and easy way of diagnosing a vaginal infection known as bacterial vaginosis. This methodology is based on the electrochromic properties of a second polyoxometalate, phosphomolybdic acid (PMA) and the UV light influence over its redox behaviour. PMA in the presence of UV light is reduced by lactic acid, excreted out by healthy lactobacilli bacteria that inhabit in the vagina. However, it is not reduced by acetic acid, which is excreted out by the pathogenic bacteria that cause the vaginal infection. In this way, with a simple colorimetric method it is possible to differenciate between a healthy situation (blue) and an infected one (colourless).

5. We have revealed the mechanism by which probiotic bacteria allow iron absorption at digestive level, a fact which has been known from decades but it has not been previously interpreted. This mechanism resides in the excretion of a molecule, *p*-hydroxyphenyllactic acid which has ferric-reducing properties. Due to the fact that the Fe(III) to Fe(II) reduction in the duodenum is a needed process to its absorption by the enterocyte through the DMT1, the presence of HPLA favours this absorption. In fact, the enterocyte contains a membrane protein, DcytB, responsible for this function. In this sense, HPLA favours the iron absorption by assisting or substituting DcytB role.

6. We have achieved the isolation and characterization of *L. fermentum* EPS. Because of the importance of these EPS in the colonization and proliferation processes of the bacteria (healthy or pathogenic ones) in a tissue, there is a huge interest in their characterization. However, the existing examples are relatively limited. By chemical methods, we have accomplished the *L. fermentum* EPS isolation. The NMR study showed that these are a mixture of polymers: dextran (glucose polymer) and levan (fructose polymer).

7. The natural EPS of *L. fermentum* act as a platform for the different morphologies, spherical, rods or prisms, gold nanoparticles aggregation. As a consequence of this aggregation, the optical properties of gold nanoparticles change, appearing a new band of absorption at lower energies in the visible spectra.

8. EPS on their own show reducing capacity and are able to create, in the absence of an additional reductant, gold nanoparticles aggregates with heterogeneous shapes.